Università degli Studi di Verona

Department of Biotechnology

PhD School in Natural Sciences and Engineering

PhD Course in Biotechnology

Cycle XXX

Characterization of the capping layer of selenium nanoparticles synthesized by environmental bacterial strains and new hypothesis on selenium nanoparticles transport in *Bacillus mycoides* SeITE01

PhD Thesis

Author:

Alessandra Bulgarini

Advisor:

Prof. Giovanni Vallini

Co-advisors:

Prof. Raymond J. Turner

Dr. Silvia Lampis

Characterization of the capping layer of selenium nanoparticles synthesized by environmental bacterial strains and new hypothesis on selenium nanoparticles transport in *Bacillus mycoides* SeITE01

Alessandra Bulgarini

November 23, 2018

Abstract

Selenium nanoparticles (SeNPs) are 10 to 400nm spheres composed of zero-valent selenium. SeNPs can be synthesized either chemically or biologically by microorganisms, plant extracts or enzymes. Biogenic SeNPs display a capping layer of organic molecules, which confer unique characteristics to such SeNPs, e.g. a major stability over time and a more efficient antimicrobial activity. Composition and role of the capping layer are mostly unknown and currently under investigation.

In this study, environmental strains *Bacillus mycoides* SeITE01, *Stenotrophomonas maltophilia* SeITE02, *Achromobacter* sp. R2A, *Ensifer* sp. R2D and *Lysinibacillus* sp. R1E are considered, which are able to biosynthesize SeNPs.

In the first section, SeNPs from the five bacteria are analyzed: microplate colorimetric assays are performed in order to quantify total carbohydrates, protein and lipids contents of such SeNPs capping layers. Moreover, SeNPs are treated with different protocols to remove part of the organic layer. Effect of such treatments on capping composition and SeNPs stability are studied and compared for all the five strains.

In the second section, SeNPs produced by *B. mycoides* SeITE01 are analyzed from a proteomic point of view: biogenic SeNPs capping layer proteins are identified. Chemical SeNPs exposed to a SeITE01 cell free extract are analyzed as well. Identified proteins are compared in order to establish which proteins bind specifically biogenic SeNPs and are more probably involved in SeNPs formation. Finally, a model for SeNPs transport through SeITE01 cell wall is formulated, based on proteomic evidence. Native proteins activity assay and microscopy analysis are performed, in order to confirm the new model.

In conclusion, studying the organic capping layer of biogenic SeNPs from different strains is of paramount importance to understand the effect of such molecules on SeNPs characteristics and formulate hypotheses on biosynthesis mechanism. SeITE01, SeITE02, R2A, R2D and R1E biosynthesized SeNPs show a different ratio of carbohydrates, proteins and lipids components of the capping layer and differently respond to treatments. Particularly, Gram-negative strains (SeITE02, R2A, R2D) show similar composition and respond to treatments in a similar fashion, while Gram-positive strains (SeITE01, R1E) show more variability. For SeITE01, proteomic and microscopy analyses led to a new model formulation for SeNPs transport outside the cell. Together with previous studies, this new hypothesis can contribute to a more complete vision of SeNPs synthesis in this aerobic strain.

Glossary

Abs Absorbance. 133

Abs Polydispersity index. 48

ANOVA Analysis of variance. 60

BioSeNPs Biogenic Selenium nanoparticles. 15

BSA Bovine Serum Albumin. 15

CFX Cell Free Extract. 29

ChSeNPs Chemically synthesized Selenium nanoparticles. 15

Dh Hydrodynamic diameter. 48

DLS Dynamic Light Scattering. 8, 48

EDX Energy Dispersive X-ray Analysis. 29

EPS Extracellular Polymeric Substance. 23, 30

FTIR Fourier Transform Infrared Spectroscopy. 29

GSH Glutathione. 17

MS Mass Spectrometry. 93

SDS Sodium Dodecyl Sulfate. 15

SDS-PAGE Sodium Dodecyl Sulfate - PolyAcrylamide Gel Electrophoresis. 9, 92

SEM Scanning Electron Microscopy. 36

SeNPs Selenium nanoparticles. 7, 13

TEM Transmission Electron Microscopy. 33

TR Thioredoxin reductase. 18

Trx Thioredoxin. 13

Contents

Part I

Introduction and Objectives

Chapter 1

Introduction

1.1 Selenium nanoparticles (SeNPs): chemical vs biological synthesis and relative specific applications

1.1.1 Selenium: characteristics, environmental occurrence and interaction with microbes

Selenium, chemical element with atomic number 34, belongs to the chalcogen group of the periodic table, having chemical properties similar to Sulfur and Tellurium. It was discovered by Jöns Jakob Berzelius in 1818 and named after the greek moon goddess "Selene" in resemblance to Tellurium, named after latin word "tellus" (earth) (*1*). Because of its similarity to Sulfur, Se generates compounds structurally related to Sulfur compounds, but more toxic due to different reactivity properties (*2*).

Selenium is an essential element for human diet, but at the same time it is considered a toxic element depending on the dosage. Daily Se intake should range from 50 to 200µg/day for adults (*3*, *4*), where an intake less than 40µg/day is considered dietary deficiency and an intake major than 400µg/day can lead to toxic effects (*5*).

It is essential as it is a component of amino acids selenocysteine and selenomethionine, and of enzymes such as glutathione peroxidase and thioredoxin (Trx) reductase (*2*, *4*). Being a metalloid, it displays characteristics similar to metals, as for example photovoltaic and semiconducting properties, finding application in photocells and rectifiers (*2*). However, Se is also used in medicine due to antioxidant and cancer prevention activities (*6*, *7*).

In the environment, Se is generally found in sedimentary rocks and soils, in both inorganic and organic forms. In inorganic forms, it occurs naturally in four oxidation states, depending on pH and redox potential of the soil: selenide (Se^{2-}), elemental selenium (Se^{0}), selenite (Se^{4+}) and selenate (Se^{6+}). Elemental Se has various possible forms: amorphous (as red powder, or

black in vitreous form), crystalline monoclinic (red) or hexagonal (grey). In Figure 1.1, the Se cycle in the environment is schematized, showing how anthropic activity is currently influencing the presence of this element in soils, waters and atmosphere. Notably, microrganisms also have an important role in Se cycle, converting Se forms (e.g. reduction, alkylation) (*8*). Selenium is in fact naturally present in the environment mainly due to natural erosion of rocks, and mobilized in waters. Anthropogenic activities, such as metal mining and smelting, accumulation in municipal landfills, oil refining, production of pigments, glass manufacturing and irrigation of Se-rich soils contribute to increase Se presence in the environment (*3*). Se concentrations of 1200 mg/kg are registered in particularly rich soils or toxic areas (*9*).

However, Se toxicity is not only related to its quantity in contaminated areas, but also to its form: oxyanions selenate and selenite are the most soluble and thus bioavailable forms. Since biogenic reactions play an important role in Se cycle and many microorganisms have been characterized, which are able to convert Se forms, bioremediation is considered a promising technology for the treatment of contaminated soils and waters (*2*, *10–14*).

Particularly, bacteria are able to reduce Se oxyanions to less toxic and/or less bioavailable forms through accumulation, reduction or methylation (*2*):

- In accumulation, they uptake or immobilize the compounds with surface biomolecules
- In bioreduction, they reduce oxyanions to elemental form Se^0
- In biomethylation, they volatize oxyanions and disperse the contaminant.

Consequently, Se oxyanions can be reduced and removed from contaminated water and soil through bioremediation, followed by removal of the less toxic forms to prevent reoxydation. Another alternative could be combining bioremediation with phytoremediation, as some plants are able to bioaccumulate Se (*10*).

Interestingly, some of the microbial strains able to convert Se oxyanions to less toxic form Se^0 are also able to synthesize Se nanomaterials in the form of nanoshpheres or nanorods composed of so-formed Se^0.

1.1.2 Selenium nanoparticles: definition, synthesis methods and applications

Selenium nanoparticles (SeNPs) are defined as 10 to 400nm (*15*, *16*) zero valent elemental Se spherical aggregates. Production of such particles is mainly possible through chemical or biological methods. Chemical synthesis generally consists in selenite reduction through the addiction of a reducing agent, like ascorbic acid, cysteine, cytochromes or glutathione (*17*), or using

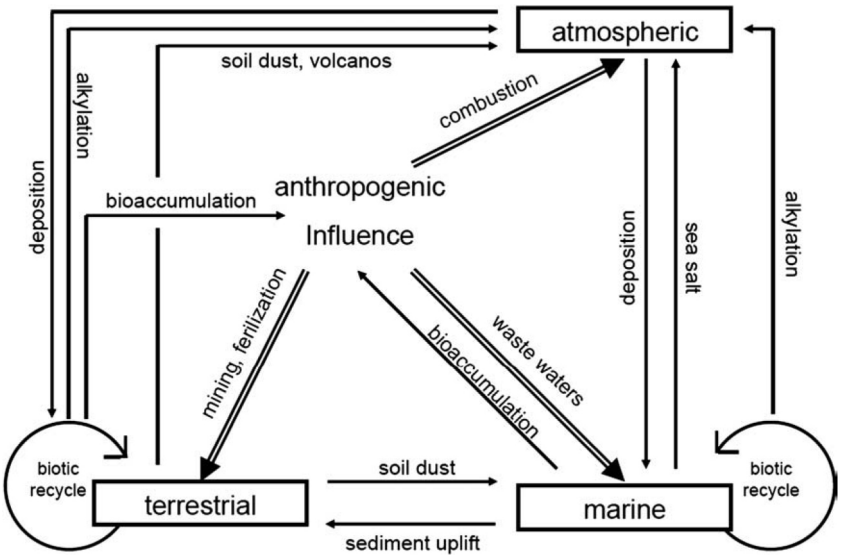

Figure 1.1: Selenium cycle in the environment is strongly influenced by anthropic activities. Image is from Lenz and Lens, 2009 (*8*)

selenous acid as a precursor and Sodium Dodecyl Sulfate (SDS) as stabilizer (*18*). Biological methods include reduction of selenate or selenite by microorganisms, microbial consortia, plant extracts or enzymatic preparations (*11*, *13*, *19–21*).

Other methods include chemical synthesis in the presence of organic molecules, for example the protein Bovine Serum Albumin (BSA) (*22*) or polysaccharides or extracellular matrix (*23*).

The main advantage of chemical synthesis is the homogeneity of produced SeNPs in size, while the main disadvantages are a susceptibility to photocorrosion and, in some cases, the use of hazardous chemical products or need of extreme temperature or pressure.

On the other hand, biological synthesis is a much more environmentally friendly production system, and can also be coupled with bioremediation (*24*, *25*). Also, it does not require expensive or hazardous chemicals and occurs at ambient temperature and pressure. Moreover, biogenic SeNPs (BioSeNPs) tend to be more stable over time than chemical SeNPs (ChSeNPs). The main disadvantage of this kind of synthesis lays in inhomogeneity in size of produced SeNPs. Yet, BioSeNPs size can be influenced changing some culture condition (e. g. temperature, pH, medium composition), but compared to ChSeNPs, biogenic ones tend to be less controllable. Similarly, BioSeNPs yeld can vary from batch to batch, while it is more controllable for ChSeNPs production processes.

ChSeNPs are more suitable for applications in electronic industry, where size uniformity is important, while BioSeNPs have been shown to be efficient

as antioxidants (*26*), anti-cancer and antimicrobial agents (*27–31*).

1.2 Mechanisms and hypothesized pathways for bacterial Se-metabolism and biosynthesis of SeNPs

Se resistance is generally characterized by the absence of specific determinants, as Se is both an essential and toxic element. By contrast, strains which are resistant to Tellurium, also a chalcogen, show very specific resistance mechanisms, being tellurite 100- to 1000-fold more toxic than selenite (*2*). Moreover, Se resistant strains often detoxify Se oxyanions with more pathways at the same time. For these reasons, study of Se resistance is particularly challenging.

The most widespread mechanism of Se-oxyanions resistance is their reduction to insoluble elemental Se and subsequent bioprecipitation. This can be either extra- or intracellular or in association with cell wall or membrane, with possible formation of SeNPs (*2*).

Overall, when Se is present in sub-toxic concentrations, it is incorporated in other molecules, such as Se amino acids; while in presence of toxic concentrations, Se oxyanions are converted and disposed by the cell. The two kinds of metabolism are referred to as "assimilatory" and "dissimilatory" metabolism, respectively.

In case of dissimilatory metabolism, Se oxyanions can be reduced through interaction with various enzymes or cell components, depending on strain and conditions (aerobic or anaerobic):

- Reaction with thiols (Painter-type reaction, see below)
- Inorganic reaction with bacterial metabolites
- Reaction with enzymes:

  Enzymes specific of Se metabolism

  Enzymes specific of other pathways (e.g. denitrification or sulfur metabolism pathway enzymes) reacting with Se compounds

  Methylation pathway enzymes

Reaction with enzymes can occur intracellularly or extracellularly, and usually involves oxidoreductases, including electron transport chain enzymes. In fact, in anaerobic conditions some strains can use Se oxyanions as final electron acceptor. During respiration, Painter type reaction and enzymatic reduction often lead to the reduction of Se oxyanions to elemental Se and formation of SeNPs, while methylation results in volatilization of reduced Se.

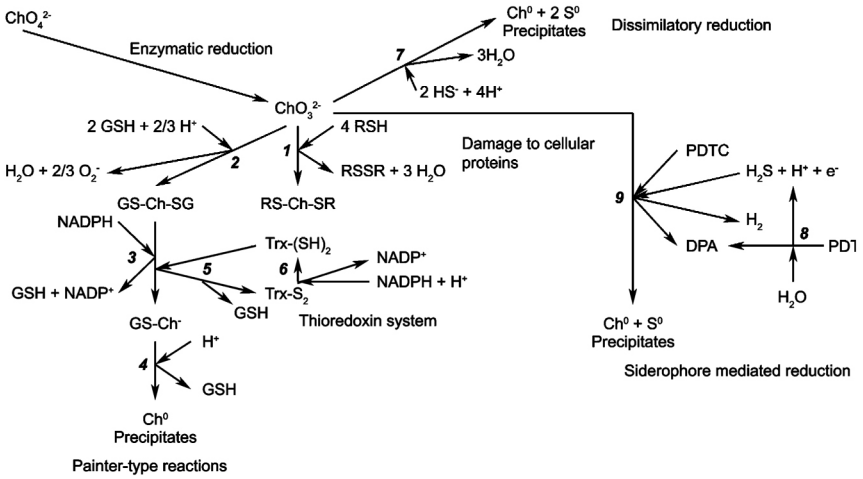

Figure 1.2: Scheme of proposed pathways for a selenium oxyanion reduction in a bacterial cell. Such pathways are likely to occur for all chalcogens ("Ch" in the figure). Image is from Zannoni *et al.*, 2008 (*2*)

1.2.1 Possible pathways for Se oxyanions reduction: coexistence of different reduction mechanisms

Despite the aforementioned difficulties in Se metabolism study, several groups so far have analyzed possible pathways of Se conversion. Zannoni *et al.* (2008) proposed that selenite conversion to SeNPs occurs through 4 possible mechanisms (*2*):

- Painter-type reaction of Se-oxyanions with reduced thiols, like glutathione (GSH) (*32*)
- Enzymatic reduction by periplasmic or cytosolic oxydoreductases
- Inorganic reaction with bacterial metabolites
- Redox reaction with siderophores

The so-called "Painter-type reaction" takes the name from Painter, who in 1941 observed the high reactivity of selenite with thiol groups and demonstrated the formation of selenotrisulfides (*32*).

In Figure 1.2 possible pathway are illustrated. First, selenate is reduced to selenite via enzymatic (or abiotic) reduction. Starting from selenite, different reactions can occur: Painter-type reaction (1) with thiols (RSH), forming selenotrisulfide (RS-Se-SR) (*32*). If the same reaction occurs with glutathione (GSH), products are selenodiglutathione (GS-Se-SG) and superoxide anions (2), which are then removed by catalase or superoxide dismutase. GS-Se-SG is reduced (3) by GSH-reductase to GSH and unstable

intermediate glutathione selenopersulfide (GS-Se-), which reacts with protons regenerating GSH and elemental Se (4). Alternatively, GS-Se-SG can be reduced by Trx reductase (TR) (5). Oxidised Trx is reduced again by Trx reductase using NADPH as electron donor (6).

Selenite could also be converted to Se^0 by dissimilatory reduction: various enzymes including nitrate and nitrite reductases or sulfate and sulfite reductases could reduce selenate or selenite. Alternatively, an inorganic reaction could occur (7). Some authors also postulated a precipitation of sulfur during inorganic reduction of selenite (*33*). Finally, chelator molecules called siderophores could interact with selenite (9): pyridine-2,6-bisthiocarboxylic acid (PDTC) was observed to interact with metal oxyanions forming insoluble precipitates (*2*, *34*).

1.2.2 Painter-type reaction with thiols

Previously described Painter-type reaction can occur in different strains as the main Se-reduction mechanism, or concomitantly with other mechanisms. For example, Butler's research group in 2012 observed this kind of interaction with thiols in the previously described Se-respirer *Enterobacter cloacae* SLD1a-1 (*20*, *35*). In *Escherichia coli* K-12, GSH is the most likely candidate for bacterial intracellular selenite reduction. Kessi *et al.* observed an induction of Trx and Trx-reductase (TR) at mM Se concentration. Trx-TR system could be responsible of GS-Se-SG conversion to Se^0 (*36*). However, other mechanisms seem to contribute to selenite reduction: Dobias and colleagues identified a propanol-preferring alcohol dehydrogenase (AdhP) which could be involved in controlling the size of final SeNPs. It is however not clear, if AdhP and other SeNPs-strictly bound proteins could be involved in Se^0 formation as well (*37*). Moreover, Se could be at the same time partly dispersed through methylation (*38*).

Thauera selenatis, Se-respiring bacterium with some Se-specific enzymes (see below), also seems to reduce selenite through GSH interaction (*20*). *Rhodospirillum rubrum* forms SeNPs intracellularly, as selenite probably reacts with thiols as soon as it enters the cells, while it would be kept outside until the reduction system is operating. GSH is also probably involved in both methylation and dissimilatory reduction pathways (*19*). Reduction of selenite was observed to induce GSH-reductase activity in *Rhodobacter sphaeroides* (*36*). For *Bacillus subtilis*, at mM selenite concentration, a significant induction of Trx and TR was observed (*39*).

1.2.3 Reduction in anoxic conditions: Se-respiring bacteria

One of the first and most studied mechanism of Se oxyanions conversion into Se^0 is reduction by Se-respiring bacteria, which are able to use Se oxyanions as terminal electron acceptors in the respiratory electron transport chain.

In the following examples, reduction to Se^0 is followed by SeNPs formation.

Bacillus selenitireducens MLS10 is able to produce extracellular SeNPs in the size range of 200 to 400nm (*40*). Switzer and Blum (1998) proposed a periplasmic reducing activity leading to dissimilatory reduction of selenite (*41*). Moreover, they proposed that reduction of selenite would be coupled with lactate oxidation. Oremland and colleagues hypothesized, that the strain could have Se-specific dissimilatory enzymes, as the strain does not reduce selenite through enzymes associated to sulfate dissimilatory reduction. They also observed, in agreement with Switzer and Blum, that no lactate oxidation was detected in the absence of selenite, nor coupled reduction of nitrate, fumarate, sulfate or thiosulfate. Interestingly, the MLS10 SeNPs appear to be encapsulated with a polymer, providing them stability for several months (*40*).

Another Se-respiring strain, *Sulfuspirillum barnesii* SES-3, was observed to produce 200 to 400nm SeNPs. Curiously, SeNPs were observed in large extracellular aggregates when the strain was grown on selenite, while when the strain was grown on selenate (or provided with selenate after growing with nitrate), SeNPs were observed intracellularly (*40*).

Selenihalanaerobacter shriftii DSSE1 also produces intra- or extracellular SeNPs when Se oxyanions are provided after growth on nitrate (*40*).

Finally, metalloid reductase (RarA) was also observed by Lenz *et al.* associated with *S. barnesii* DMSZ 10660 SeNPs (*42*).

Notably, SeNPs produced by all aforementioned Se-respiring bacteria are stable for several months.

Enterobacter cloacae SLD1a-1, a facultatively-anaerobic gamma-proteobacterium, is a Se-respirer, but in this case selenite is not the only electron acceptor. Starting from selenate, SLD1a-1 can produce SeNPs intracellularly and extracellularly, adherent to the cell surface. It was hypothesized, that membrane bound selenate reductases could release selenite in the periplasm, where it would be reduced to Se^0 (*20*, *35*). Leaver *et al.* (2008) observed, that selenate reduction was unable to support growth with selenate as the only electron acceptor. However, they hypothesized that some energy conservation could be derived by selenate reduction, as the selenate reductase is directly linked to the Quinol-pool (Q-pool), allowing the enzyme to support low level of ATP production (Figure 1.3) (*35*, *43*). Notably, the strain *E. cloacae* SLD1a-1 can maintain growth in selenate-rich and nitrate-depleted medium, while other strains of *E. cloacae* cannot (*43*).

1.2.4 Specific enzymes and interactions with other pathways

As previously mentioned, Se oxyanions reduction and SeNPs formation and transport can occur both through specific and non specific mechanisms, interacting with enzymes specific for selenate/selenite metabolism or enzymes involved in other pathways, usually nitrate/nitrite or sulfate/sulfite.

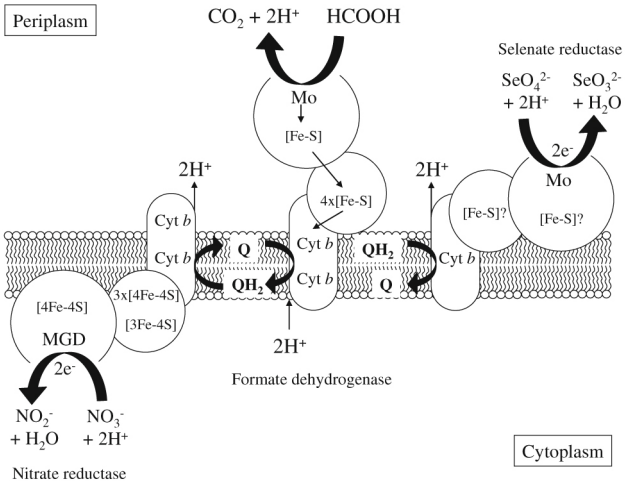

Figure 1.3: Selenate reductase catalyzes the first step of selenate reduction (to selenite). The enzyme is directly linked to the Q-pool and could consequently contribute to ATP production. Selenite is then reduced to Se^0 in the periplasm. Image is from Leaver *et al.*, 2008 (*43*)

These pathways could in fact share one or more enzymes with Se oxyanions metabolism.

Thauera selenatis was isolated from the seleniferous waters of the Joaquin Valley (CA, U.S.A.). This Gram-negative, selenate-respiring beta-proteobacterium can synthesize about 150nm SeNPs with regular size distribution (*20*). Butler *et al.* observed the production of SeNPs intracellularly and in the periplasmic compartment during the exponential phase of growth, usually one Se deposit per cell. Entering the stationary phase, SeNPs were exported via secretion by a specific protein: Selenium factor A (SefA). SefA was observed to be exported with SeNPs and has a possible function in stabilizing such particles before secretion. It was also observed that SefA was up-regulated by selenite and its accumulation in the medium increased with time during selenite reduction. Periplasmic selenate-reductase SerABC and SerD were also identified, which could be involved in selenate conversion to Se^0 (*20*, *44–46*). The proposed reduction mechanism is shown in Figure 1.4.

A specific selenite reductase could be constitutively expressed in *Rhodospirillum rubrum*. Kessi *et al.* propose a tightly regulated selenite transport system, as selenite is kept outside the cells until the end of exponential phase of growth. *R. rubrum* also displays different strategies for selenite, sulfite and nitrite reduction, keeping all pathway separated (*19*, *36*). However, SeNPs formation was observed to be intracellular, possibly through interaction with thiols.

Kessi *et al.* also analyzed SeNPs formation in *Rhodobacter capsulatus*. Differently from *R. rubrum*, selenite, sulfite and nitrate follow different path-

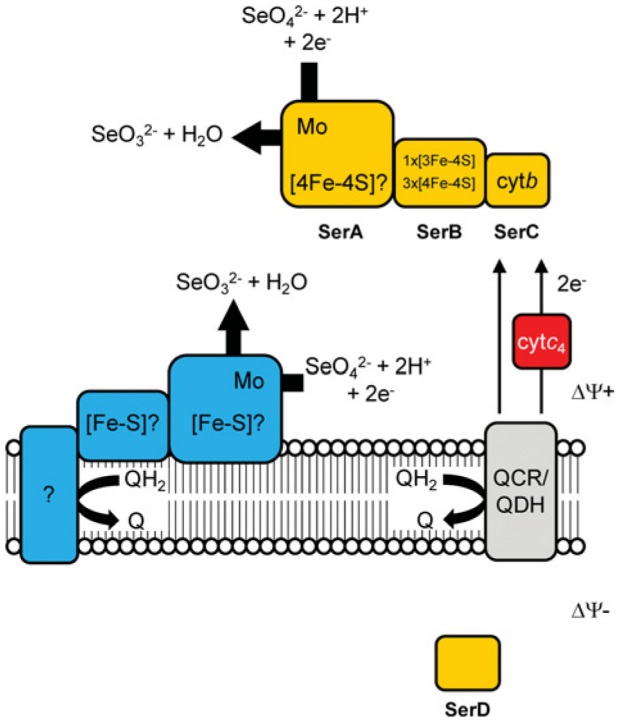

Figure 1.4: Proposed model for reduction of selenate: molybdoenzyme SerABC reduces selenate to selenite accepting 2 electrons from Q-pool via cytochrome c_4. So produced selenite is probably reduced in the cytoplasm, forming intracellular SeNPs. SerD is probably a chaperone for proteins involved in cofactor insertion in SerA. Image is from Butler *et al.*, 2012 (*20*)

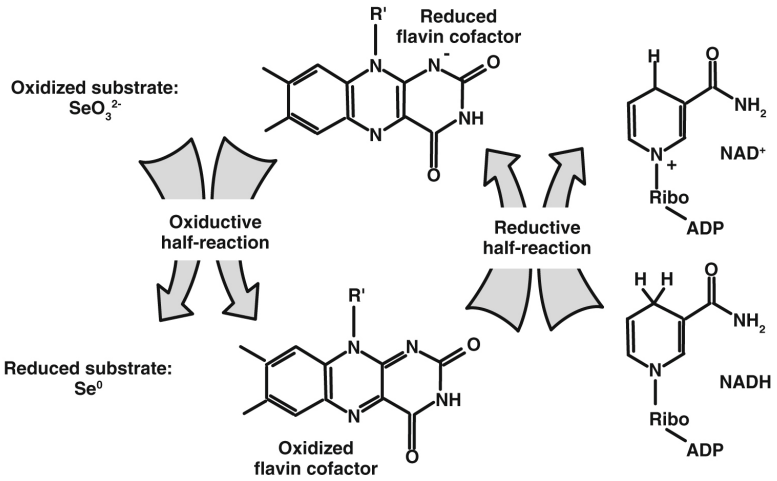

Figure 1.5: Reduction of selenite by flavin-cofactor of NADH:flavin oxidoreductase. Image is from Hunter *et al.*, 2014 (*47*)

ways, but are metabolized simultaneously, causing interferences. The authors hypothesize that nitrite and selenite pathways could share an electron transfer protein, while interference between selenite and sulfite pathways would occur at transport system level (*19*).

In 2014, Hunter and colleagues analyzed *Rhizobium selenitireducens* proteins involved in selenite reduction (*47*). Other than a nitrite reductase, which could specifically reduce selenite, another enzyme was identified which may be also involved. This protein, a NADH:flavin oxidoreductase, may be able to produce Se^0 through redox reaction of selenite with a flavin cofactor (Figure 1.5).

Tugarova *et al.* (2014) studied selenite metabolism in *Azospirillum brasilense* Sp7 and Sp245, where selenite reduction probably occurs specifically through denitrification pathway. In fact, the strains are not able to reduce selenate (*48*).

Also *Veillonella atypica* reduces selenite by a specific pathway, forming selenide, which subsequently precipitates forming NPs with other metals. Selenide formation involves a hydrogenase-coupled reduction mediated by ferredoxin. Notably, the strain is able to reduce various metals and metalloids oxidizing hydrogen (*49*).

1.2.5 Formation of SeNPs: extracellular reduction and maturation

Formation of SeNPs following Se oxyanions reduction to Se^0 is also under investigation. For some strains, it starts inside the cell, forming nucleation seeds that are subsequently secreted.

In some of those cases (*16*, *50*), SeNPs maturation is described as an

"Ostwald ripening" mechanism, a thermodynamically spontaneous process where small and unstable Se^0 clusters dissolve and aggregate to form bigger and more stable particles. Such particles in fact work as nucleation seeds for the forming SeNPs: other small Se particles dissolve and redeposit on forming SeNPs until they reach stability (*51*).

Alternatively to secretion, SeNPs growth inside the cell can lead to cell lysis. On the other hand, Se oxyanions can also be reduced to Se^0 directly by periplasmic or extracellular enzymes or other secreted molecules. In fact, in some cases the capping layer typical of biogenic SeNPs has a composition similar to Extracellular Polymeric Substance (EPS) (*11*).

For some strains, intra- and extracellular/periplasmic maturation processes can coexist. For example, a synthesis model developed by Jain and colleagues for SeNPs synthesis by a community of anaerobic granular sludge bacteria. The model is shown in Figure 1.6. The authors propose a two-step process for SeNPs production by different bacterial species present in anaerobic granular sludge: first, selenite is reduced to Se^0, then, Se^0 forms 50 to 250nm SeNPs. Reduction of selenite is proposed to occur intracellularly, in the periplasmic space, and extracellularly, depending on the microorganism. For periplasmic and extracellular synthesis, SeNPs grow in the presence of EPS, resulting in a capping layer composed of EPS molecules (proteins, carbohydrates, DNA and humic-like substances). For intracellular production, SeNPs likely develop a capping layer mainly composed of proteins. Depending on secretion pathway, such SeNPs could further grow extracellularly in the presence of EPS, or grow intracellularly, causing cell lysis (*52*).

In *Pseudomonas* strains *P. aeruginosa* JS-11 and *P. alcaliphila*, synthesis of SeNPs was proposed to be caused by interaction with extracellular material. For *P. aeruginosa*, Dwivedi *et al.* suggested the involvement of NADH and NADPH-dependent reductases and phenanzine-1-carboxylic acid (released by bacteria) in extracellular SeNPs formation from selenite (*53*). Also for *P. alcaliphila*, selenite reduction would occur by secreted proteins, and SeNPs would grow with an Ostwald ripening mechanism (*50*).

Interestingly, extracellular SeNPs synthesis was also observed in 1992 in *Pseudomonas stutzerii*, where less than 200nm SeNPs were observed associated to the tips of bacterial cells (*54*).

Extracellular reduction was also observed in *Bacillus* strains: for Se-respiring *B. selenitireducens* MLS10, a periplasmic reducing activity was also proposed for dissimilatory reduction of selenite (*41*), while for *B. cereus* CM100B, extracellular surface-attached SeNPs were observed, but also intracellular SeNPs production was evidenced (*55*). The hypothesis for CM100B is an intracellular reduction by membrane-associated reductases, followed by an accumulation of Se^0 in the cytoplasm or in the periplasmic space, followed by excretion of SeNPs. Notably, such SeNPs are tightly bound to cell-produced substances and display a highly negative surface charge, which confers stability to SeNPs (*55*).

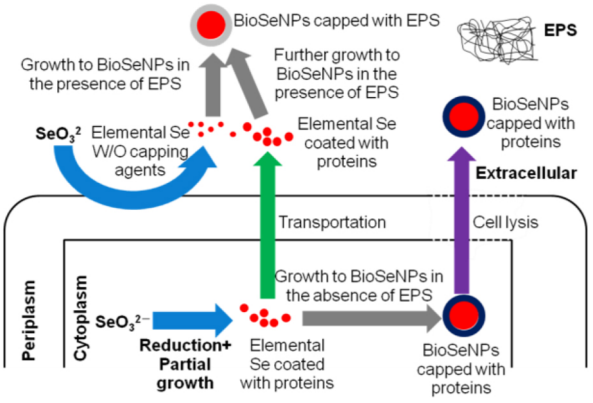

Figure 1.6: Proposed pathways of SeNPs synthesis by anaerobic granular sludge bacteria: reduction of selenite can occur extracellularly, in the periplasmic space or intracellularly. SeNPs can grow extracellularly in the presence of EPS or intracellularly in the presence of proteins, developing a capping layer mainly composed of EPS molecules or proteins. Otherwise, SeNPs can partially grow intracellularly, then be secreted without damaging membrane or cell wall and completely grow extracellularly. In this last case, EPS molecules are added to the mainly proteinaceous capping layer. Image is from Jain *et al.*, 2015 (*52*)

Extracellular activity was also observed for *Bacillus mycoides* SeITE01 (see Section 1.5.1). Another *Bacillus* strain, *B. subtilis*, was studied by Garbisu and colleagues in 1999 because of a peculiar behavior of a bacterial culture subpopulation (*39*). The authors observed what they called "dark granules" starting to form on the surface of about 10% of the cells after 6h of exposition of bacterial culture to 1mM selenite. Cell content of these cells was then extruded through a discontinuity in the cell envelope, forming protoplast-like structures called "round bodies" by the authors. After 10h of selenite exposure, such round bodies separated and left dark granules within the cell envelope. This happened to about 5% of the population. After 20h, round bodies developed crystal-like structures on the surface and lysed. Most of selenite reduction was reported to happen between 10h and 20h of selenite exposure by this subpopulation. Interestingly, no round bodies were observed in cultures previously exposed to selenite stress (induced cultures). For induced cultures, cell wall was apparently sufficiently strong to confine Se^0 within the cells. In fact, structures similar to round bodies were observed in induced cultures only after lysozyme treatment. The whole process is shown in Figure 1.7.

Trx level increased 2 to 4 fold in cells adapted to selenite stress, while NADPH-Trx reductase increased 2 to 3 fold. Such increased level was maintained in induced cells (*39*).

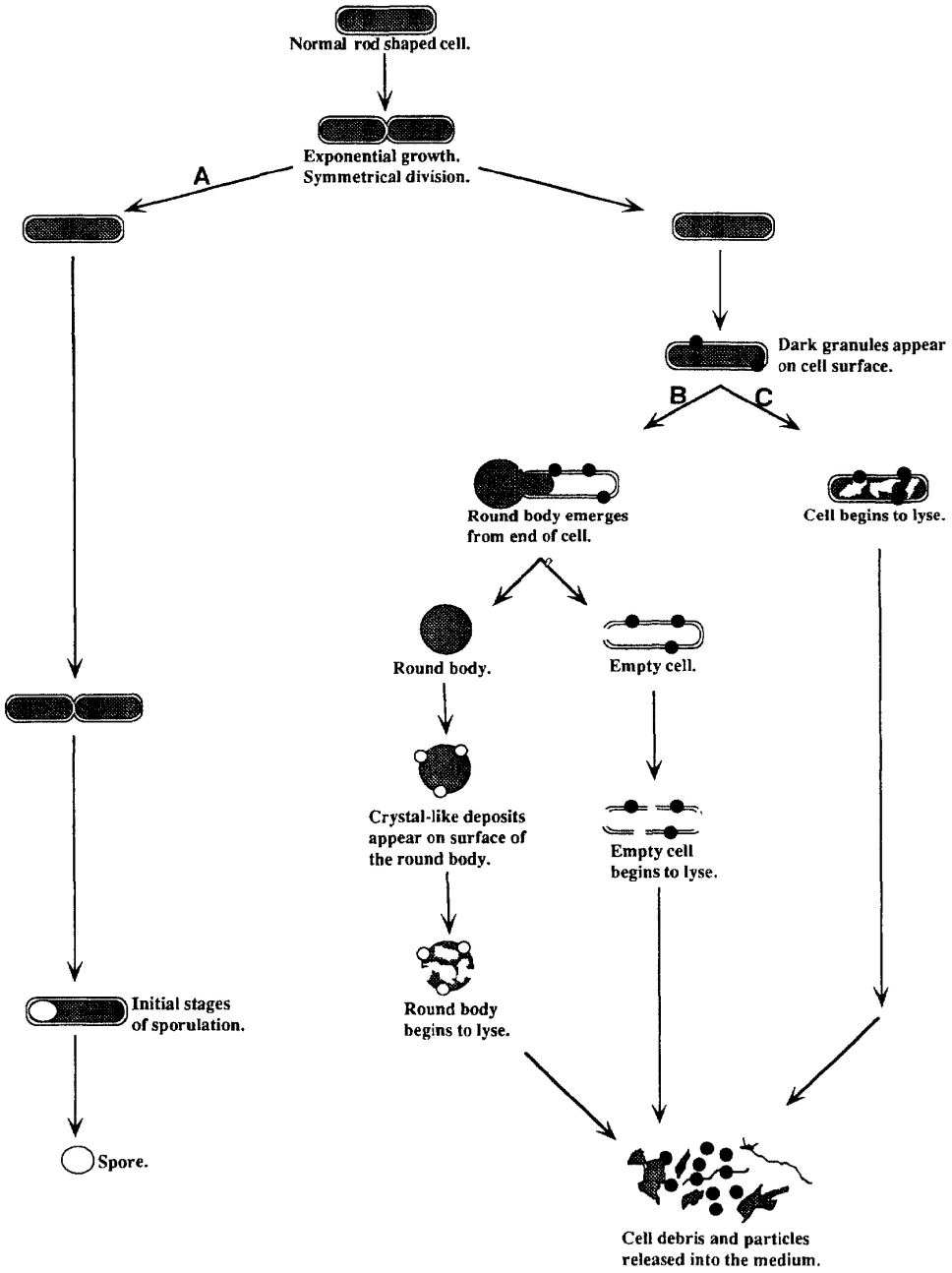

Figure 1.7: After selenite exposure, *B. subtilis* culture differentiated in 3 subpopulations. A: 90% of cells continued to grow normally and eventually sporulated. B: 5-10% of cells developed dark granules on the surface, formed round bodies and lysed. C: 1-5% of cells lysed and released cytosolic content after the appearance of dark granules, but without forming round bodies. Image is from Garbisu *et al.*, 1999 (*39*)

1.2.6 Pathways coexistence: volatilization and assimilation in SeNPs forming strains

Notably, different pathways for Se resistance can coexist in the same strain. For example, even in strains able to reduce Se oxyanions to Se^0 (and synthesize SeNPs), some of the Se can be dissimilated though volatilization by methyl groups addition (methylation). Kessi *et al.* proposed that in *R. rubrum* and *R. capsulatus*, methylation and formation of Se^0 could share some enzymes, as inhibition of GSH system leads to strong decrease of both volatile and non volatile Se compounds formation (*19*). Curiously, *E. coli* K-12 is able to methylate selenite (but not selenate) through a tellurite-specific methyltransferase (*38*).

For *R. sphaeroides*, Van Fleet-Stadler and colleagues observed that sulfur compounds positively influenced selenite metabolism, as low concentration of sulfates led to a decrease in biomass and Se volatilization, while high concentration of sulfates led to a major release of Se organocompounds (*56*). Together with volatilization, some chaperones and enzymes associated to oxidative stress reactions seem to be involved in selenite reduction (*57*).

In *Ralstonia metallidurans* CH34, Sarret *et al.* (2005) suggested the coexistence of an assimilatory pathway forming alkyl selenide and a detoxification (dissimilatory) pathway forming Se^0 (*58*).

1.3 Presence of a capping layer

A specific characteristic of BioSeNPs is the presence of associated molecules on the surface (*2*, *24*, *42*). Composition, structure and role of this associated capping are currently under investigation. However, it has already been observed that molecules change SeNPs properties such as surface charge and stability over time. Moreover, some of the associated molecules have been observed to be strongly attached to SeNPs surface, while others can be removed by mild or stringent treatments (e. g. detergent treatments, organic solvent treatments, SeNPs washing, etc.) (*37*). Despite the associated molecules being characteristic of biogenic SeNPs, chemically synthesized SeNPs can be functionalized with specific molecules or exposed to cell free extracts or solutions of proteins, polysaccharides or other organic molecules. After such exposure, organic molecules form a capping layer on chemical SeNPs surface (*23*, *59*, *60*).

In this study, such associated organic material will be referred as "capping layer", as it surrounds the surface of biogenic SeNPs here analyzed. Currently there is not a common definition in the literature for this associated material and many questions still remain open, such as their origin, role, composition, strain-specificity and strength of the bound interaction. The current hypothesis for biogenic SeNPs is that there is a layer of molecules strongly associated and surrounding such NPs. On the other hand, it has

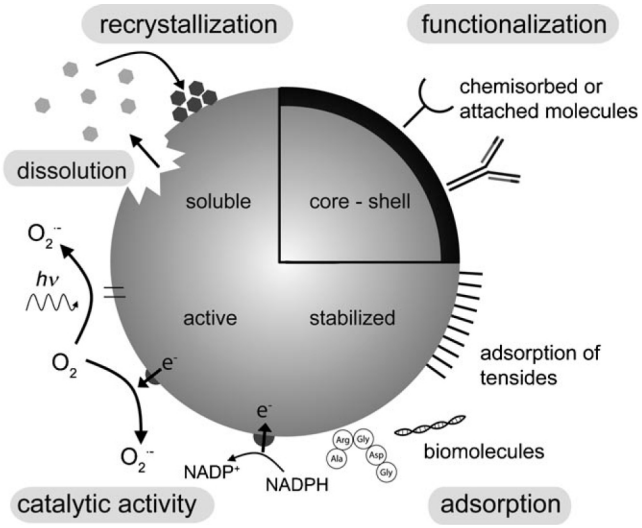

Figure 1.8: Scheme of the surface of a metallic NP: processes like dissolution, recrystallization and catalytic activity can be modified by adsorption of organic molecules or functionalization with specific molecules. Image is from Stark *et al.*, 2011 (*61*)

been observed that for biogenically synthesized NPs, the capping layer is provided by the organism through its biochemical molecules.

However, it is also clear that the capping layer provides SeNPs and NPs in general with different properties compared to ChSeNPs. Stark *et al.* (2011) highlight how associated molecules can change NPs properties like stability and reactivity. Such properties are of paramount importance when considering the use of metallic NPs in medicine. In Figure 1.8 the surface of a nanoparticle is schematized. For metallic and metalloid based NPs, processes as dissolution, degradation and recrystallization can alter the NPs themselves (*61*). Such processes can be modified by the presence of molecules on the surface. Such molecules also change catalytic activity of NPs, making them suitable or unsuitable for specific applications. Adsorption of biomolecules is a typical method to stabilize NPs, while functionalization with specific molecules (e. g. antibodies) confers new properties to NPs. In the last case, NPs can also act like delivery agents for the attached molecules (*61*).

The capping layer also determines the efficiency of NPs in applications such as antimicrobial or anticancer treatments. Uptake of NPs by other cells (microorganisms or cancer cells) in fact is likely mediated by the capping molecules. In Figure 1.9 the uptake of different molecules is schematized. However, the mechanism of uptake itself is still under debate (*61*).

The authors also stress the role of the associated molecules in NPs stability and their tendency to aggregate when the single NP stability is com-

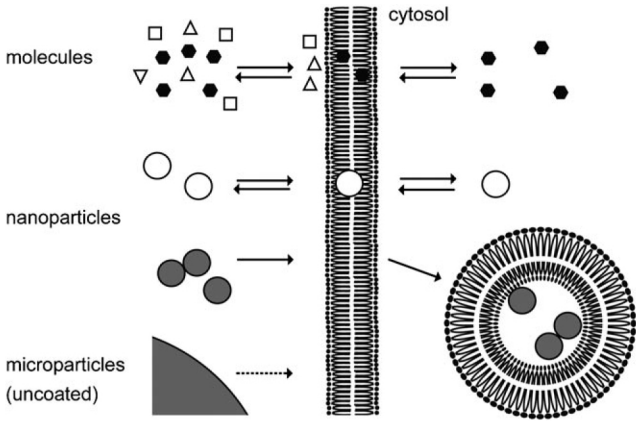

Figure 1.9: Scheme of cell uptake: lipophilic molecules (above) easily pass the membrane lipid bilayer. Depending on their surface, NPs can also diffuse inside the membrane (NPs in white) or bind vesicles (NPs in grey) to enter the cell. Uncoated microparticles (below) rarely enter the cell. Image is from Stark *et al.*, 2011 (*61*)

promised (for example by a change in pH from extracellular environment to the cytosol) (*61*). In fact, such molecules give rise to electrosteric and electrostatic stabilization to overcome the thermodynamics that lead to aggregation (*11*). Another clear aspect of the capping layer is its influence on the mobility of NPs. This has important consequences on antimicrobial efficiency or molecular carrier properties. For this reason, also ChSeNPs are functionalized with organic molecules: ions, surfactants, or polar polymers are added in order to provide stability or additional properties to NPs (see below). A particularly interesting and challenging aspect of the capping layer is in fact its origin: it is clear that for BioSeNPs, the capping layer is formed during synthesis, transport and maturation by the microorganism. However, how the capping layer is formed, if the association with the single molecules is specific or just occurs by chance, is still under investigation. What is clear, is that some of these molecules have an affinity with the metalloid, as it is possible not only to functionalize a ChNP with specific molecules, but it is also possible to induce the formation of a capping layer just exposing ChNPs to a cell extract (or enzymatic extract) or adding it to the chemical synthesis reaction mixture.

1.4 Study of composition and role of the organic capping layer: state of the art

Many bacteria have been found to be able to convert selenite or selenate to elemental Se, and to synthesize SeNPs. Another possible way to biosynthesize SeNPs is by means of cellular or enzymatic extracts. Such solutions can be used directly to reduce selenate/selenite or added to a chemical synthe-

sis reaction mixture to influence the chemical synthesis and obtain different particles.

For example, in 2011 Dobias and colleagues identified proteins belonging to *E. coli* SeNPs capping layer and added one of such proteins to chemical synthesis mixture, obtaining a decrease in synthesized SeNPs size. The authors also exposed ChSeNPs to a Cell Free Extract (CFX) and observed that proteins also associate with pre-formed ChSeNPs (*37*).

Jain *et al.* observed that ChSeNPs exposed to extracellular components (mainly polysaccharides) or to BSA tend to be more stable and spherical in shape than ChSeNPs without any capping agent, which formed wires due to SeNPs destabilization (*11*).

Capping layer can also affect SeNPs properties. For example, Cheng *et al.* compared BioSeNPs synthesized by *Bacillus paralicheniformis* SR14 with BSA capped ChSeNPs for antioxidant properties. The SeNPs biosynthesized by the bacterium displayed a more complex capping (compared to just BSA) and better antioxidant properties (*62*). BioSeNPs are also more effective as antimicrobial agents than ChSeNPs, which is probably due to the presence of capping organic molecules. The mechanism(s) of the antimicrobial activity is, however, still unknown but is now under investigation (*30*, *63*).

Capping layer of Biogenic SeNPs

In order to understand which classes of molecules are associated to the surface of BioSeNPs, the capping layer has been analyzed mainly by spectroscopic techniques such as Fourier Transform Infrared Spectroscopy (FTIR) or Energy Dispersive X-ray Analysis (EDX) (*23*, *24*, *64*).

Moreover, proteomic analyses have been performed to identify proteins possibly involved in the synthesis or transport of SeNPs (*37*, *42*, *65*) with the hypothesis that they could remain attached to SeNPs surface following selenite reduction or growth and transport of the NPs outside the cell.

In 2015, Jain *et al.* studied the capping layer of SeNPs produced by granular sludge in anaerobiosis, confirming their hypothesis that molecules belonging to the EPS constitute the capping layer. EPS in such granular sludge is composed by proteins, carbohydrates, DNA and humic-like substances (*24*, *52*); the authors used FTIR to define chemical functional groups typical of carbohydrates and proteins. Additionally, Dubois reaction (phenol-sulfuric acid method) and Lowry method were used to verify the presence of carbohydrates and proteins, respectively (*24*).

Similarly, Cheng and colleagues analyzed EPS-SeNPs synthesized by *Bacillus paralicheniformis* SR14 and quantified proteins and carbohydrates using phenol-sulfuric acid method for carbohydrates and bicinchoninic acid assay (BCA) assay for proteins (*62*). Yang *et al.* analyzed SeNPs produced by a microbial consortium growing in a biofilm, using Scanning Transmis-

analyzed component(s)	origin	reference
proteins	*E. coli*	(*37*)
.	Se-respiring bacteria	(*42*)
.	microbial community	(*65*)
EPS	granular sludge	(*24*, *67*)
carbohydrates, proteins	*B. paralicheniformis* SR14	(*62*)
EPS, lipids	microbial community (biofilm)	(*66*)

Table 1.1: Capping layer components analyzed for BioSeNPs of different origin. EPS is defined as "extracellular polymeric substance" and includes proteins, carbohydrates, DNA and other biomolecular compounds

sion X-ray Microscopy (STXM) to localize SeNPs inside the biofilm without previous treatment: SeNPs were surrounded by EPS proteins and carbohydrates present in the biofilm structure. The authors also observed lipid association with SeNPs through STMX, suggesting a possible role for lipids in selenite reduction (*66*). An overview of components found and analyzed is given in Table 1.1.

Many authors propose a stabilizing role for the organic capping regardless of the involvement of these proteins (or other molecules) in the synthesis process of the NPs. Jain *et al.* (2015) hypothesize that the main function of capping EPS is to stabilize SeNPs (*24*).

A stabilizing effect was also evidenced by Piacenza *et al.*: after testing different recovery conditions for SeNPs produced by *B. mycoides* SeITE01 and *Stenotrophomonas maltophilia* SeITE02, it was observed that SeNPs tent to aggregate when associating molecules were removed. It was also observed, that part of the material tent to remain attached on SeNPs even after detergent or organic solvent treatment (*68*). A working hypothesis in this thesis is that while part of the material is strongly attached to SeNPs, other molecules could be in thermodynamic equilibrium with SeNPs, associating only under particular conditions. Dobias *et al.* demonstrated, that in the case of their biogenic nanoparticles, the protein fraction associated to *E. coli* SeNPs includes protein strongly attached to SeNPs. These proteins could not be removed even with a harsh detergent treatment (10% SDS at 100°C). Contrarily, proteins loosely associated to SeNPs were removed with milder treatments (*37*).

Construction of a capping for Chemically synthesized SeNPs

Stabilizing effect has also been explored by associating various molecules to ChSeNPs. Such artificial capping layer also makes it possible to study the role of single capping elements and their influence on SeNPs properties

(antimicrobial or antioxidant effects). Moreover, synthesis in the presence of organic molecules has been used to formulate models for SeNPs formation or stabilization. For example, Dobias *et al.* in 2011 synthesized ChSeNPs in the presence of an alcohol dehydrogenase that was identified strongly associating with *E. coli* BioSeNPs. The authors noticed a three-fold decrease in the average dimension of ChSeNPs when the protein was present during the synthesis. Moreover, ChSeNPs synthesized in the presence of an *E. coli* CFX resulted perfectly spherical compared to standard ChSeNPs and were reported to bind bacterial proteins. Presence of CFX in the synthesis also restricted size distribution (*37*).

To shed light on the possible role of associated EPS, Jain *et al.* compared BioSeNPs to ChSeNPs exposed or not to EPS or the protein BSA: ChSeNPs without any capping agent tent to form wires due to SeNPs destabilization. On the other hand, ChSeNPs exposed to EPS or BSA were spherical and more stable. The authors hypothesize that the EPS stabilizing effect is due to electrostatic repulsion and, partially, to steric hindrance (*11*). However the authors also demonstrate that the shape of SeNPs also affected stability: biosynthesized Se-Nanorods were surrounded by a corona of EPS, mostly composed of proteins and carbohydrates, but the stabilizing effect of EPS was stronger for NPs than for Nanorods (*67*).

Xiao and colleagues added EPS from the microorganism *Cordyceps sinensis* to ChSeNPs reaction mixture, obtaining EPS-conjugated SeNPs (EPS-SeNPs). They proposed a model for EPS-SeNPs formation: Se is attracted by terminal hydroxyl groups present in large number on the surface of EPS. Small clusters of Se atoms end up forming Se nuclei, which grow to form SeNPs by aggregation (Figure 1.10). The authors hypothesize that EPS stabilizing effect is due to high viscosity: EPS molecules trap SeNPs, preventing further aggregation and precipitation (*23*). Focusing on a single EPS molecule, Zhang *et al.* demonstrated in 2003 that synthesis of ChSeNPs in the presence of polysaccharides increased SeNPs stability: obtained SeNPs were monodispersed and stable in solution up to 6 months (*59*).

Addition of an artificial capping layer has also been used to analyze SeNPs properties such as antimicrobial and antioxidant activities. Prateeksha *et al.* synthesized SeNPs using polyphenols extracted from honey in order to obtain honey polyphenol-conjugated SeNPs (SeNPs@HP) as a drug delivery vector against *Pseudomonas aeruginosa* biofilms. SeNPs@HP proved to be more effective to inhibit biofilm formation than ChSeNPs and HP alone (*69*). In this case, reduction of selenite to elemental Se and SeNPs formation is due to redox active polyphenols, that remain on the surface of final SeNPs (Figure 1.11).

Palomo-Siguero and Madrid recently demonstrated that the toxicity of SeNPs is strongly affected by coating agents (*60*): ChSeNPs were synthesized in the presence of different stabilizers including chitosan and a non-ionic surfactant. So obtained SeNPs were tested against *Lactobacillus del-*

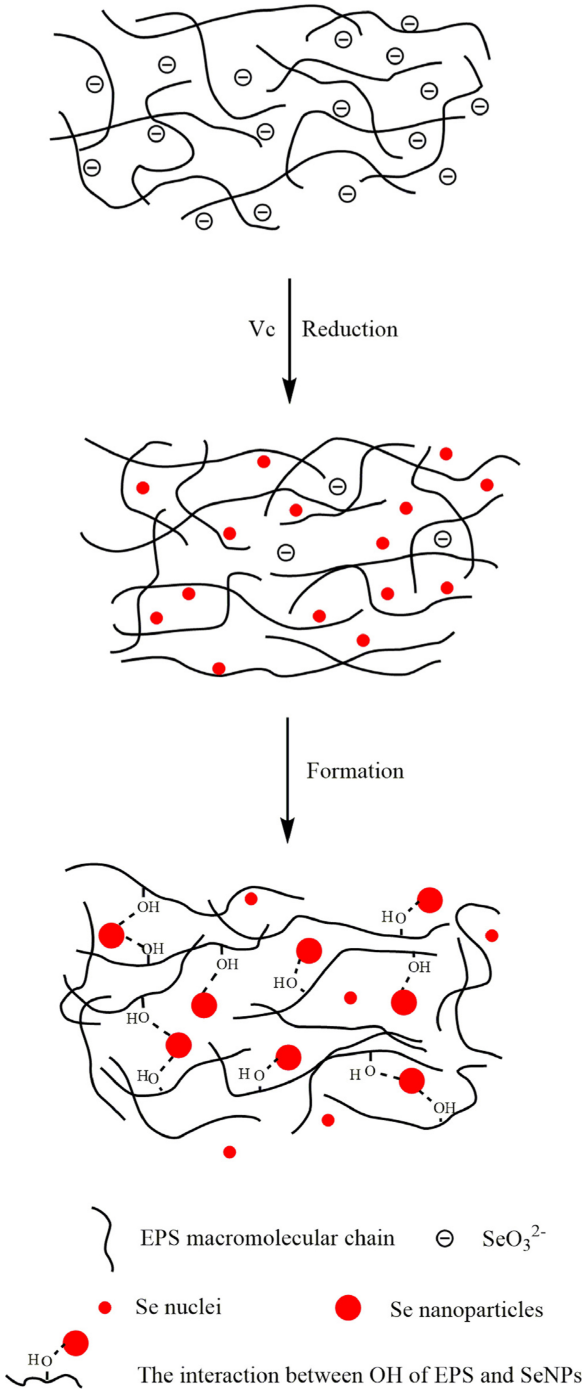

Figure 1.10: Scheme for EPS-SeNPs synthesis: small clusters of Se atoms end up forming Se nuclei, which grow to form SeNPs by aggregation. EPS molecules, characterized by high viscosity, trap SeNPs, preventing further aggregation and precipitation. Image is from Xiao *et al.*, 2017 (*23*)

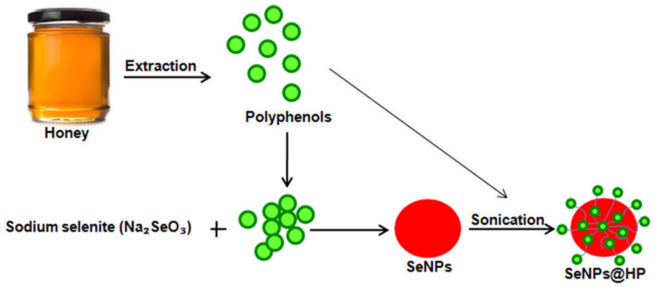

Figure 1.11: Scheme of SeNPs@HP synthesis: SeNPs are synthesized using polyphenols extracted from honey (HP). Reduction of selenite to elemental Se and SeNPs formation is due to redox active polyphenols, that remain on the surface of final SeNPs, forming SeNPs@HP. Image is from Prateeksha *et al.*, 2017 (*69*)

Chemical composition analysis (mg/ml)			
Samples	Total sugar	Protein	Se content
EPS-BioSePs	0.102	0.095	0.186
ChSePs	—	0.133	0.192

Table 1.2: Quantification of carbohydrates and proteins for EPS-SeNPs and BSA-ChSeNPs. Table is from Cheng *et al.*, 2017 (*62*)

brueckii subsp. *bulgaricus* LB-12, a strain able to metabolize inorganic Se. Transmission Electron Microscopy (TEM) observations suggest that chitosan-capped SeNPs enter the cells without damaging the cell wall, and about 90% of Se is metabolized by the cells into organic Se-compounds. On the other hand, capping ChSeNPs with detergent leads to cell death due to cell wall disruption and only about 10% of Se from these ChSeNPs is metabolized by the cells. The authors concluded, that toxicity of SeNPs is mainly due to capping molecules rather than SeNPs themselves. Finally, Cheng and colleagues analyzed EPS-BioSeNPs synthesized by *Bacillus paralicheniformis* SR14 (Figure 1.12) for coating composition and different antioxidant properties compared to BSA-ChSeNPs. Presence of the EPS coating leads to better antioxidant properties (*62*). The authors quantified and compared Se content and total carbohydrates and proteins of two samples: EPS-SeNPs and ChSeNPs synthesized in the presence of BSA. Protein content is higher in the case of BSA-ChSeNPs, where carbohydrates are obviously not present (Table 1.2). Components forming the artificial capping layer and study aims are summarized in Table 1.3.

In conclusion, given the importance of the capping layer, many studies so far attempted to determine its composition, especially from a proteomic point of view. Proteins, EPS-like molecules, carbohydrates, humic acids and lipids have been found associating to BioSeNPs by different microorganisms. Attempts have been made to quantify proteins and carbohydrates. One of

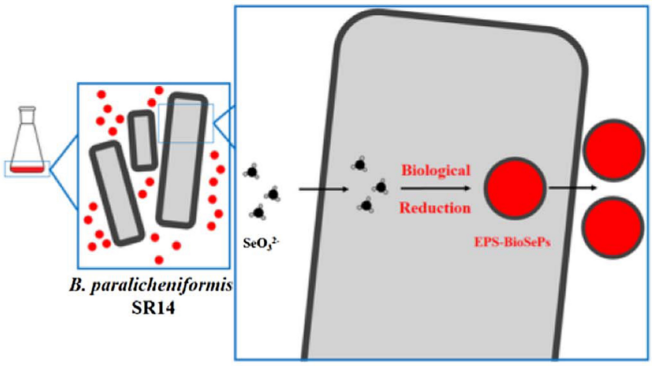

Figure 1.12: Synthesis of EPS-SeNPs by *B. paralicheniformis* SR14. Reduction of selenite and biosynthesis by the bacterium lead to the formation of SeNPs associated to EPS molecules (EPS-BioSeNPs). Image is from Cheng *et al.*, 2017 (*62*)

component(s) added to ChSeNPs	effect	reference
alcohol-dehydrogenase	stabilizing (dimension decrease)	(*37*)
EPS from granular sludge, BSA	stabilizing	(*24*)
polysaccharides	stabilizing	(*59*)
EPS from *Cordyceps sinensis*	stabilizing; synthesis model	(*23*)
honey polyphenols	drug delivery; synthesis model	(*69*)
chitosan, surfactant	antimicrobial	(*60*)
BSA	comparison of antioxidant properties; synthesis model	(*62*)

Table 1.3: Components added during ChSeNPs synthesis and analyzed effects

the main problems in quantifying the capping layer components is the quantity of SeNPs to refer to. In fact, SeNPs extracted from bacterial cultures are suspended in the liquid media, not dissolved, and quantification analyses were made directly on the extracted suspension (*62*) (Table 1.2). Moreover, no study so far has quantified the capping layer components directly on SeNPs.

Another concern is the structure of the capping layer: it is still unclear, what kind of association exists between the extracted SeNPs and the organic material. Part of this material could just co-purify with SeNPs, part could be strongly bound and part weakly, or it could be bound not to the Se surface, but to other molecules. Also, SeNPs could in some cases be surrounded by an EPS-like structure. However, some authors demonstrated that some molecules are more strongly bound than others (*37*).

Finally, understanding what kind of molecules constitute the capping layer could help understanding the biosynthesis mechanism, or give information about transport and maturation of BioSeNPs. Moreover, composition could be strain specific or community specific, providing information about one strain in particular. However, the specificity of the SeNPs-capping layer molecules bound is still under investigation, and many molecules could bind BioSeNPs during maturation processes or extraction procedures, making it challenging to understand which ones are actually involved in biosynthesis mechanisms. Understanding the capping layer composition can be the first step to investigate the biosynthesis of SeNPs and hypothesize some models. In this case, proteomic analysis is probably one of the most informative techniques to understand involved pathways.

1.5 Microorganisms studied in this thesis

In this study, five microorganisms are utilized, which are able to synthesize BioSeNPs: Gram-positive *Bacillus mycoides* SeITE01 and *Lysinibacillus* R1E and Gram-negative *Stenotrophomonas maltophilia* SeITE02, *Achromobacter* sp. R2A and *Ensifer* sp. R2D.

R2A, R2D and R1E strains were isolated from a selenate-contaminated soil in Hungary and tested for resistance to Se and Te oxyanions. Finally, the strains have recently been identified in our group through 16S rRNA gene sequencing.

R2A, identified as *Achromobacter* sp., a Gram-negative aerobic motile rod, was able to grow in the presence of 100mM selenite and 100µM tellurite.

R2D, identified as *Ensifer* sp., a Gram-negative nitrogen-fixing rhizobium, could tolerate up to 100mM selenite in the medium, even if little growth was also observed when exposed to 150mM selenite. Similarly, it could grow in the presence of 650µM tellurite, with a little growth also observed at 700µM.

For R1E, identified as *Lysinibacillus* sp., a Gram-positive rod, growth was observed in the presence of 75mM selenite. It is able to tolerate 100µM tellurite in the medium, but with very little growth. It can however grow in 10µM tellurite.

All of the three strains isolated from selenate-contaminated soil are able to produce BioSeNPs (unpublished data).

Both SeITE01 and SeITE02 have been isolated from the same environment, the rhizosphere of Se hyperaccumulator plant *Astragalus bisulcatus*, and are able to synthesize SeNPs (*10*, *70*).

S. maltophilia is an ubiquitous Gram-negative, rod-shaped, aerobic and non fermentative Gamma-proteobacterium, found in the rizosphere of many plants (e.g. wheat, potato, cucumber, maize). The strain SeITE02 is able to grow in the presence of up to 50mM selenite and synthesize SeNPs (*70*).

Overall, SeNPs synthesis mechanism is still unclear, but synthesis localization (*70*), interaction with nitrite reduction pathway, role of GSH (*3*) have been investigated for this strain. A Painter-type reaction was finally hypothesized to occur. However, a concomitant reduction pathway involving an alcohol dehydrogenase (AdH) was also investigated (*15*). Moreover, since selenite was not completely reduced to Se^0, other pathways such as volatilization and assimilation could also be present.

Formation of SeNPs from Se^0 was investigated as well: TEM and Scanning Electron Microscopy (SEM) observations led to the hypothesis of a release mechanism from the cells followed by a nucleation mechanism, resembling Ostwald ripening mechanism, once SeNPs are secreted in the extracellular matrix. Presence of EPS-like material associated to BioSeNPs was also evidenced, with FTIR analysis indicating the presence of N-H, C-H, C-O, C-N, C=O and S-H bounds (*15*).

To date the SeNPs from SeITE01 and SeITE02 strains have been investigated mainly for antimicrobial activity, especially against biofilms (*30*, *31*, *63*). It has been observed, that BioSeNPs are more efficient as an antimicrobial agent compared to ChSeNPs and to oxyanion selenite. It is presently unknown if the presence of the organic molecules on the surface of BioSeNPs could play a role in this activity.

The high effectiveness of SeITE01 and SeITE02 BioSeNPs as antibacterial agents and long time dependent stability of BioSeNPs in aqueous solution (at least 3 months) is believed to be due to the organic capping layer provided by the bacteria.

Of the five strains here analyzed, SeITE01 and SeITE02 pathways are currently under investigation (see below), and a possible model for SeNPs synthesis by SeITE01 has already been proposed (*16*).

1.5.1 *Bacillus mycoides* SeITE01: origin, isolation and features of SeNPs synthesis

B. mycoides SeITE01, isolated from Se-hyperaccumulator plant *Astragalus bisulcatus* (*10*), is a Gram-positive, aerobic rod belonging to *Firmicutes* phylum and part of *Bacillus cereus sensu lato* group together with *B. cereus*, *B. anthracis*, *B. thuringiensis*, *B. pseudomicoydes* and *B. weihenstephanensis* (*16*, *71*). The name "mycoides" is due to its typical fungal-like growth. SeITE01 is able to grow in the presence of up to 25mM selenite and to produce nearly spherical, 50 to 400nm SeNPs, depending on incubation time, but overall inhomogeneous in size.

Synthesis mechanism is still under investigation. Lampis *et al.* observed that selenite negatively affected SeITE01 growth rate, as the culture reached stationary phase more rapidly when exposed to selenite than when not exposed. However, it has been shown that selenite reduction started without a lag phase, and thus hypothesized that reduction pathway may be constitutive (*16*).

On the other hand, a delay of 24h was observed between the reduction of selenite and the appearance of Se^0. According to models listed in Section 1.2, GSH reacts with selenite forming an intermediate selenodiglutathione (GS-Se-SG), which is later metabolized by GSH reductase and TR (*2*, *36*). Thus, it was hypothesized that the reduction mechanism could involve a Painter-type reaction with thiols: first, a selenium-diglutathione intermediate would quickly form, then the intermediate would be more slowly converted into elemental Se.

To further clarify this mechanism, an activity assay was performed on native proteins extracted from cytosolic and periplasmic compartments, and from the supernatant of the culture, to localize selenite reduction activity (*16*). Since selenite reduction could occur in the EPS matrix, EPS fraction was assayed as well. The appearance of a red color (typical of amorphous Se^0) was observed in the membrane and supernatant fractions after the addition of NADH as electron donor, while no activity was evidenced in EPS fraction. On the other hand, only little activity was observed in the cytosolic fraction. The authors proposed, that the main pathway for selenite reduction could involve proteins secreted by the cell or at the membrane/cell wall level. However, at cytoplasmic level, reduction was proposed to occur through a Painter-type reaction as ancillary mechanism.

Another hypothesis could be that selenite is reduced at cytoplasmic level and then released after cell lysis. In Figure 1.13 all pathways proposed by Lampis *et al.* are schematized.

TEM observation showed the presence of electron-dense particles mainly extracellularly (and rarely intracellularly) after 12 and 24h of cultivation with 2.0mM selenite. Such SeNPs also seemed to be embedded in EPS-like material. Interestingly, lysed cells or cell-like structures without internal

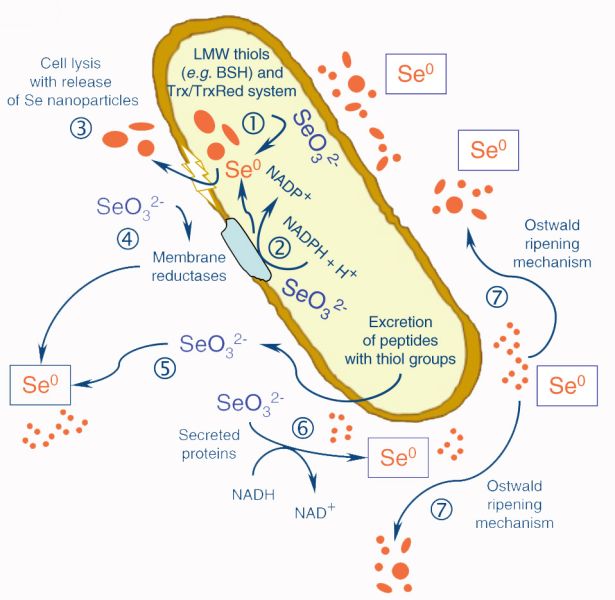

Figure 1.13: Proposed model for SeNPs synthesis by *B. mycoides* SeITE01: (1) Cytosolic precipitation of selenite as Se^0 nanoparticles due either to the reaction with low molecular weight thiols including bacillithiol (BSH) or with the Trx/TR system. (2) Intracellular selenite reduction and formation of SeNPs as a consequence of activity of membrane reductases. (3) Release of intracellularly generated SeNPs after cell lysis. (4) Membrane reductases may even catalyze extracellular selenite precipitation. (5) Peptides and other compounds carrying thiol groups may be released from the bacterial cell and directly react with selenite. (6) NADH dependent reductases mediating selenite precipitation (7) Nascent SeNPs are inherently unstable due to their high surface area and therefore tend to grow and increase their average size. Figure and description are from Lampis *et al.*, 2014 (*16*)

organization were rarely observed, while effects of selenite stress were evidenced as presence of hydroxibutyrate granules and a slight increase of cell length. SEM observation showed presence of SeNPs after 6h (exponential phase of growth), as spherical or oblong particles from 50 to 100nm in size, but overall inhomogeneous. Average dimension was observed to increase to 50-400nm after 48h of growth (stationary phase), leading to the hypothesis of an Ostwald ripening-like growth mechanism (Figure 1.13, reaction number 7).

Beside microscopy observations, presence of EPS-like material and the proposed model for SeNPs biosynthesis, composition of the capping layer is still under investigation. Further analyses are necessary to find out which specific molecules associate to SeNPs produced by this strain in order to clarify both the synthesis model and eventually the role of such molecules in SeNPs application as antimicrobial agent (see below).

1.5.2 Application of SeITE01 and SeITE02 SeNPs as antimicrobial agents

Capping layer seems to contribute to the efficiency of BioSeNPs as antimicrobial agent. In 2017, Piacenza *et al.* tested both ChSeNPs obtained by different protocols and SeITE01 BioSeNPs against planktonic cells or biofilms of *Pseudomonas aeruginosa* NCTC 12934 and *Staphylococcus aureus* ATCC 25923. SeITE01 BioSeNPs, here called Bio Se-NEMO-S (Spherical biogenic Se-Nanostructures Embedded in Organic material) to stress the presence of the capping layer, were observed to be more efficient than ChSeNPs as antimicrobial agent. Growth of both *P. aeruginosa* and *S. aureus* was in fact inhibited by Bio Se-NEMO-S at the concentration of 0.3125mg/ml using SeNPs synthetized in 24h, and of 0.078mg/ml for 6h-SeNPs. Efficiency was the same for planktonic and biofilm forms, the most resistant form of bacterial growth. Since Bio Se-NEMO-S differs from ChSeNPs for the presence of the associated organic material, this was proposed to be responsible of Bio Se-NEMO-S high efficiency as antimicrobial agent (*63*).

SeITE02 SeNPs were also tested against *P. aeruginosa* PAO1, *S. aureus* ATCC 25923 and *E. coli* MJ109 strains in both planktonic and biofilm forms. SeNPs were effective in killing 100% of bacteria after 4h of exposure at the concentrations of 125mg/l for *E. coli* and 250mg/l for *P. aeruginosa* and *S. aureus*, regardless the growing form (*30*).

Finally, the effects of ChSeNPs and BioSeNPs from both strains were tested against *P. aeruginosa* PAO1, *P. aeruginosa* strains isolated from clinical samples and two strains of *Candida*: *C. albicans* and *C. parapsilosis*. Moreover, as NPs are a promising technology for treatment of antibiotic-resistant microorganisms, SeNPs effect was investigated on human dendritic cells and fibroblasts. No cytotoxic effect was observed on investigated human cell lines.

SeNPs from both strains and ChSeNPs showed a Minimum Inhibitory Concentration (MIC) of 128mg/l against *P. aeruginosa* PAO1. Contrarily, when tested against *P. aeruginosa* and *Candida* strains from clinical samples, MIC values tent to differ. For SeITE01 SeNPs, MIC values ranged from 32 to 512mg/l for *P. aeruginosa* strains, and 512mg/l for *Candida* strains.

For SeITE02 SeNPs, MIC values ranged from 8 to 512mg/l for *P. aeruginosa* and from 256 to 512mg/l for *Candida* strains. ChSeNPs were much less effective against such strains, with MIC values ranging from 128 to more than 512mg/l for *P. aeruginosa* and more than 512mg/l for *Candida*. Biofilm synthesis was also inhibited by BioSeNPs for both bacterial and yeast strains. BioSeNPs efficiency against yeasts could also be explained by the presence of the capping layer, which could possibly interact with the yeast outer wall layer (*31*).

Biofilm synthesis by the same isolates was inhibited by 70-90% in the presence of 50-100 mg/l BioSeNPs for the most sensitive strains and by 70% in the presence of $\geq$250mg/l BioSeNPs for the most resistant ones. On the other hand, ChSeNPs were only active between 250 and 500mg/l (*31*).

In conclusion, BioSeNPs by both SeITE01 and SeITE02 showed a high efficiency as antimicrobial agents against pathogenic strains. Interestingly, such BioSeNPs are highly effective also as antibiofilm agents. Moreover, BioSeNPs were observed to be overall more effective than ChSeNPs. Since the major difference between the two types of SeNPs is the presence of the capping layer, this is probably involved in BioSeNPs antimicrobial activity, likely through interaction with the pathogens cell wall components or even biofilm matrix.

1.6 General objectives

Concluding, this study focuses on the characterization of the capping layer of BioSeNPs and subsequent hypothesis on its role in and possible synthesis pathways for the nanomaterials. The thesis is structured in two main parts.

In the first part the objective is to characterize, in terms of composition, the organic capping layer of BioSeNPs synthetized by Gram-positive *Bacillus mycoides* SeITE01 and *Lysinibacillus* R1E and Gram-negative *Stenotrophomonas maltophilia* SeITE02, *Achromobacter* sp. R2A and *Ensifer* sp. R2D.

Study of capping layer composition would in fact be of paramount importance to clarify the possible involvement of capping molecules in both synthesis process and in determining the efficiency of SeNPs as antimicrobial agent. Main components will be analyzed through a quantification approach. Moreover, effects of different treatments on main components will be investigated in terms of change in components ratios and effects on SeNPs stability.

In previous studies, carbohydrates content has been investigated by Jain

et al. and Cheng *et al.*, using Dubois reaction, while proteins has been quantified using Bradford or BCA methods (*72*, *73*). For both studies, these two components have been quantified starting from a solution of SeNPs, which makes it possible to compare different samples, but does not give any information about the quantity of such molecules on the surface of SeNPs. Cheng et al. compare proteins and carbohydrates content to elemental Se content of SeNPs solutions, but no study so far has ever quantified capping layer molecules per mg of SeNPs. Such quantification would be extremely useful to compare SeNPs biosynthesized by different microorganisms, particularly when there are significant differences in SeNPs properties or even between microorganisms themselves. In this study, in order to characterize BioSeNPs by the previously studied SeITE01 and SeITE02, and the recently isolated R2A, R2D and R1E, biomolecular quantification assays are proposed, to quantify total carbohydrates, protein and lipid contents directly on and/or associated with BioSeNPs. Such assays have been developed to make it possible to compare capping layer compositions of BioSeNPs produced by different microorganisms. Moreover, being performed directly on SeNPs and not on solutions, quantifications can be expressed in terms of carbohydrates, proteins and lipids content per mg of BioSeNPs, despite different BioSeNPs recovery yields being different for various microorganisms. Also, elimination of the molecules extraction step from SeNPs prior to analysis makes it possible to avoid underestimation of capping components, as even very stringent treatments (e.g. 10% SDS, 100°C) cannot completely recover all the organic material associated to SeNPs (*37*).

In the second part, the study focuses on further investigating the synthesis process in BioSeNPs by *B. mycoides* SeITE01 by proteomic and microscopy approaches. Proteins can be in fact very informative molecules about possible synthesis pathways and microscopy makes it possible to visualize SeNPs during synthesis steps. A new hypothesis will be formulated about SeNPs secretion by the bacterium considering the current model for SeITE01 and the results of proteomic and microscopy study.

Chapter 2

Introduction Summary

2.1 What is known about the capping layer

Differently from ChSeNPs, BioSeNPs display a surrounding layer of organic molecules, associating to SeNPs during synthesis and/or maturation. Many authors agree that this organic layer plays an important role in SeNPs stabilization (*23*, *24*, *37*, *74*). Biomolecules such as proteins, carbohydrates, DNA, humic-like substances (*24*, *52*) and lipids (*66*) have been identified by spectroscopic techniques (*23*, *37*, *42*, *64*, *65*) and similarities to EPS composition was found for some strains (*24*, *52*).

Quantitative analyses were also performed on carbohydrates and proteins, but without distinction between molecules associated to SeNPs or present in the supernatant (*24*, *62*). It is also evident that some proteins bind more strongly to SeNPs than others, and that different denaturing treatments using detergents and high temperatures could only remove part of the associated proteins (*37*). Associated molecules also provide additional properties to SeNPs, such as antimicrobial or antioxidant effects: the addition of an artificial capping layer to ChSeNPs provides such particles more stability and additional properties (e.g. antioxidant) (*23*, *60*, *62*).

2.2 Open questions

- How does the capping layer originate?
- Which molecules do constitute the capping layer?
- Does composition change depending on the strain?
- Do molecules associate specifically or by chance to SeNPs?
- Do all molecules associate with the same strength to SeNPs?

- What happens to SeNPs if the capping layer is partially or completely removed?

2.3 What is new in this research

In the first part of this thesis, quantitative assays are proposed for a routine use in order to make it possible to quickly compare samples from different strains, culture conditions and treatments. Such assays can be performed directly on SeNPs and allow distinctions between strongly and weakly bound molecules. Different strains were used to biosynthesize SeNPs in order to investigate the influence of the strains in capping layer composition. SeNPs were also treated with detergents to partially remove the capping layer: together with components quantification, SeNPs stability was also monitored. Finally, a new model was proposed to explain different responses to detergent treatments in terms of composition of the layer and stability of SeNPs.

In the second section of this thesis, the origin and specificity of proteins constituting the capping layer of SeNPs synthesized by *B. mycoides* SeITE01 are investigated. The current model of biosynthesis by this strain is discussed in context of proteomic and microscopy analysis.

Part II

Biogenic SeNPs capping layer characterization

Chapter 3

Materials and methods

3.1 Bacterial strains

Microorganisms used in this thesis were previously isolated as follows. R2A, R2D and R1E were isolated from a selenate-contaminated soil in Hungary through enrichment culture in liquid R2A-medium added with 10mM sodium selenite. R2A and R2D strains were isolated from soil contaminated with 18ppm sodium selenate, while R1E was isolated from a soil added with 6ppm sodium selenate. After isolation, the strains were passed in solid culture in the presence of 10mM selenite and stored at 4°C. Minimum inhibitory concentration of sodium selenite was determined by cultivating the strains in the presence of 5 to 150mM selenite. For identification, 16S rRNA was sequenced. SeITE01 and SeITE02 have been isolated from the rhizosphere of Se hyperaccumulator plant *Astragalus bisulcatus* as described in (*10*, *70*).

3.2 Bacterial strains cultivation and SeNPs synthesis

The five bacterial strains were grown aerobically at 27°C in Nutrient medium added with Na_2SeO_3 on a rotary shaker (150rpm). Production of BioSeNPs was visible as a brick-red color after 24h for SeITE01, SeITE02, R2A and R2D; after 72hfor R1E. Culture medium was added with 0.5mM Na_2SeO_3 for SeITE02; 2mM Na_2SeO_3 for SeITE01 and R2D; 5mM Na_2SeO_3 for R2A and R1E.

3.2.1 Extraction method

Cells were pelleted by centrifugation at 12000xg for 10min (Sorvall RC-5C Plus centrifuge, SS-34 rotor), washed twice with 0.9% NaCl and resuspended in ice cold 1.5M Tris-HCl pH 7.4. Cells were then sonicated in ultrasonic processor UP50H (Dr. Hielscher GmbH) (7 cycles of 30sec sonication + 30sec

rest in ice). Cells and cell debris were precipitated through centrifugation at 4300xg, 4°C for 20min (Sorvall Super T21 centrifuge, SL-50T rotor) and discarded. In order to separate BioSeNPs from the lysate, the supernatant was fractionated by mixing with octanol (2ml octanol every 5ml supernatant). The mixture was stirred 10sec on a vortex and centrifuged for 5min, 480xg. SeNPs migrated to aqueous phase overnight at 4°C. Aqueous phase was collected and centrifuged 18000xg, 20min. Supernatant was discarded, the pellet was washed once, then resuspended in sterile water. For quantification, SeNPs were pelletted in a 2ml tube by centrifugation (16000xg, 20min) and air-dried under the chemical hood. The 2ml tube was then weighted and SeNPs dry weight was determined subtracting the weight of the empty tube. SeNPs pellet was then immediately resuspended in sterile water.

3.3 SeNPs treatments

Two treatments were performed at the end of the standard extraction. BioSeNPs were precipitated at 16000xg for 30min and resuspended either in 500µl 2% Triton X-100 or 1ml 10% SDS. Samples resuspended in 2% Triton X-100 were shaken for 20min at 27°C. The samples were then centrifuged at 18000xg for 20min, and the pellet was washed twice and resuspended in sterile water. Samples resuspended on 10% SDS were treated at 100°C for 30min, then centrifuged at 18000xg for 20min and the pellet was washed twice and resuspended in sterile water. All samples were stored at 4°C.

3.4 SeNPs characterization

3.4.1 Dynamic Light Scattering (DLS) and Z-potential analyses

Samples were analyzed with Malvern Zetasizer Nano Series instrument for Hydrodynamic diameter (Dh), Polydispersity index (Abs) and Zeta-potential characterization. Dh and PdI values were obtained using the software provided by Malvern with the instrument. All the samples were then resuspended in sterile water and transferred to a disposable cuvette (10 mm path length). Zeta-potential at pH 7 was measured at 25°C in sterile water using the Malvern software (*68*).

3.4.2 Capping composition analyses

Total carbohydrates content assay

Total carbohydrates were quantified using a modified protocol from Masuko *et al.* (2005) (*75*). Calibration curve was based on Chow and Landhäusser

(2004) (*76*) work: first, GFG solution was prepared as a 1:1:1 glucose, fructose and galactose mixture. Then, 50µl of 0 to 10µM GFG (0 to 9000 ng/well, 0 to 180 ng/µl) and 50µl of samples and blanks were added in a 96-well plate. In order to minimize interference of selenium, different calibration curves were set based on background absorbance. Background absorbance was read at 490nm and ChSeNPs were added to calibration curves to reach the same values. 150µl of sulfuric acid were added to each well, quickly followed by 30µl of 2% phenol. The plate was incubated 5min at 90°C in a static water bath and cooled for 5min at room T. Absorbance was measured at 490nm. All samples were analyzed in triplicate. For further details, see Appendix A.

Total protein content assay

Total proteins were quantified using a modified protocol from Minamide and Bamburg (1990) (*77*): 8µl of samples, blanks and BSA standard solutions (0 to 2µg/µl BSA) were applied on 1x1cm squares pencil drawn on a Whatman sheet. The sheet was then rinsed in absolute methanol for 20sec, air-dried, placed in 200ml of staining solution (0.5% Coomassie Brilliant Blue G in 7% acetic acid) and gently agitated for 30min at room T. Subsequently, the sheet was placed in 200ml of destaining solution (7% acetic acid) for 30min/3h in order to decrease background, and air-dried. Squares were cut and placed in eppendorf tubes and mixed on a vortex with 1ml of extraction buffer (66% methanol, 33% water, 1% ammonium hydroxide). Samples were incubated at room T for 5min, then vortexed again. 200µl of each sample, blank and BSA standard were transferred to a 96-well plate. Absorbance was measured at 595nm. All samples were analyzed in triplicate. For further details, see Appendix A.

Total lipid content assay

Total lipid content was quantified using a modified protocol from Cheng *et al.* (2011) (*78*). Oleic acid was chosen as a standard for lipids and solubilized in chloroform:methanol 2:1 (calibration curve: 0 to 100 µg/well). Lipids were extracted from SeNPs: chloroform:methanol 2:1 was added and samples were shaken at 150rpm for 30min. SeNPs were subsequently pelleted at 18000xg 20min and discarded. The solvent containing the extracted lipids (or oleic acid for the calibration curve) was pipetted in a 96-well plate. Solvent was evaporated under chemical hood, leaving extracted lipids in the wells. 100µl of sulfuric acid were immediately added for each well. Microplate was heated at 90°C for 20min in a static water bath and cooled for 2min in ice water. 50µl of VP reagent (0.2mg/ml vanillin in 17% phosphoric acid) were added for each well. Microplate was incubated at room T for 10 min. Absorbance was measured at 540nm. All samples were analyzed in triplicate. For further

details, see Appendix A.

Chapter 4

Results and discussion: Capping layer characterization

4.1 Summary

- BioSeNPs are associated to EPS-like molecules, here referred as "capping layer"
- Composition of such layer is still under investigation
- It is likely that associated molecules have a stabilizing effect on BioSeNPs

4.2 Aim of the project

In this study, in order to characterize BioSeNPs synthesized by five different bacterial strains, biomolecular quantification assays are proposed, to quantify total carbohydrates, protein and lipids contents directly on and/or associated with BioSeNPs. Such assays have been developed to make it possible to compare capping layer compositions of BioSeNPs produced by different microorganisms. Moreover, such assays have been used to investigate the effect on BioSeNPs of treatments meant to remove the capping layer. Finally, effect of the capping layer removal on BioSeNPs stability has been investigated.

4.3 Experimental design

Quantification assays have been designed mainly as a tool for screening BioSeNPs produced by different microorganisms, in this case the Gram-positive *B. mycoides* SeITE01 and *Lysisnbacillus* R1E, and the Gram-negative

S. maltophilia SeITE02, *Achromobacter* sp. R2A and *Ensifer* sp. R2D. It was hypothesized, that the produced BioSeNPs will have different capping layer composition in terms of quantity of molecules belonging to different classes. Since specific molecular identification of proteins, carbohydrates and lipids is challenging, time consuming, and expensive; quantification was chosen as a more realistic parameter for sample comparison. Moreover, with the prospect of also comparing metal NPs synthesized by other microorganisms, quantification assays have been developed aiming to the following characteristics:

- Sensitivity to µg level of sample
- Cost effectiveness
- Quick response
- Possibility to compare multiple samples at the same time

Sensitivity is of paramount importance, as SeNPs and NPs in general are precious samples and assays should be projected in order to use as less material as possible. Therefore, nano-scale analysis requires sensitivity at least to the µg order. Another important characteristic for the assays is cost-effectiveness: techniques such as FTIR, EDX or chromatographic techniques are widely used to collect data about capping layer molecular figureprints, but are expensive, making it unrealistic to compare multiple different sets of SeNPs produced by different organisms or differently treated on a routine basis. Of course, such expensive techniques would be ideal to further investigate samples once the microbial protocol is defined and established.

Finally, to compare different samples, the assay would be ideally quick and have the possibility to process many samples and replicas at the same time. A microplate assay has been considered as the ideal format to satisfy all previous requisites. Such assays have been optimized starting from microplate versions of sensitive and cost-effective protocols, such as phenol-sulfuric acid method (Dubois reaction) for carbohydrates, Coomassie binding for proteins and sulfo-phospho-vanillin reaction for lipids. All of these methods are based on stable colorimetric reactions and make quantification possible through a simple absorbance read. Moreover, very short time is needed to perform the assays.

Challenges in analyzing other capping components

In previous studies, carbohydrates and proteins have been investigated by EDX or FTIR analyses or quantified after a purification step. Other articles analyze the effect of single components on the chemical synthesis of SeNPs (*23*, *59*, *60*), but do not quantify the associated molecules.

Components such as carbohydrates, proteins, lipids, nucleic acids and humic-like substances have been analyzed in previous studies. Here only carbohydrates, proteins and lipids are quantified in order to compare the five strains BioSeNPs. The main challenges in analyzing BioSeNPs components were:

- The nano-scale of the samples required a very sensitive technique, in order to detect less than 1µg of material
- The intrinsic variability of the samples, mainly due to the use of microorganisms (SeNPs yeld variability from batch to batch, and depending on culture and extraction methods)
- The interference of red amorphous Se in colorimetric measurements

Methods so far used for protein quantification, such as Bradford assay or BCA assay are sensitive techniques, but can lead to protein content overestimation (see Section 6.3.4). Consequently, a solid-support assay based on protein-Coomassie staining bound has been chosen: such indirect quantification avoids Se interfering effect on absorbance reads.

As for carbohydrates, the most used method for quantification is based on Dubois reaction, but it is usually used to verify the presence of carbohydrates, or to quantify carbohydrates in a SeNPs solution (*24*, *62*).

On the other hand, other components such as lipids, DNA and humic-like substances have been identified as components of EPS (*24*), but have never been quantified. In the case of DNA, interference of Se with absorbance made the quantification impossible, while a protocol has been developed for lipids.

4.3.1 Optimization of assays for different components quantification

Optimization of an assay for total carbohydrates content quantification

Total carbohydrates content was assayed through a protocol based on so-called Dubois reaction or phenol-sulfuric acid method (*79*). Such method is easy and reliable, and has been optimized for 96-well plates measurements. Reagents needed for Dubois reaction are also inexpensive (*75*).

Briefly, carbohydrates are treated with concentrated sulfuric acid (acid hydrolysis), then phenol is added for color development. Carbohydrates concentration can be detected after incubation at 90°C by reading absorbance at 490nm.

Detailed protocol can be found in Appendix A

Standard carbohydrates for calibration curve, linearity range and Se interference have been optimized for this assay.

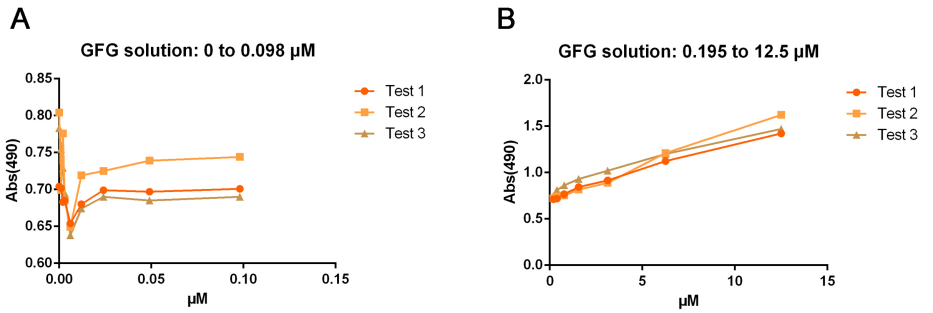

Figure 4.1: Correlation between carbohydrates concentration and Abs_{490}: linearity ranges from 0.195µM to 12.5µM (B), while below 0.098µM, correlation is non linear (A)

The issue with carbohydrates standard consisted in different carbohydrates (e.g. glucose, fructose, sucrose) resulting in different calibration curves. Chow and Landhäusser (*76*) further optimized the microplate Dubois reaction method using a mixture of glucose, fructose and galactose in equal amounts ("GFG" solution). Glucose, fructose and galactose are in fact produced during acid hydrolysis for any kind of carbohydrates samples, making GFG solution a good approximation for any kind of carbohydrates sample, especially when carbohydrates composition is unknown.

Linearity range was investigated for the chosen standard to determine the limit of quantification: concentrations from 0 to 12.5µM/well (corresponding to 11µg/well) were plotted versus Abs_{490}. As shown on Figure 4.1, linearity range is from 0.195µM to 12.5µM, while below 0.195µM (0 to 0.098µM), correlation is non linear. Therefore, calibration curve for subsequent analyses was set from 0.2 to 10µM GFG (corresponding to 0.18 to 9µg/well).

Interference was an issue for carbohydrates assay. ChSeNPs were used to test interference by adding to samples containing known concentrations of carbohydrates and performing the assays. Adding ChSeNPs to the carbohydrates assay strongly influenced the absorbance values, making it impossible to correctly quantify samples carbohydrates content when referring to the standard curve without ChSeNPs. However, the linearity range was not influenced by the presence of ChSeNPs. In Figure 4.2, different calibration curves are plotted: a standard calibration curve and 4 different curves added with ChSeNPs to a final Abs_{490} of 0.07, 0.1, 0.15 and 0.2 (Abs_{490} values typically found in BioSeNPs samples) before the Dubois reaction. All calibration curves remain linear within the previously established linearity range.

Therefore, subsequent carbohydrates assays were performed differently setting the calibration curves: before starting the assay, BioSeNPs absorbance values were measured and different calibration curves were pre-

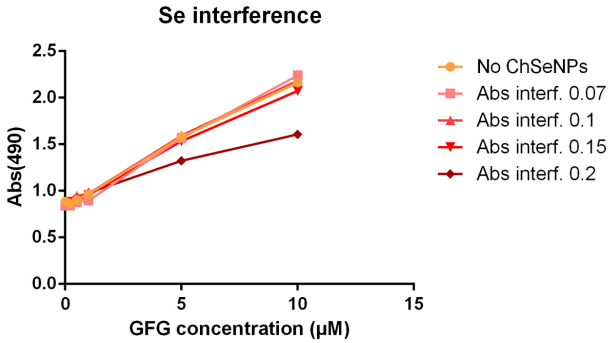

Figure 4.2: Calibration curves with or without ChSeNPs. Regardless the presence of Se interference, linearity is maintained within the same range as the standard curve

pared adding ChSeNPs to carbohydrates solutions to reach the same absorbance values. After the reaction, carbohydrates quantification was estimated for each sample referring to the corresponding calibration curve.

Optimization of an assay for total protein content quantification

Protein quantification assays are usually based on the colorimetric reaction of dyes that bind proteins. SeNPs protein content can be detected with Bradford or Bicinchoninic acid assay (BCA assay) in microplate after the extraction of proteins from the SeNPs. However, Se residues tend to interfere with absorbance reading, leading to overestimation of protein content. Separation of proteins from SeNPs could also lead to underestimation of the real protein content (see Chapter 6.3.4).

In this study, indirect measurement of protein content was performed directly on SeNPs through a solid support assay. Such assay was optimized from a work of Minamide and Bamburg (*77*), it is based on the quantity of Coomassie-Blue dye which binds proteins fixed on a filter paper. The process is similar to a polyacrylamide gel staining: the solid paper support is stained in an acidic solution containing the Coomassie-Blue dye. The acidic environment allows the interaction of the dye with proteins by Van der Waals hydrophobic non covalent interactions and through electrostatic bonds. Since the affinity of Coomassie-Blue dye for the paper is lower than for proteins, destaining is performed using the same acidic solution without the dye (*80*). Subsequently, protein content is indirectly quantified by extracting the Coomassie-Blue dye from the spots and reading Abs at 595nm. Indirect measurement also allows to avoid the interference of reducing agents (i.e. Se) and detergents (in our study, possible traces of Triton-X 100 or SDS).The detailed protocol can be found in Appendix A. As with carbohydrates assay, linearity range and Se interference have been optimized

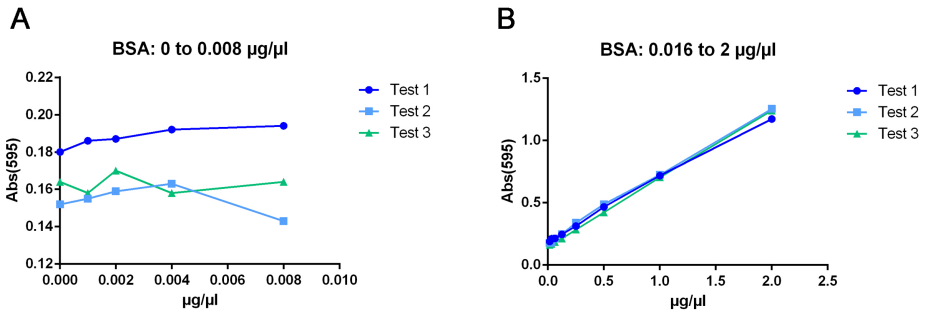

Figure 4.3: Correlation between proteins concentration and Abs_{595}: linearity ranges from 0.016 to 2µg/µl (B), while below 0.008µg/µl, correlation is non linear (A)

for this assay.

For linearity range determination, BSA concentrations from 0 to 2µg/µl were plotted versus Abs_{595}. Correlation is shown in Figure 4.3: from 0 to 0.008µg/µl , there is no linearity, while the correlation is linear between 0.016 to 2µg/µl. Thus, calibration curve was set between 0.016 and 2µg/µl BSA.

In order to test possible Se interference, ChSeNPs were added to protein samples at known concentrations: presence of ChSeNPs did not lead to any interference in protein content determination. Therefore, solid phase protein quantification assay was performed directly on BioSeNPs samples without needing addition of ChSeNPs to calibration curve.

Optimization of an assay for total lipid content quantification

Lipid quantification is based on the colorimetric sulfo-phospho-vanillin (SPV) approach, adapted for a 96-well plate assay (*78*). This method consists of a first reaction of the C=C double bonds of lipid acyl chains with sulfuric acid, followed by a second reaction with phosphovanillin, leading to the formation of a colored compound (*81*). The SPV assay in 96-well plate was optimized in this study for SeNPs. Lipids were extracted from SeNPs with chloroform: methanol 2:1 solvent and precipitated. As SeNPs could not be resuspended in the extraction solvent and precisely pipetted in a microplate, only the solvent with lipids was then placed in a 96-well plate for SPV reaction. The detailed protocol can be found in Appendix A. Calibration curve, possible interferences and linearity range have been optimized for this assay.

For calibration curve, choice of a standard is of paramount importance (*78*, *81*). Contrarily to the original article, in which seed oils were used as controls for the assay of microalgae lipid content (*78*), oleic acid was chosen in this study as a standard for cost effectiveness and composition similarity to membrane phospholipids. In Figure 4.4, oleic acid structure is

shown along with phosphatidylethanolamine, a typical bacterial membrane phospholipid (*82*). SPV reaction needs a C=C bond, consequently, the assay makes it possible to detect phospholipid and oleic acid hydrophobic tails, without detecting SDS traces.

Contrarily, Triton X-100 traces could possibly interfere with the assay and was tested for interference with Abs reading. Adding 6µl of 0.5 or 1.2% Triton X-100 (corresponding to 0.03 and 0.072µg/well) to the wells prior performing the assay led to an overestimation of lipids content below 50µg/well, while it had little to no effect in the presence of more than 50µg/well oleic acid. Differently, adding 6µl of a more diluted Triton solution (0.16%, corresponding to 0.009µg/well), led to no interference effect even to low concentrated samples (0.78µg/well oleic acid).

To simulate the experimental situation, 60µl of the extraction solvent with different known concentrations of lipids was added to micro tubes previously filled with 2% Triton X-100 solution, washed twice with sterile water and air dried. The extraction solvent was then recovered and assayed for lipid content as a control. In such conditions, Triton X-100 was found to not interfere with lipid assay.

Se interference was not an issue for lipids assay, as BioSeNPs cannot be resuspended in the extraction buffer, nor be correctly pipetted in 3 wells to have 3 replicates. Consequently, the assay had to be performed on lipids extracted from BioSeNPs.

Since the efficiency of lipids extraction was unknown, extraction of lipids from SeNPs was repeated twice. Finally, the remaining SeNPs were pipetted into one well to quantify lipids still attached to SeNPs (ChSeNPs were used as a blank for the latter samples).

Linearity range was investigated plotting concentrations from 0 to 100µg/well versus Abs_{540}. As shown in Figure 4.5, linearity ranges between 0.78 to 100µg/well, while below 0.39µg/well and above 100µg/well, correlation is non linear. Calibration curve was set from 0.78 to 100µg/well oleic acid.

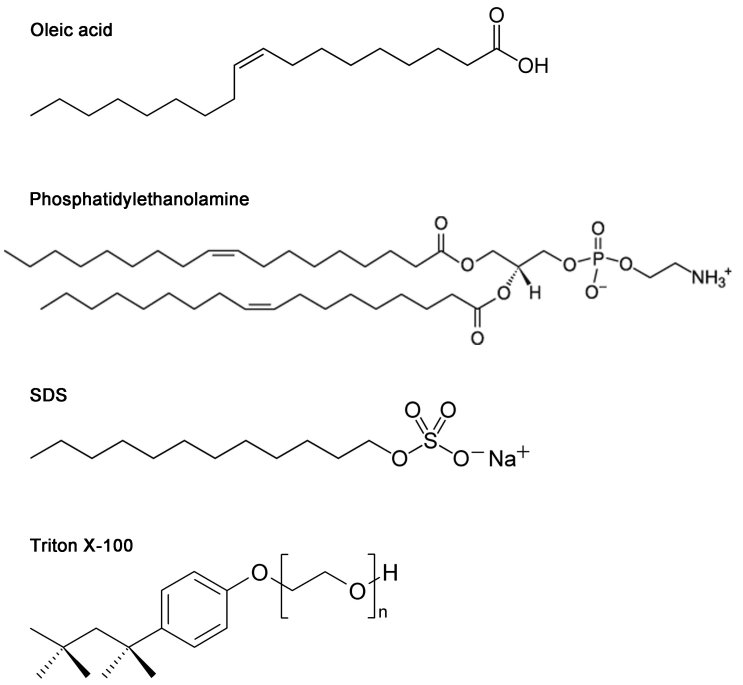

Figure 4.4: Structures of oleic acid, phosphatidylethanolamine and detergents SDS and Triton X-100

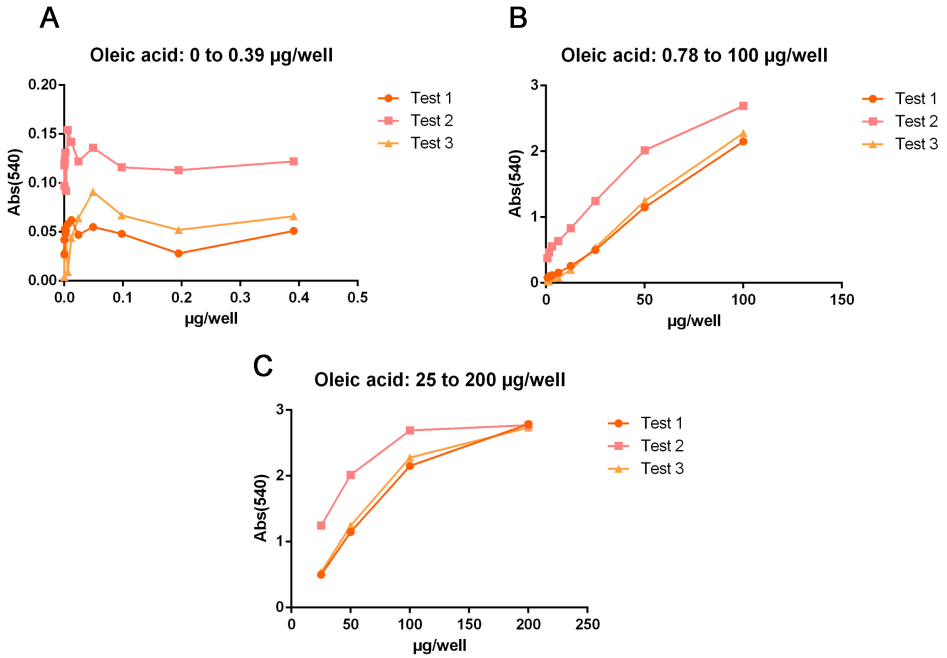

Figure 4.5: Correlation between lipids concentration and Abs_{540}: linearity ranges from 0.78 to 100µg/well (B), while below 0.39µg/well (A) and from 100 to 200µg/well (C), correlation is non linear

4.4 Results and Discussion

The goal of this study was to evaluate the amount of each of the different biomolecules (carbohydrates, proteins and lipids) that may associate during the formation of the SeNPs or as a result of the extraction protocols. In order to do this, protocols were developed for routinely screening of SeNPs samples (or other biogenically produced metal nanomaterials), with characteristics such as rapid execution, flexibility, cost-effectiveness and ability to compare a variety of different samples at the same time.

With the assays established, the effect of differences in biomolecules composition (considering carbohydrates, proteins and lipids) on SeNPs extraction and stability was investigated.

Five strains were compared, the Gram-positive SeITE01 and R1E and the Gram-negative SeITE02, R2A and R2D. SeITE01 and SeITE02 were previously studied in our group for SeNPs production and for the application of such SeNPs as antimicrobial agents (*10*, *15*, *30*, *31*, *63*, *70*). R2A, R2D and R1E were isolated from a selenate-contaminated soil and tested for selenite Minimum inhibitory concentration. The isolates were able to grow at 100mM for R2A and R2D and 75mM for R1E (*83*, *84*). For identification, 16S rRNA was sequenced: R2A shows identity of 99% to *Achromobacter* sp.; R2D of 98% to *Ensifer adherens*; R1E of 99% to *Lysinibacillus* sp. (unpublished data).

SeNPS extractions were carried out by the standard fractioning protocol (see Section 3.2.1). Samples obtained with the standard protocol were also subsequently treated under mild detergent conditions with either 2% Triton-X100 (Triton) or with higher stringency detergent of 10% SDS at 100°C (SDS).

After treatment with various solutions, samples were centrifuged to collect the SeNPs. This pellet was analyzed for different capping layer components. In order to better understand how molecules associate to SeNPs, supernatant of SeNPs extracted using standard procedure was also assayed for protein and carbohydrates content.

Following colorimetric assays, Analysis of variance (ANOVA) was performed to detect significant ($p<0.05$) difference between samples.

4.4.1 Quantification of total carbohydrates, protein and lipid contents: *B. mycoides* SeITE01

SeNPs extracted from SelTE01, containing associated biomaterial, were evaluated for carbohydrates, proteins and lipids levels. SeNPs samples extracted from a 24h SeITE01-sodium selenite culture were used. Quantifications were compared for each of the three treatments. All samples were tested with 3 biological trials, then for each biological trial, 3 technical trials were performed. ANOVA analysis was performed to assess for statistically

SeITE01	µg carbohydrates/mg NPs	µg proteins/mg NPs	µg lipids/mg NPs
Standard	10.4±4.1	7.2±3.5	64.9±10.6
Triton	12.0±2.2	3.2±4.1	27.5±16.2
SDS	0.0±0.0	0.6±1.0	67.1±5.4
Supernatant	1.1±1.5	1.0±1.0	

Table 4.1: Quantifications of main components and standard deviations. All quantifications are expressed as µg per mg SeNPs

significant differences ($p<0.05$). Table 4.1 and Figure 4.6 (panel A) show quantifications of carbohydrates associated after the different extractions with the SeNPs.

For carbohydrates, as visible in Table 4.1, mean values for standard samples are about 10µg/mg SeNPs. Differences between samples extracted with standard protocol and treated with Triton are not statistically significant, but there is a significant difference between standard and Triton-treated samples versus samples treated with SDS. At the same time, carbohydrates content in the supernatant of standard samples significantly differs from re-pelleted standard or samples treated with Triton, but does not significantly differ from samples treated with SDS (Figure 4.6).

Difference between carbohydrates content in the supernatant of standard samples and recovered SeNPs could indicate that the majority of carbohydrates remain attached to SeNPs and do not solubilize in the solvent. Treatments also appear to be efficient in dissociating carbohydrates from SeNPs only in the case of SDS (harsh treatment).

In the case of proteins (Table 4.1 and Figure 4.6, panel B), variability is so high that differences cannot be considered significant. This could be due to sample intrinsic variability, but also may be due to the proteins being the more weakly bound component of the organic material to SeNPs. No statistically significant variation has been found in total protein content after detergent treatments. Taking account of proteomic evidence for SeITE01 (see Chapter 6.4), our current working hypothesis is that there is a core of proteins strongly bound to SeNPs which cannot be removed even after 100°C, 10% SDS treatment. This is a very harsh treatment expecting membranes to be solubilized and proteins denatured and made soluble via the SDS binding (as in traditional preparation for SDS-Polyacrylamide Gel Electrophoresis). However, although this typically denatures most proteins, membrane proteins, which do not undergo traditional thermal denaturation (*85*) and retain secondary elements, could still have the ability to interact with the NPs.

Table 4.1 and Figure 4.6 (panel C) show the mean lipids content for standard samples of about 65 µg/mg SeNPs. Detergents were expected

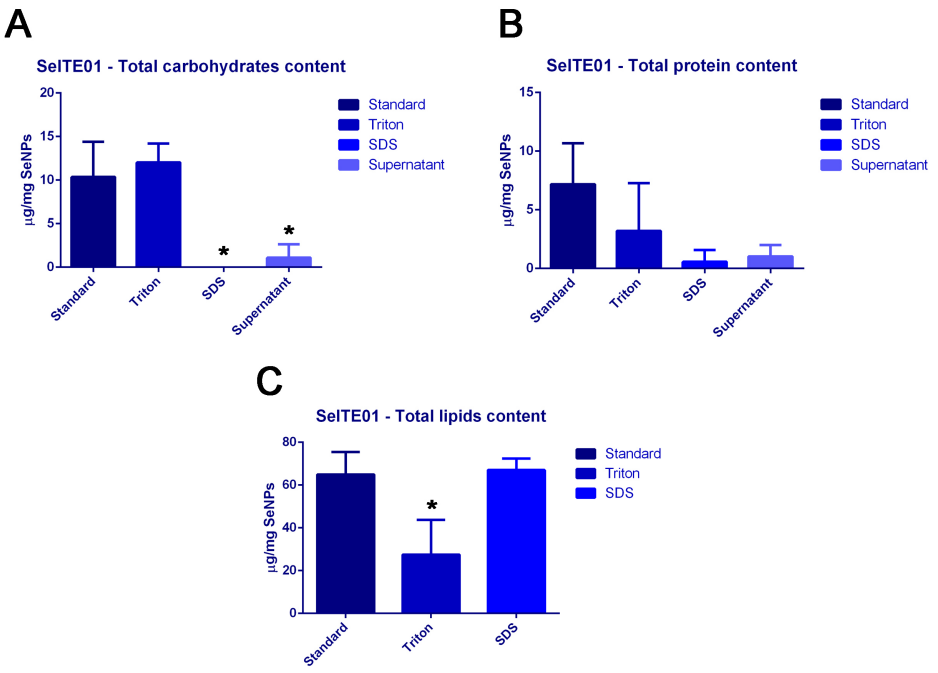

Figure 4.6: Graphic representation of Table 4.1. Stars indicate significant difference (ANOVA, $p<0.05$), while bars indicate standard deviation. All samples were performed in triplicate: 3 biological trials for each sample, then 3 technical trials for each biological trial

SeITE02	µg carbohydrates/mg NPs	µg proteins/mg NPs	µg lipids/mg NPs
Standard	11.1±4.1	39.3±3.2	124.4±14.5
Triton	10.8±1.2	36.2±4.1	65.2±50.3
SDS	0.6±1.0	1.6±2.2	72.3±21.6
Supernatant	1.5±1.5	9.0±3.9	

Table 4.2: Quantifications of main components and standard deviations. All quantifications are expressed as µg per mg SeNPs

to be able to extract away any lipid. Here Triton treatment seems to be more effective than SDS treatment. SDS-treated samples significantly differ from Triton-treated samples, but not from standard ones: there is still a considerable amount of lipid material still associated with the NPs.

Overall, we see that while the protein content from different treatments lead to non significant variations (also due to the intrinsic variability of SeITE01 protein content), the harsh SDS treatment was able to extract away the most carbohydrates from SeNPs. Differently, Triton treatment had no significant effect on carbohydrates content. For lipids, difference between the two treatments is significant, but no significant variation was observed between SDS-treated and standard samples. For carbohydrates and proteins, part of the content was also found in the sterile water the SeNPs were suspended in. High variability seems to be typical of this strain, especially in protein content and in the part of component that remains in the supernatant: this part is clearly not strongly associated with SeNPs, as it tends to dissociate in water even after 3 washing steps (the latter during sample division for the three assays).

4.4.2 Quantification of total carbohydrates, protein and lipid contents: *S. maltophilia* SeITE02

Total content quantifications for carbohydrates, proteins and lipids were carried out directly on SeNPs samples extracted from a 24h SeITE02-sodium selenite culture. All samples were tested with 3 biological trials, then for each biological trial, 3 technical trials were performed. ANOVA analysis was performed to assess for statistically significant differences ($p<0.05$).

In Table 4.2 and Figure 4.7, quantifications are shown in µg per mg of SeNPs.

Mean carbohydrates content for standard samples is about 11 µg/mg SeNPs. As shown in Figure 4.7 (panel A), there is no significant difference in carbohydrates content between standard and Triton samples. It seems that only SDS treatment is effective in removing a significant amount of carbohydrates from SeITE02 SeNPs. On the other hand, mild treatment is not effective. The part of carbohydrates content which dissociates from

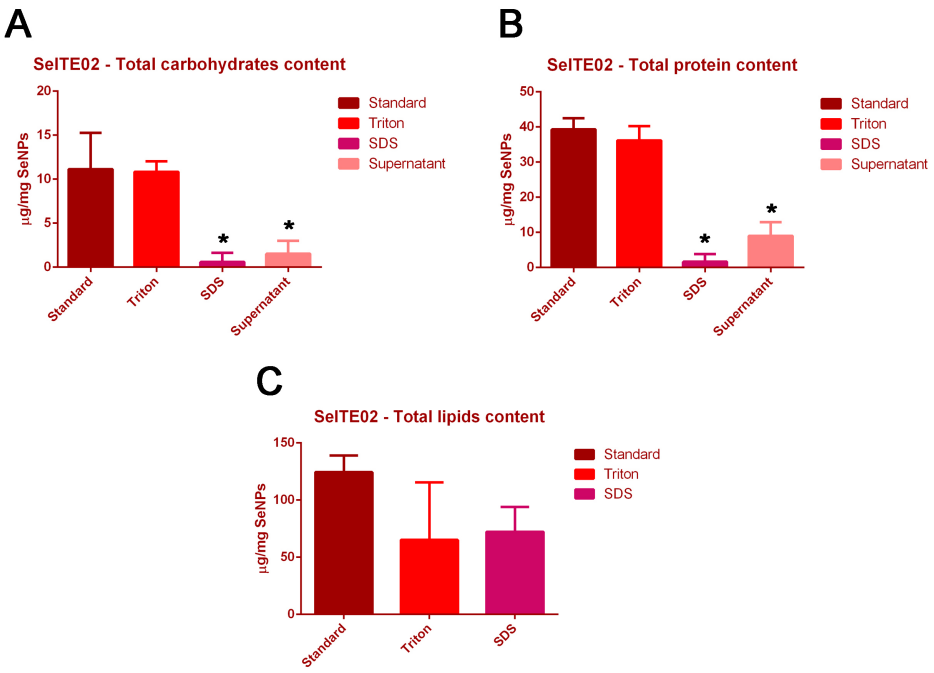

Figure 4.7: Graphic representation of Table 4.2. Stars indicate significant difference (ANOVA, $p<0.05$), while bars indicate standard deviation. All samples were performed in triplicate: 3 biological trials for each sample, then 3 technical trials for each biological trial

R2A	µg carbohydrates/mg NPs	µg proteins/mg NPs	µg lipids/mg NPs
Standard	5.1±1.8	28.2±8.4	138.9±32.0
Triton	6.6±0.5	26.0±3.1	84.0±39.4
SDS	0.2±0.3	1.2±1.2	129.7±40
Supernatant	1.2±1.2	2.5±2.2	

Table 4.3: Quantifications of main components and standard deviations. All quantifications are expressed as µg per mg SeNPs

SeNPs (supernatant samples) is significantly lower than both standard and Triton treated samples, while there is no significant difference between these samples and SDS-treated samples.

Mean protein content for SeITE02 is about 39 µg/mg SeNPs. Significant difference can be observed in Figure 4.7 (panel B). Similarly to carbohydrates, significant difference in protein content was found between standard and SDS treated samples, while Triton treatment had no significant effect. Almost a quarter of total protein content is also found in the supernatant, suggesting a weak bound with SeNPs (Table 4.2).

Lipids content is higher than carbohydrates and protein, about 125 µg/mg SeNPs, and does not seem to be influenced by treatments. Overall, both protein and carbohydrates contents are significantly affected by SDS treatment but not by milder Triton treatment. Carbohydrates and proteins are also found in the supernatant of standard samples: the difference from the standard samples is significant, while no significant variation was found between carbohydrates and protein content in the supernatant and SDS treated samples.

4.4.3 Quantification of total carbohydrates, protein and lipid contents: *Achromobacter* sp. R2A

SeNPs samples extracted from a 24h R2A-sodium selenite culture were evaluated for carbohydrates, proteins and lipids levels. All samples were tested with 3 biological trials, then for each biological trial, 3 technical trials were performed. ANOVA analysis was performed to assess for statistically significant differences ($p<0.05$).

In Table 4.3 and Figure 4.8, quantifications are shown in µg per mg of SeNPs.

Carbohydrates content for R2A is about 5µg/mg SeNPs (Table 4.3). Triton treatment has no significant effect on the total content, while SDS treatment leads to a significant decrease of total carbohydrates content. Carbohydrates are also found in the supernatant samples, with a significant difference from standard and Triton treated samples, but not from SDS treated samples (Figure 4.8, panel A).

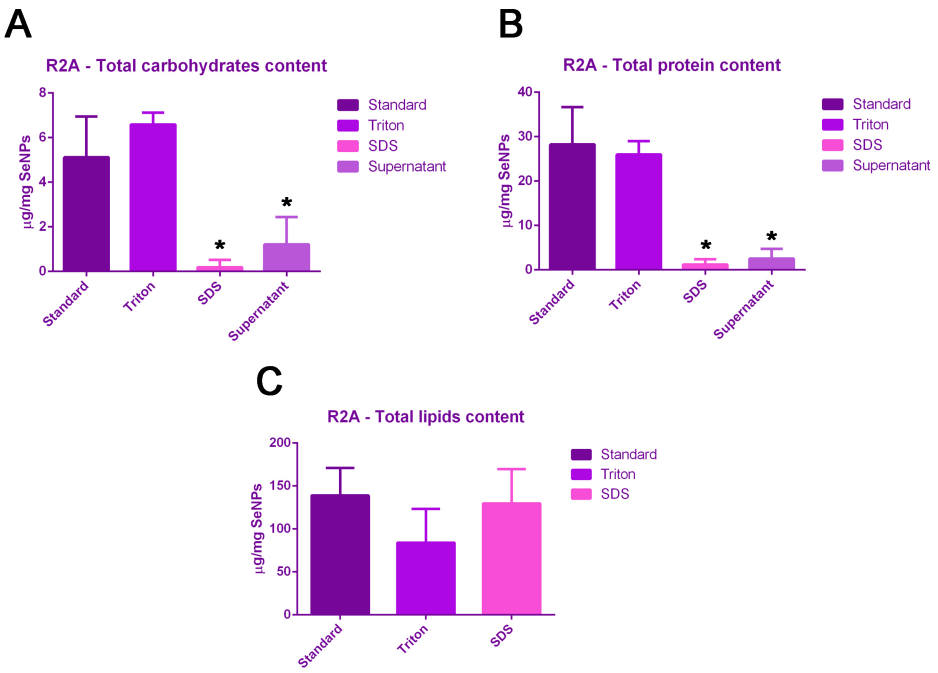

Figure 4.8: Graphic representation of Table 4.3. Stars indicate significant difference (ANOVA, $p<0.05$), while bars indicate standard deviation. All samples were performed in triplicate: 3 biological trials for each sample, then 3 technical trials for each biological trial

R2D	µg carbohydrates/mg NPs	µg proteins/mg NPs	µg lipids/mg NPs
Standard	7.9±0.4	45.0±11.4	175.2±26.6
Triton	8.5±0.1	36.4±3.6	96.1±15.5
SDS	1.2±1.1	0.1±0.1	120.9±52.0
Supernatant	0.5±0.8	1.9±1.1	

Table 4.4: Quantifications of main components and standard deviations. All quantifications are expressed as µg per mg SeNPs

Protein content is higher than carbohydrates content, about 30µg/mg SeNPs. Similarly to carbohydrates content, protein content is significantly affected by SDS treatment, but not by Triton treatment. Protein content found in the supernatant significantly differs from standard and Triton treated samples, but not from SDS treated samples (Figure 4.8, panel B).

Both mild Triton treatment and harsh SDS treatment have no statistically significant effect on total lipids content of R2A SeNPs (Figure 4.8, panel C).

Overall, protein and carbohydrates content are both significantly affected by the harsh SDS treatment, but not by milder treatment. On the other hand, lipids content is not significantly affected by any of the two treatments. Despite high variability, the difference between protein and carbohydrates contents in standard and supernatant samples is still significant.

4.4.4 Quantification of total carbohydrates, protein and lipid contents: *Ensifer* sp. R2D

Total content quantifications for carbohydrates, proteins and lipids were carried out directly on SeNPs samples extracted from a 24h R2D-sodium selenite culture. All samples were tested with 3 biological trials, then for each biological trial, 3 technical trials were performed. ANOVA analysis was performed to assess for statistically significant differences ($p<0.05$).

In Table 4.4 and Figure 4.9, quantifications are shown in µg per mg of SeNPs.

Total carbohydrates content is about 8µg/mg SeNPs for standard samples and does not significantly differ from Triton treated samples. On the other hand, SDS treatment has a significant effect on carbohydrates content. Protein content is about 45µg/mg SeNPs. SDS treatment is particularly effective, almost removing all proteins from SeNPs (Figure 4.9, panel B). On the other hand, milder treatment with Triton causes no significant difference in protein content compared to standard samples. Presence of proteins was found also in the supernatant samples, but significantly lower than the protein content still associated to SeNPs. Lipid content seems to not being affected by any of the two detergent treatments (Figure 4.9, panel C).

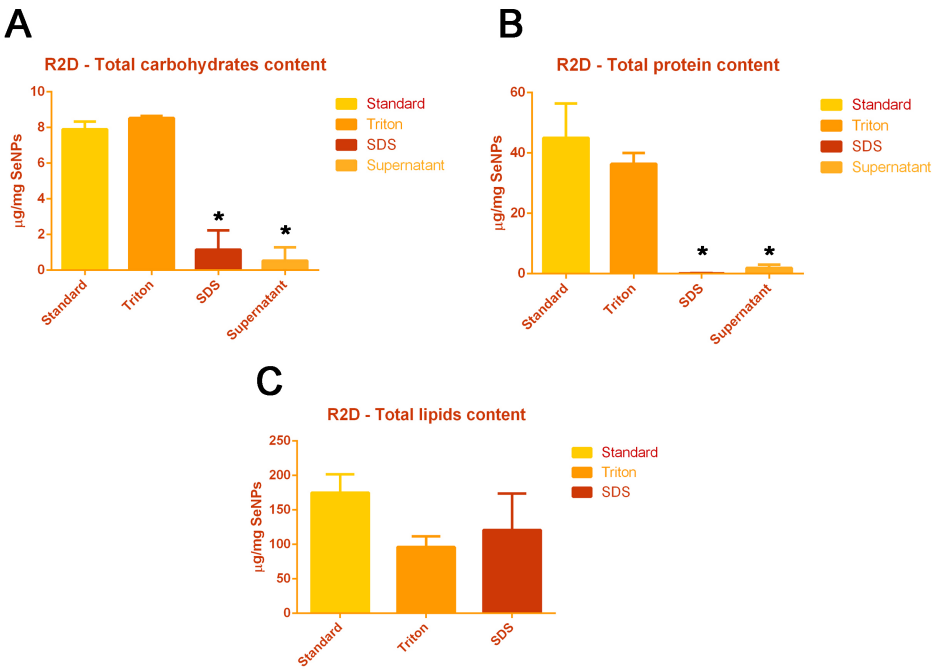

Figure 4.9: Graphic representation of Table 4.4. Stars indicate significant difference (ANOVA, $p<0.05$), while bars indicate standard deviation. All samples were performed in triplicate: 3 biological trials for each sample, then 3 technical trials for each biological trial

R1E	µg carbohydrates/mg NPs	µg proteins/mg NPs	µg lipids/mg NPs
Standard	0.7±0.8	24.4±1.7	122.0±35.5
Triton	0.3±0.4	8.4±4.2	55.8±28.9
SDS	1.5±0.6	0.3±0.5	32.7±2.2
Supernatant	1.2±1	12.4±1.5	

Table 4.5: Quantifications of main components and standard deviations. All quantifications are expressed as µg per mg SeNPs

Overall, SDS treatment has a strong effect on total carbohydrates and protein contents, while it has no significant effect on lipids. Milder Triton treatment has no significant effect on any of the three components for R2D. Carbohydrates and proteins associated to standard samples significantly differ from the supernatant fraction.

4.4.5 Quantification of total carbohydrates, protein and lipid contents: *Lysinibacillus* sp. R1E

SeNPs samples extracted from a 72h R1E-sodium selenite culture were evaluated for carbohydrates, proteins and lipids levels. All samples were tested with 3 biological trials, then for each biological trial, 3 technical trials were performed. ANOVA analysis was performed to assess for statistically significant differences ($p<0.05$). In Table 4.5 and Figure 4.10, quantifications are shown in µg per mg of SeNPs.

Total carbohydrates content for R1E shows a very high variability, with a surprisingly high content of carbohydrates also in the supernatant fraction (Figure 4.10, panel A). No significant difference was found after the two detergent treatments, while also the supernatant fraction does not significantly differ from the standard for total carbohydrates content.

On the other hand, treatments do significantly affect total protein content: standard samples significantly differ from all other samples for total protein content. SDS treatment also significantly differs from all other samples (Figure 4.10, panel B). Protein content in the supernatant fraction is surprisingly high, almost half of the standard samples protein content (Table 4.5) and not significantly differing from Triton treated samples. This could suggest a particularly weak bound between proteins and R1E SeNPs.

For lipids content, milder Triton treatment was less effective than harsh SDS treatment: standard samples lipids content significantly differs only from SDS treated samples (Figure 4.10, panel C). Overall, SDS treatment seems to be very effective in removing proteins and lipids from R1E SeNPs, while there is a very high variability in carbohydrates content.

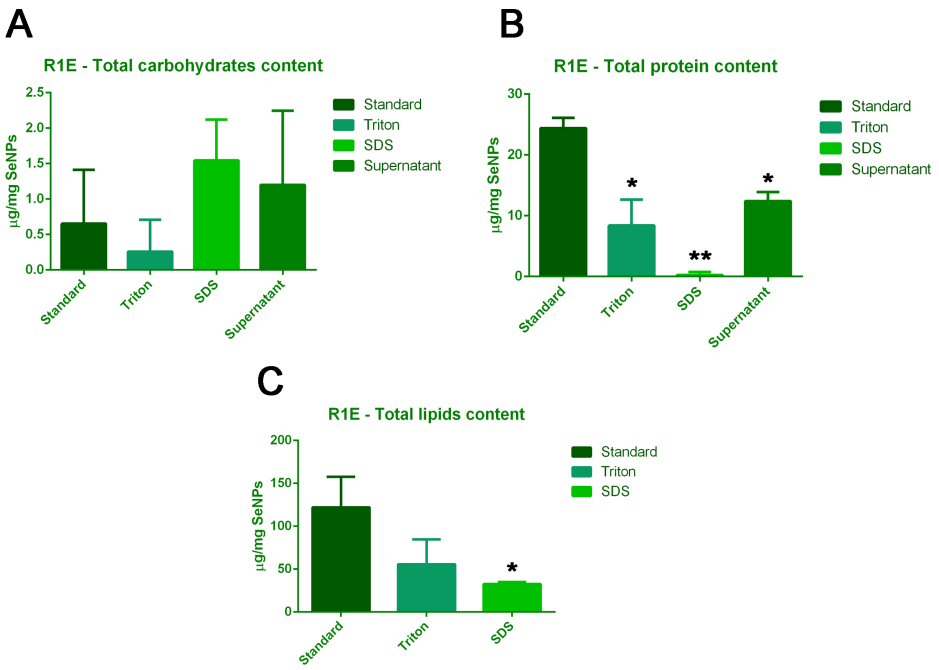

Figure 4.10: Graphic representation of Table 4.5. Stars indicate significant difference (ANOVA, $p<0.05$), while bars indicate standard deviation. All samples were performed in triplicate: 3 biological trials for each sample, then 3 technical trials for each biological trial

4.4.6 Overall differences between the five strains SeNPs capping components

Quantification of associated components was performed on five different strains: Gram-positive SeITE01 and R1E, and Gram-negative SeITE02, R2A and R2D.

Notably, all Gram-negative strains SeNPs show a similar pattern of significant differences depending on the treatment: for both carbohydrates and proteins, there is no significant difference in standard and Triton treated samples. On the other hand, SDS treatment leads to a significant decrease in both carbohydrates and protein contents. Finally, difference is significant between standard and supernatant carbohydrates/protein contents but not between SDS treated samples and supernatant fraction. Moreover, for all Gram-negative strains SeNPs, detergent treatments are not effective in causing a significant decrease in lipids content.

Gram-positive strains are characterized by a higher variability in carbohydrates and protein contents: particularly, protein content for SeITE01 and carbohydrates content for R1E show the highest standard deviations. Also, differently from Gram-negative strains SeNPs, Gram-positive strains SeNPs are affected in lipids content by detergent treatments.

For carbohydrates, significant difference in quantification was found between R1E and the other four strains (Figure 4.11). Particularly, R1E seems to have the lowest carbohydrates content of all the five strains. Interestingly, the carbohydrates contents of the supernatant fractions of all the strains do not show significant difference between each other (nor with standard R1E).

Differently from carbohydrates content, SeITE01 shows the lowest protein content of all the five strains, significantly differing from the other strains (Figure 4.12). R1E shows a similar protein content to R2A, while it significantly differs from SeITE01, SeITE02 and R2D. Finally, R2A significantly differs from SeITE02 and R2D. Only for SeITE01 the difference between standard and supernatant fractions is nonsignificant.

For lipids, SeITE01 seems to have the lowest content, significantly differing from the other strains (Figure 4.13).

Finally, for all the five strains, presence of some of the components in the supernatant of BioSeNPs could lead to interesting hypotheses. For carbohydrates, SeITE01, SeITE02, R2A and R2D show a significant difference between pelleted SeNPs and supernatant carbohydrates content, while for R1E difference is not significant. This could either be due to high variability in standard samples carbohydrates content or to a weaker bound to SeNPs of this component. The presence of a weaker bound could explain why part of the material disassociates from the pelleted SeNPs (see Section 4.6 - Figure 4.22 and relative model).

For protein content, SeITE02, R2A, R2D and R1E show a significant difference between standard and supernatant fraction. Here SeITE01 great

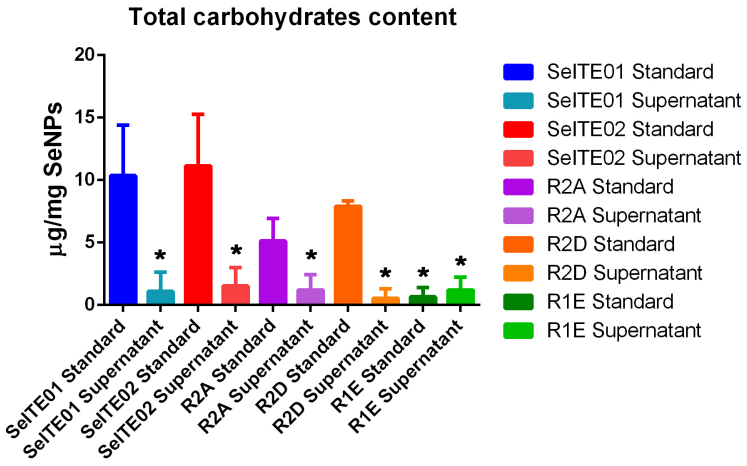

Figure 4.11: Quantification of carbohydrates content in the five strains SeITE01, SeITE02, R2A, R2D and R1E for both SeNPs and supernatant fraction. Stars indicate significant difference (ANOVA, $p<0.05$), while bars indicate standard deviation. All samples were performed in triplicate: 3 biological trials for each sample, then 3 technical trials for each biological trial

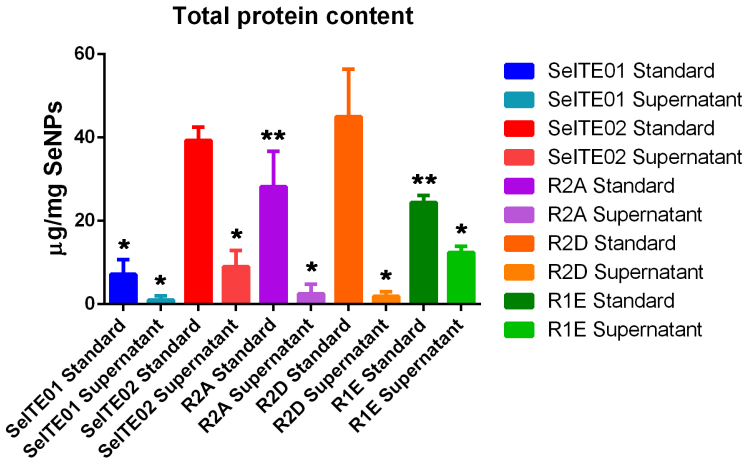

Figure 4.12: Quantification of protein content in the five strains SeITE01, SeITE02, R2A, R2D and R1E for both SeNPs and supernatant fraction. Stars indicate significant difference (ANOVA, $p<0.05$), while bars indicate standard deviation. All samples were performed in triplicate: 3 biological trials for each sample, then 3 technical trials for each biological trial

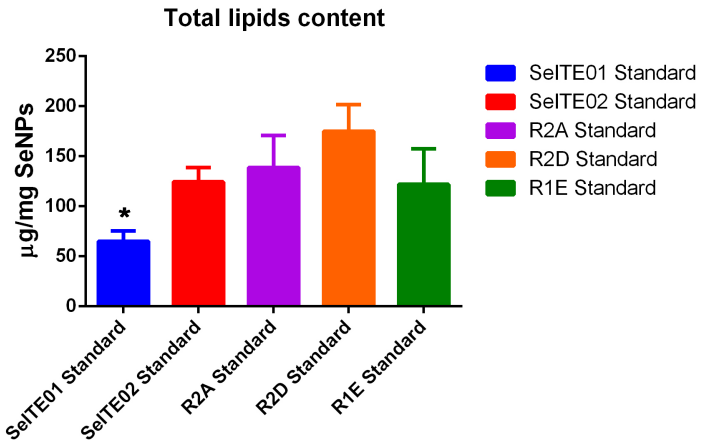

Figure 4.13: Quantification of lipids content in the five strains SeITE01, SeITE02, R2A, R2D and R1E for both SeNPs and supernatant fraction. Stars indicate significant difference (ANOVA, $p<0.05$), while bars indicate standard deviation. All samples were performed in triplicate: 3 biological trials for each sample, then 3 technical trials for each biological trial

variability could also explain the nonsignificant difference.

4.4.7 Stability of SeNPs: DLS and Zeta-potential analyses

All standard and treated samples were analyzed for hydrodynamic diameter (Dh), polydispersion (PdI) and surface charge (Zeta-potential). ANOVA analysis was also performed in order to assess significant changes in these three parameters following changes in the capping layer composition. Again, significant difference is considered with a p value of $p<0.05$.

Standard hydrodynamic dimensions for SeITE01 and SeITE02 SeNPs correspond to data already found in literature: 399nm for SeITE01 and 249nm for SeITE02, respectively (Tables 4.6 and 4.7), while there are no studies to date about R2A, R2D and R1E BioSeNPs. Analysis of size values before and after detergent treatments could help understanding the possible aggregation of destabilized SeNPs in bigger particles. Polydispersion is also an interesting parameter: PdI of 0.3 or less indicates good monodispersion of SeNPs.

The Zeta-potential measurement is correlated to stability of SeNPs (*86*): Zeta-potential values higher than 30mV or lower than -30mV indicate that SeNPs will have the ability to remain dispersed in aqueous solution and not to aggregate. Here, Zeta-potential of about -30mV to -20mV indicate that particles extracted with standard protocol are moderately stable in aqueous solution.

Size values for SeITE01 are about 400nm, with high values of polydis-

SeITE01	Dh (nm)	PdI	Z-potential (mV)
Standard	399±143	0,6±0,3	-17±4
Triton	1452±22	0,9±0,1	-10±2
SDS	340±106	0,4±0,1	-20±3

Table 4.6: Hydrodynamic diameter (Dh), polydispersity index (PdI) and surface charge (Z-potential) of SeITE01 BioSeNPs

SeITE02	Dh (nm)	PdI	Z-potential (mV)
Standard	249±63	0,3±0,1	-29±1
Triton	715±132	0,9±0,1	-20±2
SDS	268±51	0,9±0,2	-18±2

Table 4.7: Hydrodynamic diameter (Dh), polydispersity index (PdI) and surface charge (Z-potential) of SeITE02 BioSeNPs

tribution, with an average PdI of 0.6. Also, Zeta-potential indicates low stability (Table 4.6). Triton treatment seems to have a destabilizing effect on SeITE01 SeNPs: size values show a significant increase compared to standard SeNPs, indicating a possible aggregation of destabilized SeNPs.

On the other hand, SDS seems to stabilize SeITE01 SeNPs. Compared to Triton treatment, there is a significant decrease in size of SeNPs, probably due to both aggregation for Triton samples and a possible stabilizing effect for SDS samples (*18*). This is shown also for Zeta-potential values, with surface charge for Triton samples almost half of SDS samples charge. Significant difference is also present in PdI values, showing a better dispersion for SDS samples (Table 4.6 and Figure 4.14).

It can be hypothesized, that some SDS molecules associate to the capping layer during the treatment. This idea is supported by an observation of a similar effect for SDS reported by Lin and Wang in 2005, for chemically synthesized SeNPs. Small concentrations of SDS in the reaction mixture (1.5mM) keep synthesized ChSeNPs stable in solution (*18*). Thus SeNPs themselves tend to be stabilized by low concentrations of SDS regardless of the presence of other molecules in the capping layer.

For SeITE02, Triton treatment seems to cause a destabilizing effect, with a significant increase of size and polydistribution values. Differences between standard and SDS treated samples are not significant for SeITE02, as this treatment has apparently no effect on SeNPs stability. On the other hand, Zeta-potential values significantly differ between standard and treated samples, indicating an effect of both treatments on SeNPs surface charge (Table 4.7 and Figure 4.15).

Significant differences were found for R2A SeNPs after Triton treatment:

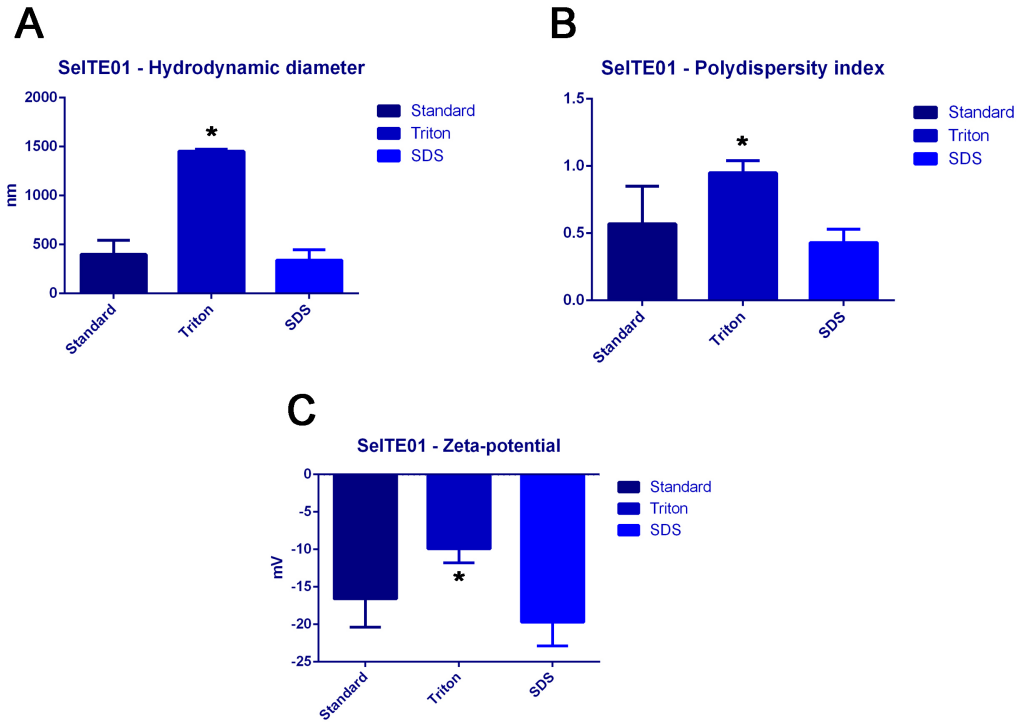

Figure 4.14: Graphical representation of Table 4.6. Stars indicate significant difference (ANOVA, $p<0.05$), while bars indicate standard deviation

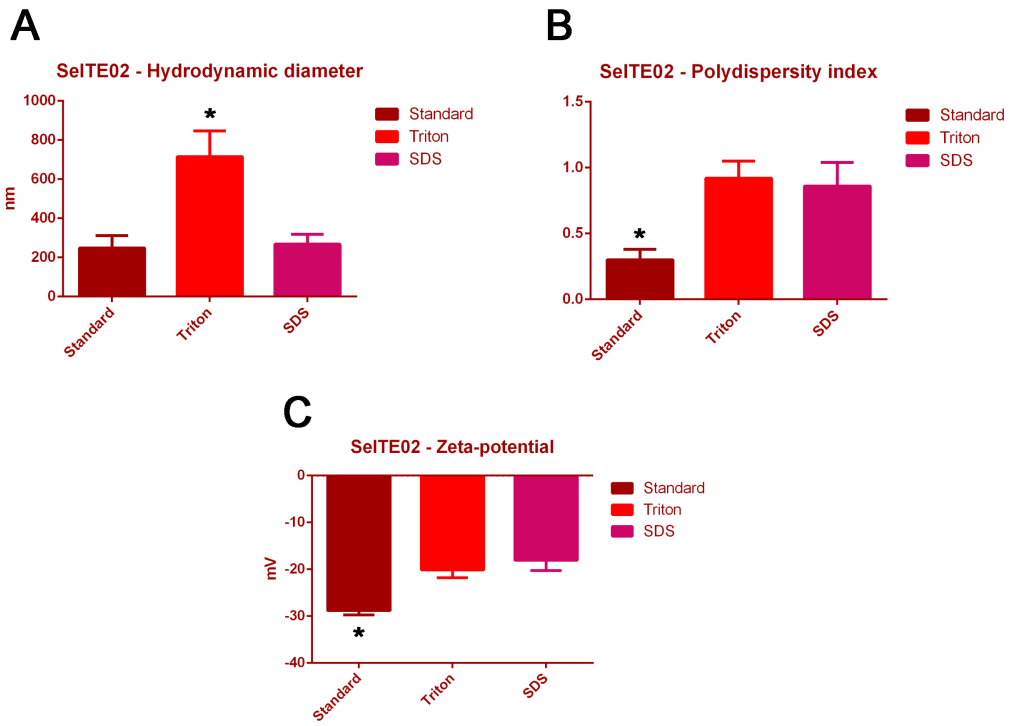

Figure 4.15: Graphical representation of Table 4.7. Stars indicate significant difference (ANOVA, $p<0.05$), while bars indicate standard deviation

R2A	Dh (nm)	PdI	Z-potential (mV)
Standard	273±93	0,3±0,1	-31±5
Triton	1354±286	0,7±0,3	-3±6
SDS	293±149	0,7±0,2	-17±4

Table 4.8: Hydrodynamic diameter (Dh), polydispersity index (PdI) and surface charge (Z-potential) of R2A BioSeNPs

R2D	Dh (nm)	PdI	Z-potential (mV)
Standard	283±45	0,2±0,0	-31±4
Triton	1368±33	1.0±0,0	-4±4
SDS	631±507	0,6±0,2	-14±3

Table 4.9: Hydrodynamic diameter (Dh), polydispersity index (PdI) and surface charge (Z-potential) of R2D BioSeNPs

size values significantly increase, indicating a possible aggregation of destabilized SeNPs. This hypothesis seems to be confirmed by Zeta-potential values, almost approaching neutrality after Triton treatment. No significant difference was reported for polydispersion.

Interestingly, SDS treatment causes a significant decrease in Zeta-potential values compared with standard samples, but size values do not significantly differ, suggesting no aggregation occurs. This could be due to SDS stabilizing effect (Table 4.8 and Figure 4.16).

For R2D SeNPs, Triton treatment leads to a significant increase of SeNPs size, while SDS treatment leads to extremely variable results. Significant differences are shown for both polydispersion and surface charge, indicating a possible destabilization and aggregation of SeNPs after Triton treatment. Notably, an increased polydispersion and decrease in Zeta-potential values were also observed following SDS treatment, despite being less severe than after Triton treatment. In this case, given strong variability in size values, it is not possible to hypothesize an aggregation of SeNPs following SDS treatment, even if a destabilizing effect could be suggested (Table 4.9 and Figure 4.17).

Finally, Triton treatment shows a significant effect on both size and polydispersion of R1E SeNPs, and while there is no significant variation in Zeta-potential for none of the samples, Triton treatment shows the major variability. Overall, SDS treatment seems to have no significant effect on SeNPs in terms of size and polydispersion, showing significant difference only with Triton treated samples for size and PdI values (Table 4.10 and Figure 4.18).

ChSeNPs synthesized by the protocol by Lin & Wang (2005) (*18*), that

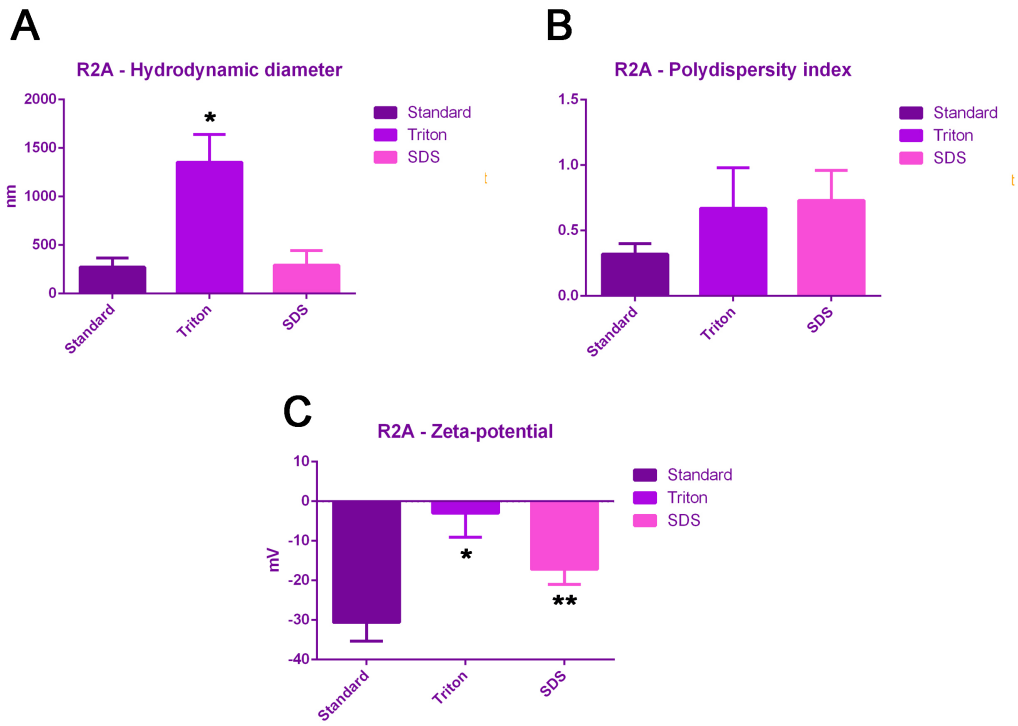

Figure 4.16: Graphical representation of Table 4.8. Stars indicate significant difference (ANOVA, $p<0.05$), while bars indicate standard deviation

R1E	Dh (nm)	PdI	Z-potential (mV)
Standard	607±121	0,3±0,0	-24±1
Triton	1667±50	0,9±0,1	-12±10
SDS	642±402	0,5±0,2	-13±2

Table 4.10: Hydrodynamic diameter (Dh), polydispersity index (PdI) and surface charge (Z-potential) of R1E BioSeNPs

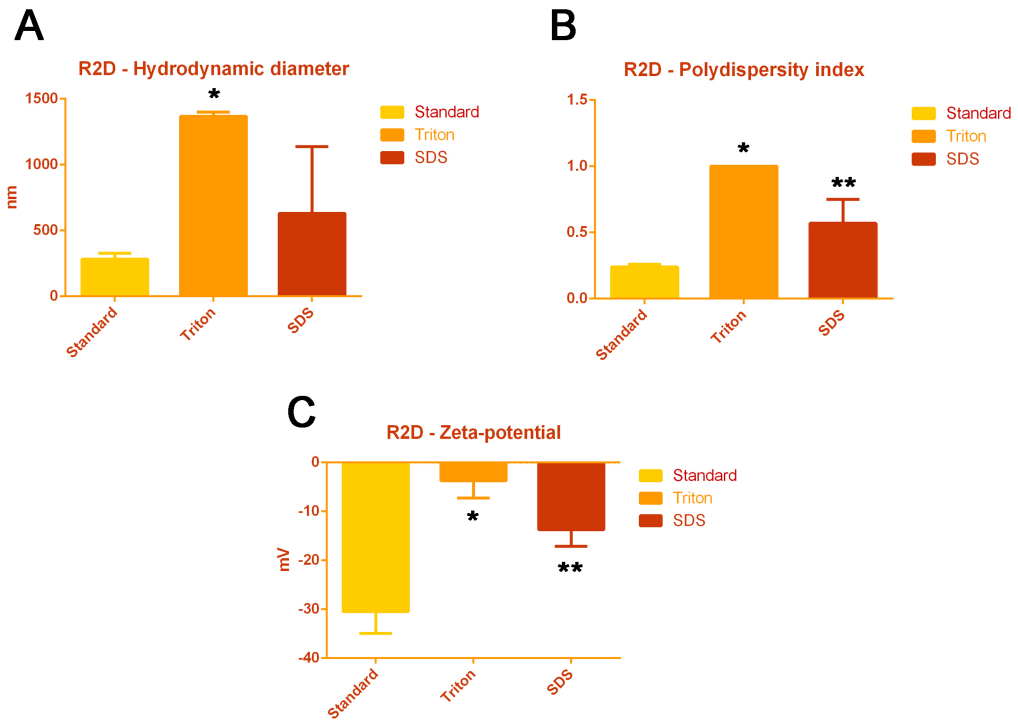

Figure 4.17: Graphical representation of Table 4.9. Stars indicate significant difference (ANOVA, $p<0.05$), while bars indicate standard deviation

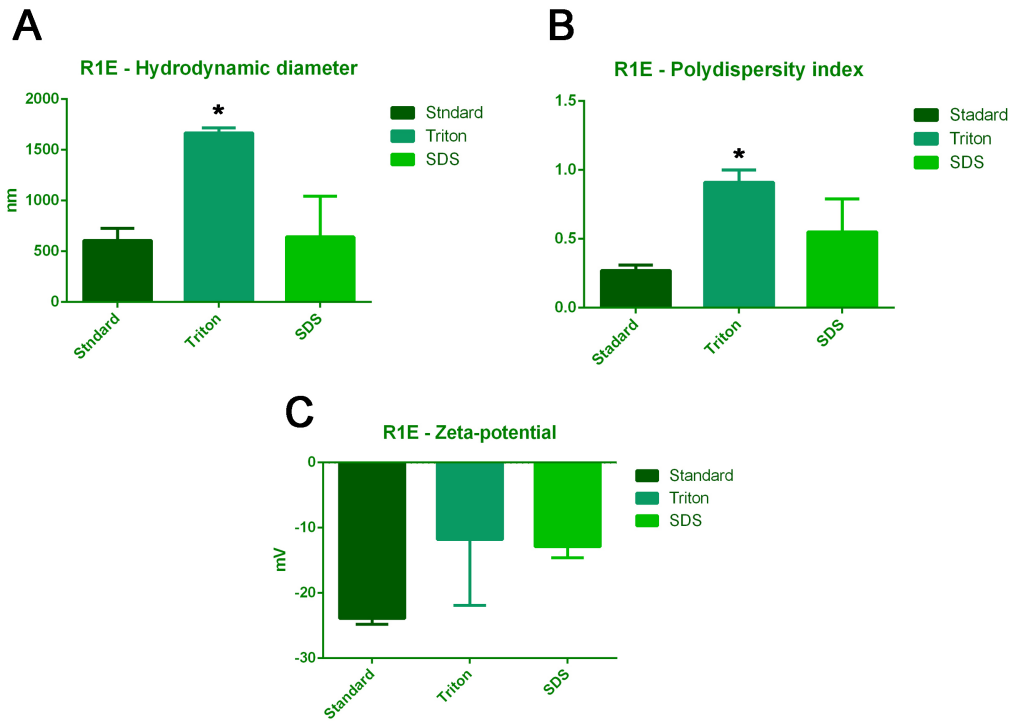

Figure 4.18: Graphical representation of Table 4.10. Stars indicate significant difference (ANOVA, $p<0.05$), while bars indicate standard deviation

ChSeNPs	Dh (nm)	PdI	Z-potential (mV)
Standard	205±25	0,2±0,0	-36±1
Triton	220±39	0,3±0,1	-29±1
SDS	225±77	0,1±0,0	-30±1

Table 4.11: Hydrodynamic diameter (Dh), polydispersity index (PdI) and surface charge (Z-potential) of ChSeNPs

do not present any associated material, were also investigated in terms of size, polydispersion and surface charge. ChSeNPs were not affected by treatments, showing similar values for size, surface charge and polydistribution (Table 4.11). In this case, strongly negative values of Zeta-potential could be due to SDS molecules stabilizing ChSeNPs. Notably, despite showing better parameters than BioSeNPs (lower Dh and PdI and more negative Zeta-potential), ChSeNPs are less stable for long time periods, and start to precipitate if stored for more than 30 days, even with SDS inside storing solution.

4.4.8 Overall differences between the five strains SeNPs stability parameters

SeNPs extracted from the five strains show interesting differences when comparing size and surface charge values. Notably, no significant differences were found comparing polydispersion. As visible in Figure 4.19, Gram-positive R1E SeNPs show the highest hydrodynamic diameter, significantly differing from the three Gram-negative strains SeITE02, R2A and R2D, but not from Gram-positive SeITE01. On the other hand, SeITE01 does not significantly differ from Gram-negative strains. Notably, Gram-positive strains show a higher variability compared to Gram-negative strains.

In Figure 4.20, Gram-positive SeITE01 shows the lowest surface charge, significantly differing from the three Gram-negative strains, but not from the other Gram-positive strain R1E. For Zeta-potential, Gram-positive R1E and Gram-negative SeITE02 show the lowest variability.

PdI values seem overall higher for SeITE01, but this strain is also characterized by a strong variability. However, no significant variation was found for PdI values in standard samples (Figure 4.21).

4.4.9 Experimental issues and significance

The main biomolecular components were evaluated by quantification analysis through microplate assays on BioSeNPs from the five strains, in order to find differences in capping layer composition. Such assays are proposed here in this thesis as a screening tool for different SeNPs samples. The goal is

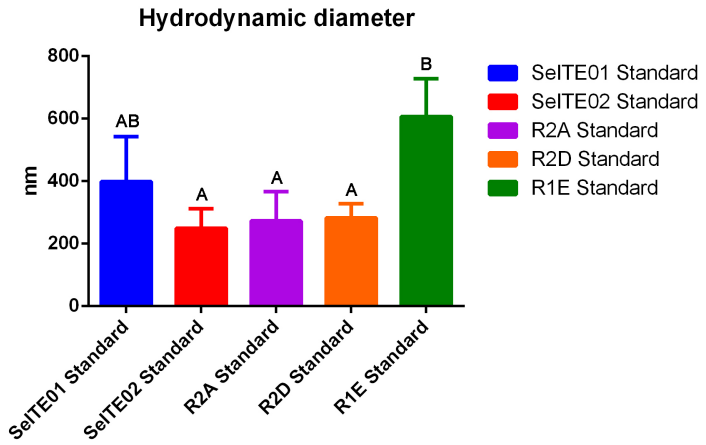

Figure 4.19: Hydrodynamic diameter of SeNPs from the five strains. Letters indicate significant difference (ANOVA, $p<0.05$), while bars indicate standard deviation

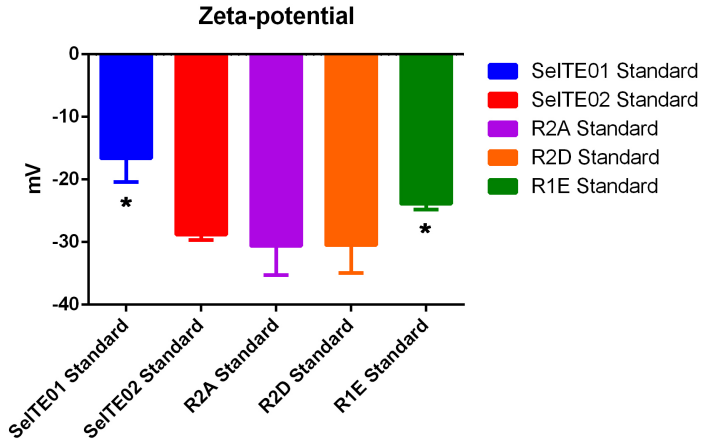

Figure 4.20: Surface charge of SeNPs from the five strains. Stars indicate significant difference (ANOVA, $p<0.05$), while bars indicate standard deviation

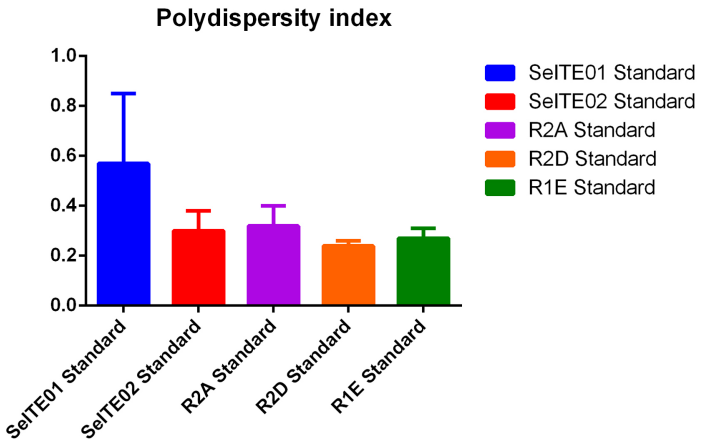

Figure 4.21: Polydispersity index of SeNPs from the five strains. Bars indicate standard deviation

to have experimental characteristics of: speed, sensibility, cost-effectiveness, and possibility to compare a variety of different samples at the same time. Overall results show the assays, even with experimental variability, have the ability to quantify the three groups of biomolecules.

Using the assays to discriminate the value of different extraction efficiencies was in some cases hampered due to the magnitude of the standard deviations. ANOVA was then utilized to evaluate the statistical significance of results. Repeatability of analyses was in fact an issue, as starting material has shown to have intrinsic variation, especially for some of the treatments.

Overall, SeNPs from Gram-positive strains showed the greatest variability: SeITE01 for protein and carbohydrates content, R1E for carbohydrates and lipids content. Interestingly, Gram-negative strains showed less variability, except for lipids content. R2A standard samples show high variability in protein and carbohydrates contents.

High variability, and consequently high values of standard deviation, has also been noticed for R2D and R1E in terms of size and surface charge after detergent treatments, and in the polydistribution of SeITE01 and R2A. It can be considered that the molecular composition of the biogenic SeNPs can be slightly different for any given extraction batch. Despite this high variability, ANOVA analysis made it possible to distinguish significant differences between some of the samples, which can reasonably be considered reliable. It can be concluded, that microplate assays need to be performed at least three times in order to detect significant differences.

Carbohydrates:Proteins:Lipids Ratios (µg/mg SeNPs)					
Sample	SeITE01	SeITE02	R2A	R2D	R1E
Standard	10 : 7 : 65	11 : 39 : 124	5 : 28 : 139	8 : 45 : 175	1 : 24 : 122
Triton	12 : 3 : 27	11 : 36 : 65	7 : 26 : 84	9 : 36 : 96	0 : 8 : 56
SDS	0 : 1 : 67	1 : 2 : 72	0 : 1 : 130	1 : 0 : 121	2 : 0 : 33

Table 4.12: C:P:L ratios expressed as µg/mg SeNPs for the five bacterial strains

4.5 Overall effect of treatments on the five strains SeNPs

Considering the average Carbohydrates:Protein:Lipids (C:P:L) ratios of the extracted NPs allows an approach to compare the different extractions. Lipids appear to be the most abundant components of the capping layer for all the five strains in terms of µg/mg SeNPs (Table 4.12). Unexpectedly, the lipid fraction is also the least affected by detergent treatments, being significantly affected only by SDS treatment for R1E and significantly differing between the two treatments for SeITE01. Gram-negative strains are not significantly affected in lipids content, suggesting a different kind of interaction of lipid molecules with SeNPs.

Following lipids, proteins are the second most abundant component in terms of µg/mg SeNPs for all the strains except SeITE01 (Table 4.12). For Gram-negative strains, proteins are effectively and almost completely removed from SeNPs by SDS treatment, while Triton treatment is not as much effective. On the other hand, Gram-positive strains show completely different results. SeITE01 is characterized by so high variability, that differences between treated and untreated samples can not be considered significant (ANOVA). Contrarily, R1E protein content significantly differs for all treatments.

Finally, carbohydrates are the least abundant component in terms of µg/mg SeNPs, except for SeITE01. Again, SeNPs from Gram-negative strains show a similar pattern, with SDS removing most of the carbohydrates content. For Gram-positive strains, contrarily to proteins, R1E shows the highest variability and non significant differences (ANOVA), while SeITE01 shows significant differences between SDS treated samples and standard samples. Triton seems ineffective in significantly removing carbohydrates from SeITE01 SeNPs. Overall, C:P:L ratios seem to maintain even when the total amount of organic capping material is removed (Table 4.12).

Detergent treatments have different effects on BioSeNPs: while SDS treatments seems to be the most effective in removing the capping layer components, Triton treatment appears to be much more effective in destabilizing SeNPs, eventually leading to aggregation. In fact, Triton and SDS

treated samples significantly differ for almost all stability parameters in all the five strains. These data were partly unexpected, as removal of almost all the capping layer (as in the case of SDS treated samples) was expected to cause destabilization and aggregation of SeNPs. On the other hand, this kind of assays do not take into account the strength of the bound between SeNPs and the organic molecules. In fact, some capping layer components can be found also in the supernatant of standard samples even after 3 washing steps. To date, the strength of the bound between organic molecules and SeNPs is still under investigation. Dobias *et al.* found proteins associating with different strength to *E. coli* SeNPs (*37*), but very few studies to date have investigated the presence of capping components and their form of association with SeNPs. Cheng *et al.* quantified the material associated to *B. paralicheniformis* SR14 SeNPs, but without a distinction between the material associating to the SeNPs and their resuspension buffer (*62*).

A TEM analysis on SeNPs from SeITE01 and SeITE02 by our research group shows interesting data about the capping layer (*68*). Despite culturing condition being different from this study, TEM analysis clearly shows the presence of the organic material associated to SeNPs. It is hypothesized, that attempts to remove the organic material lead to destabilization and aggregation of BioSeNPs. Culturing and extraction conditions also led to the presence of a greater amount of organic material compared to the methods used in this thesis, as it was also visible not only in TEM images, but also inside the test tubes, detaching from the pellet during washing steps. Therefore, it is also possible that, depending on the culture conditions and extraction protocol, part of the organic material is weakly bound and simply co-purifies with SeNPs. Consequently, it detaches from SeNPs once resuspended in water. This possibly exceeding material could however contribute to SeNPs stability, keeping SeNPs suspended in water.

However, presence of smaller amounts of organic molecules even after harsh treatments like 10% SDS at 100°C (*37*) suggests that part of the associated material constitutes a strongly bound capping layer, which do not dissociate from SeNPs. Another possible explanation of the effect of detergents on SeNPs stability could be the incorporation of some detergent molecules in the capping layer. This hypothesis could also explain the aforementioned stabilizing effect of SDS.

4.6 A possible model for capping layer composition: inner and outer layers

Considering the effect of different treatments on BioSeNPs and the associated material, it seems likely, that some of the organic molecules are more strongly bound to SeNPs and ultimately affect their stability in water solutions. Then, it could be hypothesized, that these specific capping molecules

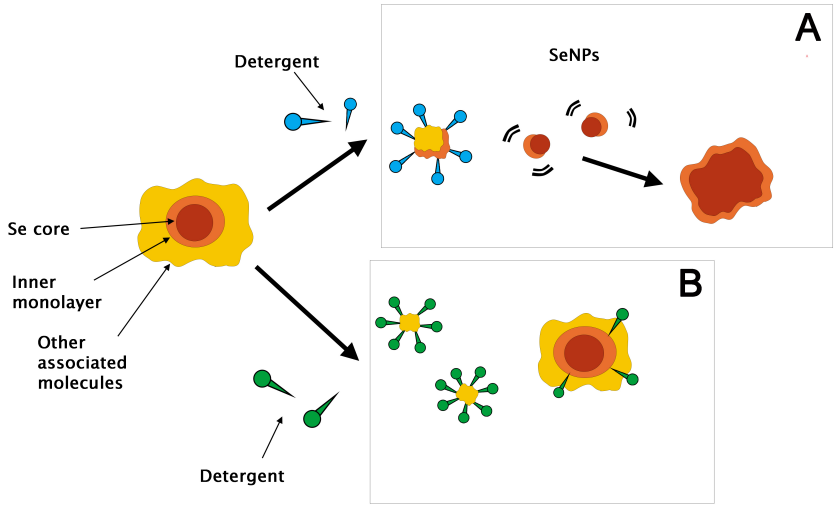

Figure 4.22: Scheme of possible interaction of detergents with the capping layer: panel A: detergents remove associated molecules and part of the inner layer, leading to destabilization and aggregation of SeNPs. Panel B: detergents remove part of the associated molecules, but not the inner layer. SeNPs are not destabilized and do not aggregate. Moreover, some detergents could incorporate in the associated material and have a stabilizing effect

more strongly associated with SeNPs are probably located in the inner part of the layer or constitute an inner monolayer of specific molecules in direct contact with the Se atoms. Whereas other molecules could constitute associated material that is interacting with the SeNPs via this inner monolayer (Figure 4.22).

With this in mind, the harsh detergent treatments could remove molecules of the surface of the layer, leading sometimes to SeNPs destabilization and less outer layer associated material.

Hypothesis shown in Figure 4.22 could also explain the effect of components and treatments on SeNPs stability assayed by DLS measurements. Unfortunately, it is not clear whether hydrodynamic diameter measured by DLS includes both the layers of the capping plus the selenium core, or only the core, or just the inner part of the layer.

Moreover, different strains could influence the composition of the inner and outer layers. Notably, SeNPs produced by the three Gram-negative strains here analyzed show a similar pattern in quantified components when treated with detergents. Also, DLS parameters are characterized by significant differences between Triton and SDS treated samples. Almost total removal of the associated material do not correspond to a major destabilization, indicating a possible difference in the role of the inner and outer layer molecules. In this case, the hypothesis is that the inner layer molecules, which are not removed after the harsh treatment, have a stronger stabi-

lizing effect than the outer layer molecules. Stabilization here would not be influenced by the quantity of molecules associating, but the nature of the molecules exposed to the solvent. Another possibility is that some SDS molecules could bind the remaining inner layer molecules, stabilizing SeNPs. In fact, hydrodynamic diameters of SDS treated molecules do not significantly differ from standard samples. This model could also be applied to SeNPs by Gram-positive bacteria, even if in this case quantification and DLS patterns are more variable.

SDS and Triton treated samples for SeITE01 still differ in carbohydrates and lipids contents. For Triton treated samples, with a higher carbohydrates content and lower lipid content, DLS parameters clearly suggest a destabilization of SeNPs. On the other hand, SDS treated samples, with a higher lipids content and undetectable amounts of carbohydrates, do not significantly differ from standard samples in terms of size, polydistribution nor surface charge. This could suggest, that lipids could more probably have a stabilizing effect compared to carbohydrates for SeITE01 SeNPs. On the other hand, it is still possible that some SDS molecules are incorporated in the inner layer (Figure 4.22, panel B), possibly bound to lipids, while Triton could be more easily washed away, leaving destabilized SeNPs, that aggregate.

Finally, the two detergent treatments have variable effects on R1E SeNPs. Triton treated samples seem to be more destabilized than SDS treated samples, even if Zeta-potential values do not significantly differ. Protein content is significantly higher for Triton treated samples than for SDS treated samples, and for both, protein content is significantly lower than for standard samples. However, strong presence of proteins in the supernatant fraction suggests a weaker bound of proteins to R1E SeNPs compared to other strains. Overall, SDS treated samples show the lower protein and lipids content, associated to a probable major stability when compared to Triton treated samples. Again, incorporation of SDS molecules is still possible, as it is possible that lipids have more stabilizing power than proteins for Gram-positive strains.

4.7 Conclusions

BioSeNPs produced by the five bacterial strains SeITE01, SeITE02, R2A, R2D and R1E have been analyzed using microplate versions of colorimetric assays in order to perform a first screening of the different classes of molecules constituting the organic capping layer. Such assays have proven to be sensitive, quick, cost-effective and with the possibility to compare many different samples at the same time. On the other hand, repeatability issues have been encountered during the study. While some issues have been solved, for some strains SeNPs still show an intrinsic variability due to

non-stoichiometric production and extraction method, and possibly quantification method. However, ANOVA analysis made it possible to distinguish significant differences.

Significant changes have been observed between SeNPs from the five strains after different treatments aimed to remove part of the organic capping layer and associated biomolecules.

Notably, Gram-negative strains SeNPs show a more similar pattern than Gram-positive strains SeNPs, which are also characterized by more variability and higher standard deviations.

Treatments affecting the organic capping/associated molecule composition also affect parameters such as hydrodynamic diameter, distribution and surface charge, which are an indicator of SeNPs stability.

A hypothesis has been proposed, that some of the molecules are more strongly attached to SeNPs than others, maybe belonging to the inner capping layer (Figure 4.22).

Also, different molecules could have a different influence on SeNPs stability, possibly interacting with detergents.

Further analyses and optimization are needed, in order to confirm hypotheses and further understand the capping layer composition and role.

Part III

SeNPs synthesis and translocation in *B. mycoides* SeITE01

Chapter 5

Materials and Methods

5.1 Procedures for SeNPs extraction from *B. mycoides* SeITE01: octanol fractioning and sucrose gradient

Cultivation conditions and extraction of SeNPs from *B. mycoides* SeITE01 culture through octanol fractioning are described in Chapter 3. Alternatively to organic solvent fractioning, sonicated samples were placed on the top of a 60% sucrose solution and centrifuged in a Sorvall Super T21 Benchtop Superspeed® Centrifuge (SL-50T rotor) at 2000xg for 50min at 4°C. All phases were collected and 200 to 800nm absorbance was scanned with an Agilent Cary 60 UV-Vis Spectrophotometer. Only the pellet showed the typical SeITE01 SeNPs spectrum. Finally, the pellet was washed three times with sterile water in order to remove sucrose.

5.2 SeNPs by chemical synthesis

SeNPs were chemically synthesized according to Lin and Wang protocol (2005) (*18*): selenous acid and a reducing agent (10mM SDS +520mM $Na_2S_2O_3$) were mixed to a final concentration of 2.5mM selenous acid, 1.5mM SDS and 75mM $Na_2S_2O_3$ and kept at room temperature overnight. ChSeNPs were collected by centrifugation (9300xg, 8min, 4°C), immediately resuspended in TrisHCl 100mM pH 7.4 and stored at 4°C.

5.3 Exposition of chemically synthesized SeNPs to *B. mycoides* SeITE01 cell free extract

SeITE01 cells were cultured 24h in liquid Nutrient medium at 27°C in a shaker, harvested by centrifugation (1100xg, 15min 4°C) and washed twice with PBS buffer. Cells were then resuspended in ice-cold 100mM Tris pH

SDS	4%
Glycerol	20%
2-mercaptoethanol	10%
Bromphenol blue	0.004%
Tris HCl, pH 6.8	0.125M

Table 5.1: Laemmli Buffer composition (*87*)

7.4 and sonicated in ultrasonic processor UP50H (Dr. Hielscher GmbH) (4 cycles of 40sec sonication + 40sec rest in ice). Cells and cell debris were pelleted by centrifugation (16000xg, 30min, 4°C). Supernatant (CFX) was filtered (Syringe Filters, Filtropur S 0.45, Sarstedt) and collected for subsequent ChSeNPs exposure. ChSeNPs were mixed with CFX overnight. Exposed ChSeNPs were recovered by simple centrifugation (16000xg, 30min) and resuspended in sterile water. Alternatively, it was fractionated by mixing with organic solvent (2ml organic solvent every 5ml supernatant). The mixture was stirred 10sec on a vortex and centrifuged for 5min, 480xg. SeNPs migrated to aqueous phase overnight at 4°C. Aqueous phase was collected and centrifuged 16000xg 20min. Supenatant was discarded and the pellet was resuspended in sterile water.

5.4 Recovery of protein fraction from SeNPs synthesized by *B. mycoides* SeITE01

BioSeNPs and exposed ChSeNPs samples were resuspended in Laemmli Buffer (Table 5.1) (*87*) and treated at 95-100°C for 10min to strip proteins off the SeNPs. SeNPs were subsequently pelleted through centrifugation (16000xg, 30min, 4°C) and discarded. Proteins were precipitated as follows: 4 volumes of cold acetone were added. Proteins were precipitated overnight at -20°C and pelleted through centrifuging 14000xg 10min and air dried. Finally, proteins were resuspended in 3% SDS and concentration was estimated through BCA assay (Peirce® Microplate BCA Protein Assay Kit, Thermo Scientific). Proteins were precipitated again with acetone in order to obtain 150µg of proteins for every sample.

5.5 Sodium Dodecyl Sulfate - PolyAcrylamide Gel Electrophoresis (SDS-PAGE)

Proteins were resuspended in Laemmli Buffer 1x and treated at 95-100°C for 10min. Samples were then immediately loaded on a polyacrylamide gel 8-10%T (Table 5.2).

Running gel (10ml)	8% T	18% T	Stacking gel (5%T)
Acrylamide 40%	1ml	2.25ml	500µl
Tris-HCl pH8.8 5x	1ml	1ml	3.265ml
SDS 10%	50µl	50µl	40µl
Glycerol	—	517µl	—
milliQ water	2.950ml	1.183ml	0.383ml
TEMED	2µl	2µl	1.6µl
APS	5µl	5µl	4µl

Table 5.2: Polyacrilamide gel composition

Glycine	192mM
SDS	0.1%
Tris	12mM

Table 5.3: Tris-glycine buffer composition

Samples ran in Tris-Glycine Buffer 1x (Table 5.3) under the following conditions:

- 5mA for 1h
- 10mA for 1h
- 20mA till blue reached bottom of gel

At the end of the run, the gel was placed in the Coomassie Stain solution overnight in a shaker, then in 5% acetic acid for destaining (ca. 6h). Gel image was acquired with VersaDoc Imaging System Model 1000 (BioRad).

5.6 Mass Spectrometry-compatible Silver staining

Alternatively to Coomassie staining, in first experiments gels were stained with a Mass Spectrometry (MS) compatible version of Silver staining.

Proteins were fixed 3 times for 30min in the fix solution (5% acetic acid, 30% ethanol), then gel was washed 3 times for 10min in H_2O. Following, gel was placed in sensitivity enhancing solution (2ml of 10% sodium thiosulfate/l in H_2O) for 1min and washed 2 times for 1min in H_2O. Bands were stained in silver stain solution (12.5ml of 1N silver nitrate/l H_2O) for 30min, then the gel was washed for 10sec in H_2O and put in development solution (30g potassium carbonate, 250µl 37% formaldehyde and 125µl 10% thiosulfate/l H_2O) for about 8min. Finally, gel was placed in stop solution for 60min and finally washed in H_2O for 30min.

5.7 Spot treatment and tripsin digestion

Bands were cut and destained with NH_4HCO_3. Proteins were then reduced and alkylated in gel with dithioerythritol (DTE) and iodoacetamide (IAA), respectively, and finally digested with Trypsin overnight at 37°C. Peptides were extracted in acetonitrile (ACN) and 0.5% formic acid through sonication, then centrifuged at 16000xg, 30min in order to remove Selenium traces from the mixture. Finally, peptides were air-dried under chemical hood at 38°C.

5.8 MS identification

Peptides were separated by reversed phase nano-HPLC-Chip technology (Agilent Technologies, Palo Alto, CA, USA) online-coupled with a 3D ion trap mass spectrometer (Esquire 6000, Bruker Daltonics, Bremen, Germany).

Identification was performed using Mascot software (*88*) searching in the National Center for Biotechnology Information non-redundant database (NCBInr).

The following parameters were adopted:

- specific trypsin digestion, up to one missed cleavage
- variable modifications: carbamidomethyl (Cys) and oxidation (Met)
- peptide and fragment tolerances: ±0.9 Da and ±0.9 Da, respectively
- peptide charges: +1, +2 and +3
- taxonomy: Firmicutes (gram-positive bacteria)

Proteins were identified as being 'significant hit' ($p<0.05$) based on individual peptide ion score. These peptide ion scores were automatically calculated by Mascot Programme as -10*Log(P), where P is the probability that the observed match is a random event. When the individual ion score exceeded the threshold value (>60) for a random event, it indicated sequence identity or extensive homology ($p<0.05$). The identity of the spot was established as protein that produced the highest score and, consequently, the best match with peptide sequences.

5.9 Bioinformatic analysis

Identified proteins were searched in SecretomeP database (*89*) in order to predict if the secretion pathway was classical (signal peptide) or non-classical (*90*). Moreover, presence of transmembrane domains was investigated: predictions of transmembrane helices of most hydrophobic protein was carried

out using the TMHMM server version 2.0 (*91*, *92*). Subcellular localization was investigated through BLAST algorithm in PSORTdb database (*93*).

5.10 Native protein extraction

SeITE01 cells were grown aerobically at 27°C in Nutrient medium for 24h on a rotary shaker. Proteins were extracted in native form for three different fractions: supernatant (extracellular), cytosolic and membrane fractions. Samples were kept in ice during all the steps. For supernatant fraction, cells were precipitated at 5000xg for 30min (Sorvall centrifuge, GS3 rotor) and kept in ice for subsequent extraction. Supernatant was filtered (Millipore filters, 0.2µm) and native proteins were concentrated with VIVASPIN 6 kit (Sartorius stedium) 10-kDa cut-off (1900xg 30min, 4°C). Protein concentration was estimated through Bradford assay (min 2mg/ml). Samples were stored at -20°C. For cytosolic and membrane fractions, cells were washed twice with 10mM Tris-HCl buffer, pH 7.4, and pelleted at 39100xg, 10 min at 4°C. Pellet was then resuspended in 50ml 10mM Tris-HCl buffer, pH 7.4 and sonicated in ultrasonic processor UP50H (Dr. Hielscher GmbH) (10 cycles of 40sec sonication + 40sec rest in ice), then centrifuged at 22540xg for 40min at 4°C (Optima L-90K, Beckman Coulter). Supernatant (cytosolic fraction) and pellet (membrane fraction) were recovered and native proteins were concentrated with VIVASPIN 6 kit (Sartorius stedium) 10-kDa cut-off (1900xg 30min, 4°C). Protein concentration was estimated through Bradford assay (about 5mg/ml). Samples were stored at -20°C.

5.11 Activity assay

For every fraction, protein activity was assayed for the capability of reducing selenite to elemental selenium. A 96 well-plate was prepared as follows. For each well:

- 100µl of McIlvane buffer (0.2M Na_2HPO_4 + 0.1M citric acid), pH 6.0 to 7.0
- 10µl 100mM sodium selenite
- 50µl native protein solution
- 20µl 20mM NADH
- 20µl H_2O

Activity was assayed at different pH: 6.0, 6.2, 6.4, 6.6, 6.8 and 7.0. Three negative controls were prepared not adding NADH, selenite or protein solution to the well. All samples were tested in triplicate. 96 well-plates

were incubated for 24-48h at room temperature. Reduction of selenite was observed as the appearance of a brick-red color.

5.12 Optical microscopy analysis

B. mycoides SeITE01 cells were cultured in liquid Nutrient medium at 27°C in a shaker, with or without the presence of 2mM sodium selenite. After 6h and 24h of selenite exposure, 100µl of culture were placed on a microscope slide. Samples were colored with Malachite Green stain, heated on a Bunsen burner and washed with water. Finally, cells were colored with Safranin. Samples were observed with a Leica DM750 instrument provided with Leica ICC50 camera.

5.13 TEM analysis

B. mycoides SeITE01 cells were cultured in liquid Nutrient medium at 27°C in a shaker, with or without the presence of 2mM sodium selenite. Cells were harvested after 0, 3, 6, 12 and 24h selenite exposure through centrifugation: 500µl of culture were precipitated at 16000rcf for 3min and resuspended in 1ml of sterile water. Samples were then diluted and 5µl were spotted on CF300-Cu-Carbon Film Copper grids (Electron Microscopy Sciences) and air dried for 24h. Samples were directly observed with high resolution electron microscope Philips CM-100 instrument.

Chapter 6

Results and discussion: SeITE01 SeNPs associated proteins and synthesis model

6.1 Summary

- *Bacillus mycoides* SeITE01 has been studied for its capacity to produce SeNPs: a possible model has been hypothesized
- Such model includes a main extracellular pathway, where protein activity and NPs growth occur outside the cell or on the membrane, and an ancillary pathway, including intracellular reduction followed by cell lysis (*16*)

6.2 Aim of the project

B. mycoides SeITE01 is able to synthesize BioSeNPs surrounded by organic material, including proteins, carbohydrates and lipids (see Chapter 4). Proteins can be particularly informative molecules, and a proteomic analysis of the proteins included in the capping layer could lead to a better comprehension of the biosynthesis mechanisms.

In this chapter the synthesis, maturation and secretion of SeITE01 SeNPs are analyzed. First, SeNPs capping layer is analyzed from a proteomic point of view: associated proteins are identified and proteomic profiles for different extraction protocols are compared. Characteristics of identified proteins are investigated: affinity for SeNPs, subcellular localization, secretion pathway and presence of transmembrane domains. Secondly, a hypothesis is formulated around SeNPs secretion out of the cell and the role of identified proteins in SeNPs maturation. Assays and microscopy analysis are performed in order to provide evidence for the hypothesis.

6.3 *B. mycoides* SeITE01 SeNPs-associated proteins: experimental design and issues

6.3.1 Experimental design

The presence of associated proteins on the surface of *B. mycoides* SeITE01 SeNPs was proposed by Lampis *et al.*, as UV-vis spectrum showed an absorption peak at 280nm, typical of aromatic amino acids (*16*). The goal of this study was to identify such proteins and consider the possible role of these proteins in SeNPs formation and maturation. In this regard, a proteomic study was carried out through protein separation with SDS-PAGE and identification by MS.

To investigate the affinity of proteins to SeNPs regardless their possible role in synthesis/transport/maturation processes, a comparison was performed with ChSeNPs exposed to a SeITE01 CFX. Proteins found on both samples are less likely involved in SeNPs formation, but could still have role in SeNPs maturation and stabilization, interacting with the forming NPs on the basis of affinity and contributing to the capping layer. On the other hand, proteins found only in biogenic samples are more likely to be involved in the first steps of selenite reduction and SeNPs seeds formation, and to be a specific part of the capping layer.

The SDS-PAGE made it possible to compare proteomic profiles of different kinds of samples, like BioSeNPs or exposed ChSeNPs differently extracted or treated. In particular, in order to compare proteomic profiles, BioSeNPs were extracted by using two different protocols: centrifugation through a dense solution or octanol fractioning. Exposed ChSeNPs were recovered from CFX through simple centrifugation or octanol fractioning.

Following identification, bioinformatics analyses were performed to assess function, subcellular localization and possible role of identified proteins. With the list of proteins in hand a hypothesis was formulated for a new model, mainly focusing on transport of SeNPs from the cytosol through the periplasmic membrane and cell wall, to the extracellular space. Additional experiments were then performed to verify this new model.

6.3.2 Comparison between octanol fractioning and sucrose gradient SeNPs extractions

Gradient centrifugation to recover SeNPs from the cell lysate is described as the safest method to prevent protein loss in all previous SeNPs proteomic studies (*37*, *42*). In this study, SeNPs were separated by centrifuging through a 60% sucrose solution. Presence of SeNPs was visible as a brick-red color in the pellet fraction. Additionally, 200 to 800nm spectrum was investigated to visualize a peak around 225nm, typical of SeITE01 SeNPs extracted after 24h (*16*). Notably, a peak around 200nm was previously observed

also for *Pseudomonas alcaliphila* BioseNPs (*50*). However organic solvent fractioning (usually hexane fractioning) is so far the most used method to separate SeNPs from cell lysate. In this study, proteomic profiles were then compared between samples obtained by gradient centrifugation and organic solvent fractioning. Octanol and sucrose extracted samples were treated and analyzed by SDS-PAGE loading the same amount of proteins for both samples (150µg). For sucrose extraction, the protocol used by Dobias for *E. coli* (*37*) was adapted to SeITE01. The major problem using this protocol was a sporadic presence of spores from our organism, which could co-migrate with SeNPs in density gradient. On the other hand, octanol fractioning makes it possible to extract SeNPs without the presence of spores. Regardless, as visible in Figure 6.1, both methods resulted in the same protein pattern. In order to avoid the presence of spores in final samples, a filtration step was added before proteomic analysis of SeNPs.

6.3.3 Comparison between biosynthesized SeNPs and chemically synthesized SeNPs exposed to CFX

Proteomic profiles obtained for BioSeNPs samples were compared to those obtained from ChSeNPs exposed to CFX recovered through octanol fractioning or simple centrifugation. Unlike BioSeNPs, CFX exposed ChSeNPs displayed different proteomic profiles depending on the extraction method. Variability in band intensity was also observed in different extraction batches. On the other hand, BioSeNPs displayed the same profile regardless the extraction method used. Proteomic profile also did not vary after 6 months from the extraction, confirming the characteristic stability of BioSeNPs over time (Figure 6.1, lane C).

Proteins were subsequently identified for both BioSeNPs and CFX exposed ChSeNPs. The results obtained suggest a possible explanation; that proteins identified with BioSeNPs are more probably linked to SeNPs formation and/or maturation than those identified for exposed ChSeNPs (*37*). Moreover, the BioSeNPs protein profile did not change regardless of the batch and the extraction method, while ChSeNPs seemed to bind proteins more randomly between trials.

6.3.4 Experimental issues: interference of capping layer components, protein quantification and profiles

Proteomic identification by MS needs a first step of protein separation. One of the most used techniques is SDS-PAGE, followed by proteins recovery from the bands of the resulting proteomic profile. Protein separation by SDS-PAGE is possible by directly loading BioSeNPs treated with a denaturing buffer (usually Laemmli buffer, see Chapter 5) and heat in order to allow proteins to detach from the SeNPs and run inside the gel. A first ex-

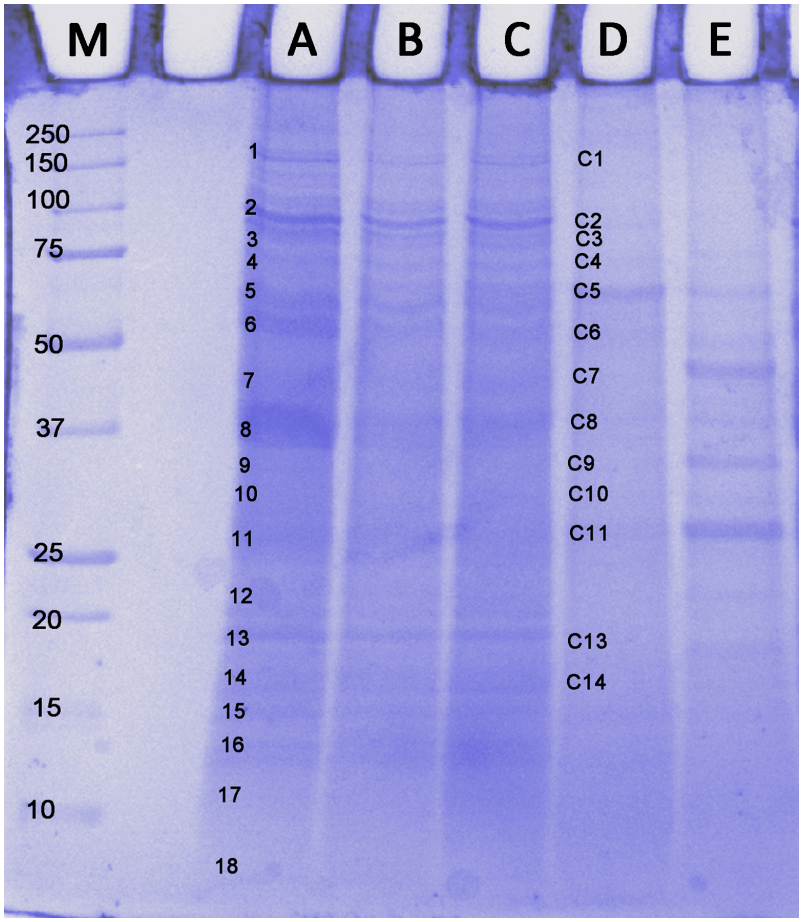

Figure 6.1: Proteomic profiles for BioSeNPs extracted by octanol fractioning (A) or gradient centrifugation (B, C) and exposed ChSeNPs recovered by centrifugation (D) or octanol fractioning (E). Sample in lane C was stored at 4°C for 6 months before analysis

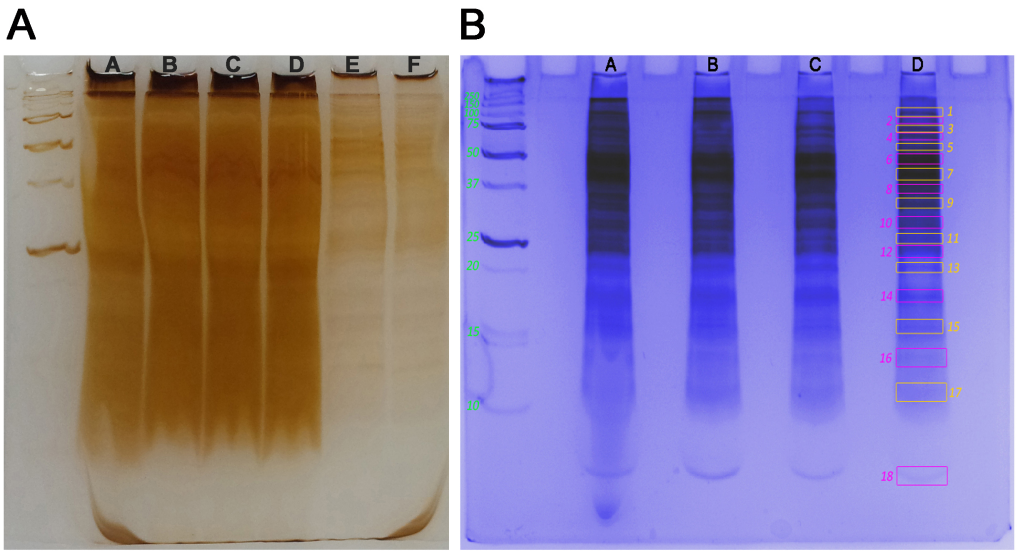

Figure 6.2: panel A: SDS-PAGE of BioSeNPs and exposed ChSeNPs directly loaded in a 12% T polyacrylamide gel. The smear caused by the other capping layer components is especially evident for BioSeNPs replicas (lanes A/D), but can be seen also in exposed ChSeNPs lanes (E-F). Traces of Se are visible on the bottom of the gel. Gel was visualized with a Silver stain. panel B: SeITE01 BioSeNPs only directly loaded in a 15% T polyacrylamide gel (lains A/D). Despite the proteomic profile being visible, the smear caused by other capping layer components is still present. Gel was visualized through Coomassie Blue staining

periment was carried out, directly loading BioSeNPs. This approach makes it possible to skip the extraction step of the organic material from SeNPs. However, the other components of the capping layer detach from SeNPs together with proteins, causing a long smear, which mostly overwhelms the protein bands. This smear was only weakly visible for exposed ChSeNPs (Figure 6.2, panel A), probably because BioSeNPs capping layer is more complex than the one associating with ChSeNPs. In fact, BioSeNPs capping could be formed by membrane fragments, as lipid content is particularly high (see Chapter 4 and Section 4.4.1), while for the CFX preparation, membranes tend to be discarded on the preparation of the CFX. Consequently, ChSeNPs do not gain lipid content comparable to BioseNPs. In Figure 6.2, panel B, shows a second attempt to run SeNPs directly on SDS-PAGE by increasing the amount of material. A smear is still visible, but protein profile can be distinguished. Proteins digestion and a clean peptides extraction from the corresponding bands were not possible. Thus an extraction step for the proteins from SeNPs was necessary in order to separate them from other capping layer components, recover corresponding peptides and identify associated proteins (Figure 6.1).

The proteomic profile in Figure 6.2, panel B, shows no difference with the one in Figure 6.1, indicating that treatment with Laemmli Buffer (*87*) successfully detaches proteins from SeNPs. Presence of a lighter smear in Figure 6.1 also indicates that precipitation with acetone makes it possible to separate proteins from the other capping layer components, but not completely. Finally, another issue was the low definition of bands corresponding to higher molecular weights. Consequently, in order to increase bands separation, polyacrylamide gel was changed from 12% to 15% T (Figure 6.2) to a gradient 8-18% T polyacrylamide gel (Figure 6.1).

Overall, two important differences between BioSeNPs and CFX exposed ChSeNPs emerged after protocol optimization (separation of proteins by acetone precipitation and gradient polyacrylamide gel). While BioSeNPs proteomic profile did not change for different samples and treatments, CFX exposed ChSeNPs proteomic profile varied depending on the batch and the recovery protocol. Regardless, the position of protein bands in CFX exposed ChSeNPs profiles tend not to change, despite differences in intensity. It is not clear if this variability is due to CFX preparation or happens during the exposition step. It can also be hypothesized, that protein association with CFX exposed ChSeNPs is much less specific than to BioSeNPs. For BioSeNPs, proteins could be in part from cell membrane fragments possibly surrounding SeNPs, while ChSeNPs tend to bind cytosolic proteins from the CFX (see below).

Other differences were noticed during protein quantification. Proteins precipitated with acetone were subsequently quantified in order to load 150µg of proteins for each lane. First, proteins were quantified using Bradford assay; this assay turned out to be imprecise. To increase precision, a BCA kit was used instead of Bradford assay. Despite an actual increase in quantification precision, BCA assay tent to either underestimate protein content in samples extracted from BioSeNPs, or overestimate samples from exposed ChSeNPs. As a result, weaker bands were visible on the gels for exposed ChSeNPs despite trying to load 150µg of protein per sample (this is also visible in Figure 6.1).

Later it was hypothesized, that trace Se preset inside the samples or other components of the layer could interfere with protein quantification, for example lipids or glycoproteins could remain attached to proteins even after precipitation with acetone. In Figure 6.1 a weak smear can in fact be observed even after the addition of the protein extraction step. It is also particularly evident, that for BioSeNPs more material was loaded into the gel (Lains A, B and C), compared with ChSeNPs samples (Lains D and E), even if for both samples 150µg of proteins were quantified using BCA assay.

Presence of proteins in the supernatant of BioSeNPs prior precipitation and extraction with Laemmli Buffer was also investigated through precipitation with acetone and BCA assay. Contrarily to Chapter 4, presence of proteins in the supernatant was not detected. This could be due to both

different extraction protocols (proteins were identified following extraction in sucrose gradient, while in Chapter 4 octanol fractioning was used) or the number of times the sample was washed with water. Even if, as previously said, BCA assay could slightly underestimate protein quantity in the presence of Se traces or capping layer components, we should consider, that supernatant proteins precipitated with acetone should contain less Se or organic residues, being precipitated from a solution with more diluted organic material.

6.4 Results and Discussion

6.4.1 Identified proteins

After protein separation by SDS-PAGE, bands were cut out, proteins digested with trypsin and peptides purified from the gel. Proteins were identified by running the peptides on a NanoHPLC-Chip, followed MS/MS and bioinformatics analysis with Mascot software. Table 6.1 shows proteins identified associated with biogenic SeNPs. Identifications listed are based on a good "Mascot score": a score >67 indicates that the matching has a probability less than 5% of being a random event (*88*). Remaining columns show estimated mass (Mr) and isoelectric point (pI) of the protein, followed by the sequence coverage of the identified peptides.

We identified BioSeNPs-associated proteins, which mainly belong to protein and amino acid, redox and cell wall metabolic pathways (Tables 6.1 and 6.5). As expected, proteins capable of reductase activity were found, which are possibly involved in selenite reduction to zero-valent SeNPs: glutamate dehydrogenase, a protein belonging to NADH dehydrogenase family and glyceraldehyde-3-phosphate dehydrogenase (GADPH).

Some membrane transporters and proteins involved in cell wall metabolism were also found, such as: penicillin-binding protein (PBP) and peptidoglycan endopeptidase, involved in peptidoglycan synthesis, and lysozyme (peptidoglycan degradation pathway), a protein translocase and an ABC transporter substrate-binding protein. A thiol:disulfide interchange protein and ATPase subunits were identified as well. Several proteins involved in polypeptide synthesis and amino acid metabolism were also identified, including: elongation factors Tu and G (EF-Tu, EF-G), ribosomal proteins, peptidase P60 and glutamate dehydrogenase. Interestingly, a stress protein was also found related to Tellurium stress (TerD domain).

Proteins associated to ChSeNPs were identified as well (Table 6.2). As for biogenic samples, proteins belonging to protein and amino acid metabolism, primary and redox metabolism were identified. GADPH, ATPase-subunit beta, EF-Tu and EF-G were found associated to both BioSeNPs and ChSeNPs. Also, proteins with a similar function (ribosomal proteins and peptidases) were identified for both samples. Following identification, proteins were compared and investigated through literature and bioinformatics for: affinity to Se, involvement in key pathways, subcellular localization, secretion pathway and presence of transmembrane domains.

6.4.2 Identified proteins and affinity to Selenium

In order to better understand the probability of identified proteins to be involved in formation or maturation of SeNPs, identifications were compared to previous studies. Dobias and colleagues in 2011 compared proteins associated to *E. coli* BioSeNPs with proteins associated to ChSeNPs and FeNPs

Spot	Name	Origin	NCBI num.	Peptides	Macot Score	Mr (Da)	pI	Seq. Cov. (%)
1	penicillin-binding protein	*B. cereus*	WP_002119238.1	2	162	91585	8.9	4
1	MULTISPECIES: protein translocase subunit SecDF	*B. cereus* group	WP_001119051.1	2	73	82588	9.48	3
1, 2	elongation factor G	*B. mycoides*	WP_033797762.1	8	383	76278	4.93	13
3	peptide ABC transporter substrate-binding protein	*B. mycoides*	WP_078206463.1	2	73	59867	6.34	3
3, 5	ATP synthase subunit alpha	*B. mycoides*	WP_042981039.1	2	79	54477	5.37	4
3, 4, 5, 14	ATP synthase subunit beta	*Bacillus*	WP_001032596.1	9	453	51020	4.92	22
5	glutamate dehydrogenase	*B. mycoides*	WP_042982821.1	3	180	47447	6.17	9
6	peptidoglycan endopeptidase	*B. mycoides*	WP_059038255.1	2	91	45197	9.55	5
5	peptidase P60	*Bacillus* sp. LK2	WP_048372757.1	3	148	44654	9.39	9
4, 5, 6, 7	translation elongation factor Tu	*B. mycoides*	WP_042981370.1	5	268	43028	4.9	13
6, 7	NADH dehydrogenase family protein	*B. mycoides*	WP_044439292.1	6	286	41526	6.47	20
13	lysozyme family protein	*B. mycoides*	WP_060751007.1	3	118	35996	6.44	13
6, 7	glyceraldehyde-3-phosphate dehydrogenase, partial	*B. cereus*	KWW52438.1	2	89	32112	5.45	9
7	lysozyme, partial	*B. mycoides*	WP_088004971.1	2	73	25108	6.89	7
13	stress protein	*B. mycoides*	WP_078213816.1	2	81	21975	5.47	11
13	thiol:disulfide interchange protein	*B. mycoides*	WP_044441543.1	2	75	20612	5.95	10
13, 14	MULTISPECIES: 50S ribosomal protein L5	*B. cereus* group	WP_016116955.1	2	88	20151	9.61	20
14	30S ribosomal protein S7	*B. cereus*	WP_063222353.1	1	93	18020	9.99	10
14	MULTISPECIES: 30S ribosomal protein S5	*B. cereus* group	WP_002063426.1	2	121	17524	9.79	15

Table 6.1: Proteins identified for BioSeNPs coating. In the first column (Spot), origin protein bands are indicated. Following: name of the protein (Name) and microorganism (Origin), NCBI database classification number (NCBI num), number of peptides identified by MS (Peptide), score attributed to the identification from the software (Mascot Score), molecular mass of the protein in Da (Mr), calculated isoelectric point (pI) and sequence coverage of the identified peptides on the whole protein sequence (Seq. Cov.)

Spot	Name	Origin	NCBI num.	Peptides	Macot Score	Mr (Da)	pI	Seq. Cov. (%)
2	5-methyltetrahydropteroyltriglutamate-homocysteine methyltransferase	*B. mycoides*	KZE07161.1	2	84	91301	5.38	2
2	formate acetyltransferase	*B. mycoides*	WP_033733733.1	3	140	84403	5.61	4
1	elongation factor G	*B. mycoides*	WP_033797762.1	4	157	76278	4.93	5
2	MULTISPECIES: molecular chaperone DnaK	*B. cereus* group	WP_000034694.1	6	262	65654	4.65	9
3	MULTISPECIES: molecular chaperone GroEL	*B. cereus* group	WP_002029451.1	3	148	57396	4.81	7
5	ATP synthase subunit beta	*B. mycoides*	WP_042981037.1	2	67	51078	4.89	4
6	aminopeptidase	*B. mycoides*	WP_003202305.1	2	101	50379	8.63	4
4, 5	dihydrolipoyl dehydrogenase	*B. cereus* group	WP_000260101.1	5	284	49410	5.32	14
5	enolase	*B. cereus*	KWW52376.1	4	200	46423	4.63	11
3, 4	branched-chain alpha-keto acid dehydrogenase subunit E2	*B. mycoides*	WP_003199953.1	3	93	45615	5.39	8
5	methionine adenosyltransferase	*B. mycoides*	WP_003208790.1	2	96	43352	5.16	6
6	translation elongation factor Tu	*B. mycoides*	WP_042981370.1	6	286	43028	4.9	16
6	alanine dehydrogenase	*B. mycoides*	WP_042980294.1	2	73	40033	5.49	8
6	MULTISPECIES: type I glyceraldehyde-3-phosphate dehydrogenase	*B. cereus* group	WP_002112805.1	3	191	35905	5.2	13
7, 8	Pyruvate dehydrogenase E1 component subunit beta	*B. cereus*	CUB10128.1	3	154	35221	4.76	10
11	MULTISPECIES: 30S ribosomal protein S3	*B. cereus* group	WP_002009771.1	5	211	24280	9.99	24

Table 6.2: Proteins identified for CFX exposed ChSeNPs coating. In the first column (Spot), origin protein bands are indicated. Following: name of the protein (Name) and microorganism (Origin), NCBI database classification number (NCBI num), number of peptides identified by MS (Peptide), score attributed to the identification from the software (Mascot Score), molecular mass of the protein in Da (Mr), calculated isoelectric point (pI) and sequence coverage of the identified peptides on the whole protein sequence (Seq. Cov.)

exposed to an *E. coli* CFX (*37*). In the same year, Lenz and colleagues identified proteins associated to BioSeNPs synthesized by two respiratory Se reducers (dissimilatory pathway): *Bacillus selenatarsenatis* and *Sulfospirillum barnesii*; as well as *Rhodospirillum rubrum*, which precipitates Se in a non-dissimilatory manner. The authors also used exposed ChSeNPs as a control (*42*). In 2016, Gonzalez-Gil *et al.* analyzed SeNPs produced by anaerobic granular sludge (mainly composed of *Veillonellaceae* and *Pseudomonadaceae*) and identified associated proteins (*65*).

Many of the proteins found on BioSeNPs in this thesis were previously observed by these authors (Table 6.3) including: peptide ABC transporter, ribosomal proteins S7 and L5, EF-Tu, EF-G, both subunits of ATPase, GADPH and NADH dehydrogenase. Most of these proteins were also found associated to ChSeNPs exposed to CFX of *E. coli* (*37*) with the exception of ATPase-subunit beta and ribosomal proteins. Some were also found on FeNPs exposed to *E. coli* CFX (EF-Tu and ATPase), suggesting an affinity to Se for these proteins. Interestingly, EFs, ATPase and GADPH were found associating to both biogenic and chemical SeNPs also in this study. However, these proteins are in high abundance in bacteria and are routinely found in proteomic studies with bacteria. Therefore, it cannot be ruled out those proteins such EF-Tu, EF-G and ribosomal constituents may be in fact artifacts.

Almost all of proteins identified for ChSeNPs in this study were found on ChSeNPs in previous studies (Table 6.4): methionine adenosyltransferase (s-adenosylmethionine synthetase), pyruvate dehydrogenase and formate acetyltransferase only for ChSeNPs; with the proteins EFs, molecular chaperones GroEL and DnaK, ribosomal protein S3, dihydrolipoyl dehydrogenase and GADPH were identified for both biogenic and chemical samples. Conversely, a putative aminopeptidase was identified for granular sludge and Se-respirers BioSeNPs, respectively, while in this study it was only found on ChSeNPs.

In conclusion, EF-Tu and ATPase do not specifically associate with biogenic SeNPs, but have probably an affinity to metal NPs in general, being found on both BioSeNPs and ChSeNPs, and FeNPs. On the other hand, EF-G and GADPH can be found on both BioSeNPs and ChSeNPs, but not on FeNPs, suggesting an affinity for SeNPs only. However, it is unlikely that such proteins are directly involved in synthesis or maturation of SeITE01 SeNPs. Conversely, protein translocase SecDF, PBP, lysozyme, peptidoglycan endopeptidase, peptidase P60, ribosomal proteins S5, S7 and L5, glutamate dehydrogenase, stress protein (TerD) and thiol:disulphide interchange protein were found only associating to BioSeNPs in this study and, when present in the other proteomic studies on SeNPs, these proteins were not found on CFX exposed ChSeNPs. The presence of a Te-stress related protein is of particularly interest, given that Te is far more toxic but chemically similar to Se. Due to higher Te toxicity (tellurite can be

tolerated in the order of µM, compared to mM for selenite), Te-resistance mechanisms are generally specific, while Se-resistance pathways are not (*2*). In fact, many indications of stress were observed by Lampis *et al.* during production of SeNPs in SeITE01 cultures: cultivation in 2mM sodium selenite negatively affected growth of SeITE01 culture and TEM analysis also revealed the presence of polyhydroxibutyrate granules inside the cells and a slight increase of bacterial cell length (*16*).

6.4.3 Localization of identified proteins: secretion pathway and transmembrane domains

Identified proteins mainly belong to protein/amino acid and primary metabolism, but there are also membrane proteins and proteins associated with the cell wall. In order to better understand the role of identified proteins, sequences were analyzed with PSORTdb database (*93*) for subcellular localization data. Similar proteins were found in the database for *B. mycoides* strains or other members of *B. cereus sensu lato* group.

BioSeNPs proteins display different localizations (Table 6.5): 9 cytoplasmic proteins (mainly protein and primary metabolism), 6 membrane proteins and 4 cell wall associated proteins (including transporters and cell wall metabolism proteins). Proteins associated to ChSeNPs are almost all localized in the cytosol (14 proteins), while one is extracellular (aminopeptidase) and one is a membrane protein (ATPase-subunit beta) (Table B.1, Appendix). Overall, the main difference between proteins identified for BioSeNPs and ChSeNPs is the presence, for biogenic samples, of membrane and cell wall associated proteins, which are absent in chemical samples. However, this could be also due to CFX preparation method: between culture sonication and ChSeNPs exposition, the culture is centrifuged in order to remove intact cells and cell debris, causing co-precipitation of membrane fragments. Consequently, total lipid content of exposed ChSeNPs is not comparable to BioSeNPs, and membrane bound proteins could be absent for this reason.

Protein sequences were also investigated for the presence of transmembrane regions on THMM database: for BioSeNPs, cell wall associated proteins peptide ABC transporter associated binding protein, and thiol:disulphide interchange protein all have one transmembrane domain. Membrane proteins PBP and NADH dehydrogenase family protein also have one transmembrane domain; while membrane protein SecDF has 12 transmembrane domains (Table 6.5).

For ChSeNPs, only the extracellular protein aminopeptidase has 2 transmembrane domains (Table B.1, Appendix).

Finally, identified proteins were investigated for the secretion pathway using SecretomeP database (*89*). Three proteins for BioSeNPs and one for ChSeNPs are predicted to be secreted based on the presence of a sig-

Name	Origin	NCBI num.	Chem	*E. coli* (*37*)	Se-reducers (*42*)	Anaerobic granules (*65*)
penicillin-binding protein	*B. cereus*	WP_002119238.1	—	—	—	—
MULTISPECIES: protein translocase subunit SecDF	*B. cereus* group	WP_001119051.1	—	—	—	—
elongation factor G	*B. mycoides*	WP_033797762.1	x	Chem	—	Bio
peptide ABC transporter substrate-binding protein	*B. mycoides*	WP_078206463.1	—	Bio, Chem	—	—
ATP synthase subunit alpha	*B. mycoides*	WP_042981039.1	—	Chem, FeNPs	Bio	Bio
ATP synthase subunit beta	*Bacillus*	WP_001032596.1	x	FeNPs	—	Bio
glutamate dehydrogenase	*B. mycoides*	WP_042982821.1	—	—	—	—
peptidoglycan endopeptidase	*B. mycoides*	WP_059038255.1	—	—	—	—
peptidase P60	*Bacillus* sp. LK2	WP_048372757.1	—	—	—	—
translation elongation factor Tu	*B. mycoides*	WP_042981370.1	x	Bio, Chem, FeNPs	Bio	Bio
NADH dehydrogenase family protein	*B. mycoides*	WP_044439292.1	—	—-	Bio, Chem	—
lysozyme family protein	*B. mycoides*	WP_060751007.1	—	—	—	—
glyceraldehyde-3-phosphate dehydrogenase, partial	*B. cereus*	KWW52438.1	x	Bio, Chem	Bio	Bio
lysozyme, partial	*B. mycoides*	WP_088004971.1	—	—	—	—
stress protein	*B. mycoides*	WP_078213816.1	—	—	—	—
thiol:disulfide interchange protein	*B. mycoides*	WP_044441543.1	—	—	—	—
MULTISPECIES: 50S ribosomal protein L5	*B. cereus* group	WP_016116955.1	—	—	—	Bio
30S ribosomal protein S7	*B. cereus*	WP_063222353.1	—	—	—	Bio
MULTISPECIES: 30S ribosomal protein S5	*B. cereus* group	WP_002063426.1	—	—	—	—

Table 6.3: Proteins found in other proteomic studies on SeNPs: name of the protein (Name) and microorganism (Origin), NCBI database classification number (NCBI num), presence of the same protein in exposed ChSeNPs (Chem), presence of the same protein in other studies: *E. coli* (*37*), Se-reducers (*42*) and anaerobic granules (*65*)

Name	Origin	NCBI num.	Chem	*E. coli* (*37*)	Se-reducers (*42*)	Anaerobic granules (*65*)
5-methyltetrahydropteroyltriglutamate-homocysteine methyltransferase	*B. mycoides*	KZE07161.1	—	—	—	—
formate acetyltransferase	*B. mycoides*	WP_033733733.1	—	Chem	—	—
elongation factor G	*B. mycoides*	WP_033797762.1	x	Chem	—	Bio
MULTISPECIES: molecular chaperone DnaK	*B. cereus* group	WP_000034694.1	—	—	Bio, Chem	—
MULTISPECIES: molecular chaperone GroEL	*B. cereus* group	WP_002029451.1	—	Chem	Bio, Chem	—
ATP synthase subunit beta	*B. mycoides*	WP_042981037.1	x	FeNPs	—	Bio
aminopeptidase	*B. mycoides*	WP_003202305.1	—	—	—	Bio
dihydrolipoyl dehydrogenase	*B. cereus* group	WP_000260101.1	—	Chem	Bio, Chem	Bio
enolase	*B. cereus*	KWW52376.1	—	FeNPs	Bio	—
branched-chain alpha-keto acid dehydrogenase subunit E2	*B. mycoides*	WP_003199953.1	—	—	—	—
methionine adenosyltransferase	*B. mycoides*	WP_003208790.1	—	Chem	—	—
translation elongation factor Tu	*B. mycoides*	WP_042981370.1	x	Bio, Chem, FeNPs	Bio	Bio
alanine dehydrogenase	*B. mycoides*	WP_042980294.1	—	—	—	—
MULTISPECIES: type I glyceraldehyde-3-phosphate dehydrogenase	*B. cereus* group	WP_002112805.1	x	Bio, Chem	Bio	Bio
Pyruvate dehydrogenase E1 component subunit beta	*B. cereus*	CUB10128.1	—	Chem, FeNPs	—	—
MULTISPECIES: 30S ribosomal protein S3	*B. cereus* group	WP_002009771.1	—	Bio, Chem, FeNPs	Bio	Bio

Table 6.4: Proteins found in other proteomic studies on SeNPs: name of the protein (Name) and microorganism (Origin), NCBI database classification number (NCBI num), presence of the same protein in BioSeNPs (Bio), presence of the same protein in other studies: *E. coli* (*37*), Se-reducers (*42*) and anaerobic granules (*65*)

Name	Origin	NCBI num.	Loc	Metabolism	Secretion pathway	Transmembrane domains
lysozyme, partial	*B. mycoides*	WP_088004971.1	Membrane	Cell wall	non-classic	no
stress protein	*B. mycoides*	WP_078213816.1	Cytoplasmic	Stress	no	no
peptide ABC transporter substrate-binding protein	*B. mycoides*	WP_078206463.1	Cell wall	ABC transporters	signal peptide	1
30S ribosomal protein S7	*B. cereus*	WP_063222353.1	Cytoplasmic	Protein	no	no
lysozyme family protein	*B. mycoides*	WP_060751007.1	Membrane	Cell wall	non-classic	no
peptidoglycan endopeptidase	*B. mycoides*	WP_059038255.1	Cell wall	Cell wall	signal peptide	no
peptidase P60	*Bacillus* sp. LK2	WP_048372757.1	Cell wall	Protein	signal peptide	no
thiol:disulfide interchange protein	*B. mycoides*	WP_044441543.1	Cell wall	Other	non-classic	1
NADH dehydrogenase family protein	*B. mycoides*	WP_044439292.1	Membrane	Oxidoreductase	no	1
glutamate dehydrogenase	*B. mycoides*	WP_042982821.1	Cytoplasmic	Protein/amino acid	no	no
translation elongation factor Tu	*B. mycoides*	WP_042981370.1	Cytoplasmic	Protein	no	no
ATP synthase subunit alpha	*B. mycoides*	WP_042981039.1	Cytoplasmic	Primary	no	no
elongation factor G	*B. mycoides*	WP_033797762.1	Cytoplasmic	Protein	no	no
MULTISPECIES: 50S ribosomal protein L5	*B. cereus* group	WP_016116955.1	Cytoplasmic	Protein	no	no
penicillin-binding protein	*B. cereus*	WP_002119238.1	Membrane	Cell wall	non-classic	1
MULTISPECIES: 30S ribosomal protein S5	*B. cereus* group	WP_002063426.1	Cytoplasmic	Protein	no	no
MULTISPECIES: protein translocase subunit SecDF	*B. cereus* group	WP_001119051.1	Membrane	Membrane	non-classic	12
ATP synthase subunit beta	*Bacillus*	WP_001032596.1	Membrane	Primary	no	no
glyceraldehyde-3-phosphate dehydrogenase, partial	*B. cereus*	KWW52438.1	Cytoplasmic	Primary	no	no

Table 6.5: Localization of BioSeNPs proteins: name of the protein (Name) and microorganism (Origin), NCBI database classification number (NCBI num), subcellular localization based on PSORTdb database (Loc), role in cell metabolism (Metabolism), type of secretion pathway based on SecretomeP database (Secretion pathway), presence of transmembrane domain based on TMHMM database (Transmembrane domains)

nal peptide (classic secretion). These include for biogenic samples: cell wall proteins peptide ABC transporter substrate-binding protein, peptidase P60, and peptidoglycan endopeptidase. An aminopeptidase (extracellular) was identified for ChSeNPs. Other proteins are not secreted or are secreted in a non-classic way: SecDF, PBP, lysozyme and thiol:disulphide interchange protein. This study is the first time that these proteins were found to be associated to BioSeNPs (Table 6.5); SecretomeP scores are shown in Tables B.3 and B.4, Appendix). In contrast, almost all proteins associated to ChSeNPs are not secreted (Table B.1, Appendix).

6.4.4 Membrane and cell wall proteins: a possible link to vesicle transport?

Localization of proteins in SeITE01 cell and analysis of secretion pathway, plus the presence of membrane and cell wall associated proteins only for BioSeNPs, lead to an interesting hypothesis: membrane and cell wall associated proteins are characteristic of biogenic SeNPs produced by *B. mycoides* SeITE01. This relates to previous studies that showed that SeNPs are mainly extracellular after 24h of incubation with selenite (*16*) and that few SeNPs are visible in the cytoplasm at any stage of growth. Thus it can be hypothesized, that SeNPs nucleation seeds formed in the cytoplasm or on the inner side of the membrane are then exported through the membrane and cell wall using vesicle-like structures. Of course this assumes that the selenite gets into the cytoplasm at all in any significant concentration. In 2012, Zhang *et al.* demonstrated that under microaerophilc conditions, the yeast *Saccharomyces cerevisiae* produces SeNPs through expulsion by vesicle-like structures. In their study, they also observed SeNPs associated to organic molecules, especially proteins. They postulated this capping layer has a stabilizing effect and its presence is due to the break down of vesicle-like structures (*94*).

Many of the BioSeNPs-associated proteins found in our study were also found associated to sporulation process in *B. cereus* group (Table 6.6). Mukhopadhyay and colleagues found GADPH, ATPase, enolase, ABC transporters, chaperones and EFs in the spore proteome of *B. anthracis* and *B. cereus sensu lato* group (*95*). Del Vecchio *et al.* also found these proteins in *B. cereus* spores (*96*). Curiously, many proteins associated to ChSeNPs are linked to sporulation process, probably because of the affinity of primary metabolism proteins for SeNPs (Table B.2, Appendix).

Presence of spores was also verified for SeITE01 in the presence of 2mM selenite (see also Chapter 6.4.5 below): in Figure 6.3 SeITE01 cells grown in the presence of 2mM selenite are shown. Presence of spores was much stronger in the case of cells grown with selenite, probably due to stress.

Considering all proteomic data and related information, a new model could be formulated for transport of SeNPs outside the cell following the

Name	Origin	NCBI num.	*B. cereus* spores (*96*)	*B. anthracis* spores (*95*)
penicillin-binding protein	*B. cereus*	WP_002119238.1	—	—
MULTISPECIES: protein translocase subunit SecDF	*B. cereus* group	WP_001119051.1	—	—
elongation factor G	*B. mycoides*	WP_033797762.1	x	x
peptide ABC transporter substrate-binding protein	*B. mycoides*	WP_078206463.1	x	x
ATP synthase subunit alpha	*B. mycoides*	WP_042981039.1	x	x
ATP synthase subunit beta	*Bacillus*	WP_001032596.1	x	x
glutamate dehydrogenase	*B. mycoides*	WP_042982821.1	—	—
peptidoglycan endopeptidase	*B. mycoides*	WP_059038255.1	—	—
peptidase P60	*Bacillus* sp. LK2	WP_048372757.1	—	—
translation elongation factor Tu	*B. mycoides*	WP_042981370.1	x	x
NADH dehydrogenase family protein	*B. mycoides*	WP_044439292.1	—	—
lysozyme family protein	*B. mycoides*	WP_060751007.1	—	—
glyceraldehyde-3-phosphate dehydrogenase, partial	*B. cereus*	KWW52438.1	x	x
lysozyme, partial	*B. mycoides*	WP_088004971.1	—	—
stress protein	*B. mycoides*	WP_078213816.1	x	—
thiol:disulfide interchange protein	*B. mycoides*	WP_044441543.1	—	—
MULTISPECIES: 50S ribosomal protein L5	*B. cereus* group	WP_016116955.1	—	—
30S ribosomal protein S7	*B. cereus*	WP_063222353.1	—	—
MULTISPECIES: 30S ribosomal protein S5	*B. cereus* group	WP_002063426.1	—	—

Table 6.6: Proteins identified also in spore proteome of other members of *B. cereus sensu lato* group: name of the protein (Name) and microorganism (Origin), NCBI database classification number (NCBI num), presence of the same protein in spore proteome of other members of *B. cereus sensu lato* group: *B. cereus* spores (*96*), *B. anthracis* spores (*95*)

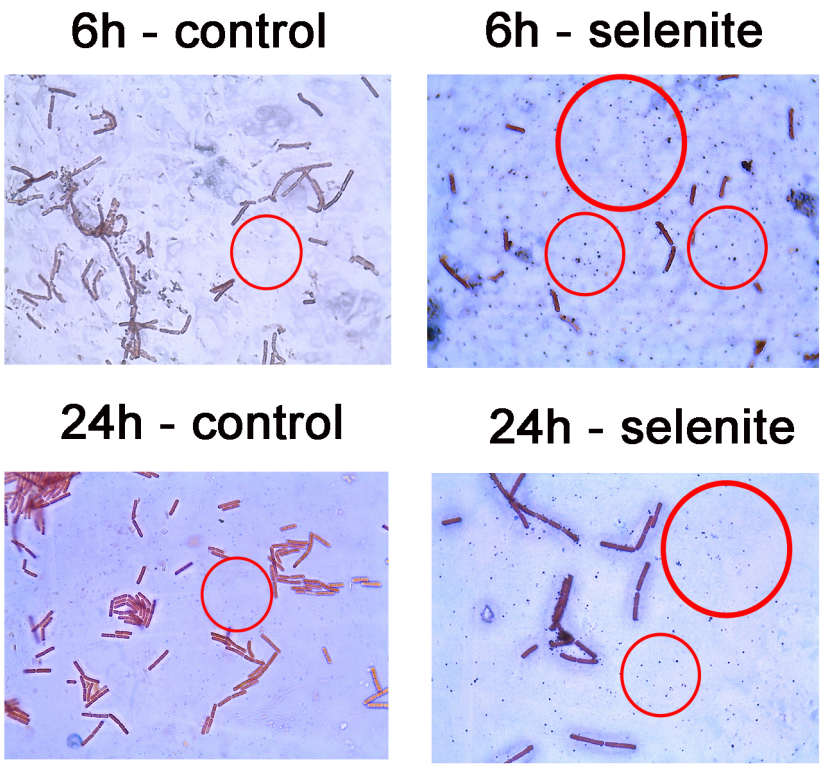

Figure 6.3: SeITE01 cells observed by optical microscopy analysis (100x) and Malachite Green spore staining. A stronger presence of spores can be observed in samples treated with selenite compared to controls

formation of nascent SeNPs inside the cell. In fact, the current model of SeNPs formation also includes a cytosolic pathway (Figure 6.10 - panel I), while cell lysis is proposed as the release mechanism of such SeNPs. Here it is hypothesized, that small sub-10nm Se^0 particles or early formation of SeNPs are released outside the cell through a mechanism possibly linked to vesiculation and/or sporulation. This new model could explain the presence of both secreted and non secreted proteins in SeNPs capping layer (Section 6.4.3): non secreted proteins would remain attached to SeNPs during nucleation seeds formation, while secreted and membrane proteins would associate to growing SeNPs during their transport outside the cell. The new proposed model is schematized in Figure 6.9.

6.4.5 Verifying the hypothesis: activity assay and microscopy study

In order to evaluate the activity of selenite reduction, an extraction of native proteins from the different cell compartments was performed. Following, activity of such proteins towards selenite was assayed. Particularly, this activity assay was performed in order to verify the presence of selenite reduction in the membrane fraction (Figure 6.4). This assay worked very well showing selenite reduction only in the membrane fraction. Surprisingly, reduction of selenite to elemental selenium occurred also in the absence of the electron donor NADH, indicating that enzymatic activity is not the only reduction mechanism (*16*). Selenite reduction activity from a membrane fraction was also previously observed for SeITE01 by Lampis *et al.* However in this case, reduction was observed only after the addition of NADH. Moreover, activity was observed in the extracellular fraction, with a very little activity also in the cytoplasm (*16*). The presence of activity in the membrane fraction could explain the presence of lipids and membrane-localized proteins in SeNPs capping layer (see Section 4.4.1). However it is not sufficient data to prove the new model.

Cultures of SeITE01 exposed to selenite were analyzed with TEM microscopy in order to visualize the localization of SeNPs during the synthesis phase. In Figure 6.5, vesicles are visible after 24h incubation in sodium selenite: vesicles are visible along the cell wall (panel A) with the impression of being secreted outside the cell through holes in the cell wall (panel B). SeNPs, being electron-dense, are visible in TEM figures as black or dark grey spots. In panels C and D (Figure 6.5), SeNPs are visible inside the cell in proximity of the holes in the cell wall.

In Figures 6.6 and 6.7, a time course analysis is shown: control cells and cells grown in the presence of 2mM sodium selenite were collected after 0, 3, 6, 12 (Figure 6.6) and 24h (Figure 6.7) of growth and visualized. Cultures do not show significant differences after 3h of growth (panel A). Growth curve also did not show any difference after 3h (Figure 6.8). After 6h culturing with or without selenite, the two samples start to show significant differences. Growth is lower for the culture supplied with selenite compared with control. Also, optic microscopy analysis indicates an increased production of spores, probably due to stressing conditions (Figure 6.3), even if spores were also observed in the control culture. TEM analysis shows the presence of vesicle-like structures at the poles of the cells even for control sample (Figure 6.6, panel B), while for selenite-treated sample, presence of vesicles (less than 100nm) was evidenced together with the presence of spores (about 500nm). Electron-dense material is associated to some of these vesicles, but we can not state it is Se.

After 12h, control cells start to show the presence of greyish material (electron-dense) surrounding the cell walls (Figure 6.6, panel C). Curiously,

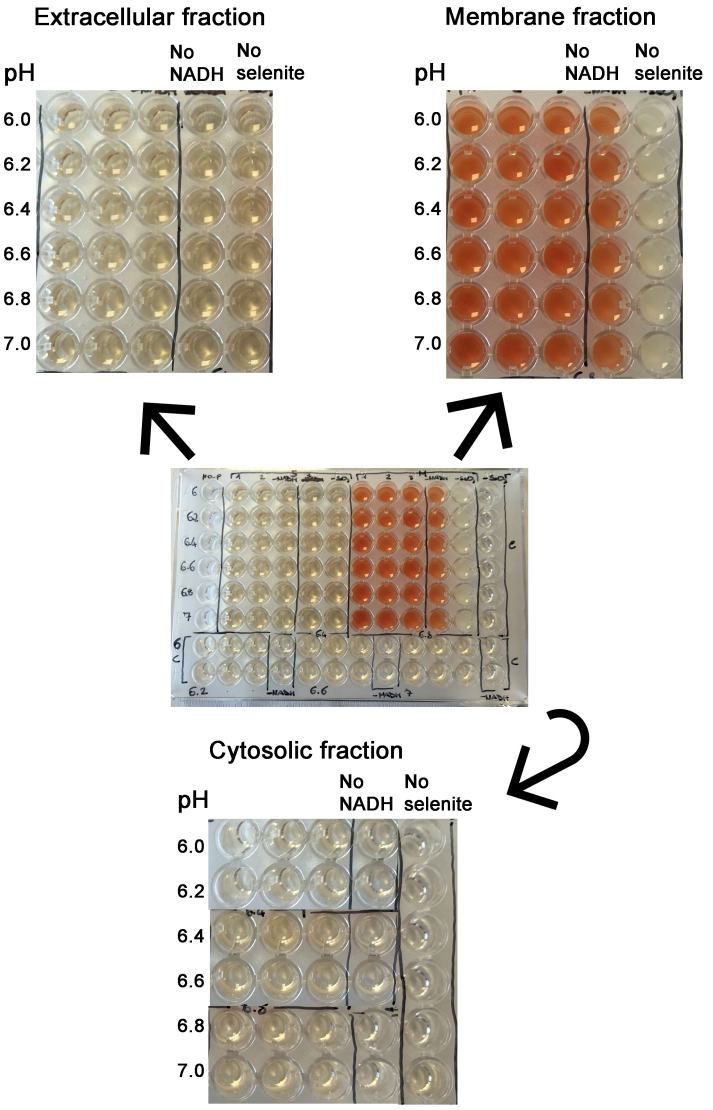

Figure 6.4: Activity assay on *B. mycoides* SeITE01 native extracts from cytosolic, membrane and extracellular fractions. Selenite reduction can be observed by the appearance of a red color in the wells corresponding to membrane fraction. Selenite reduction occurs at all pH tested (from 6 to 7) also in the absence of an electron donor

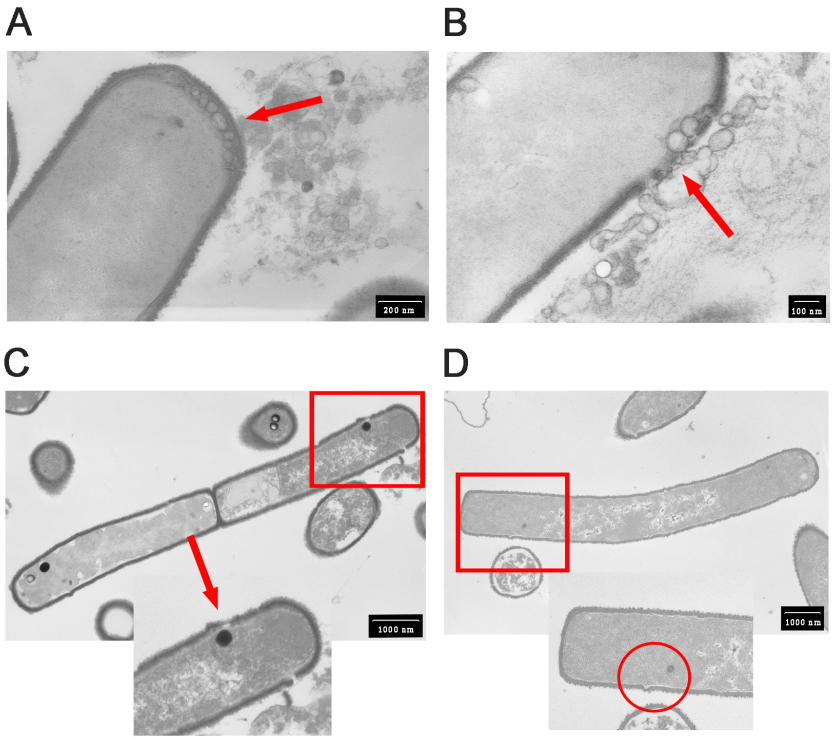

Figure 6.5: Vesicles approaching the cell wall (A). Discontinuity in the cell wall close to vesicles and SeNPs (B, C). Deformation of the cell wall (D). Images were obtained through thin section microscopy: after cell fixation and embedding in resin, thin sections were prepared with an ultramicrotome equipped with a diamond knife and subsequently observed. Images are from Lampis *et al.*, 2014, unpublished data (*16*)

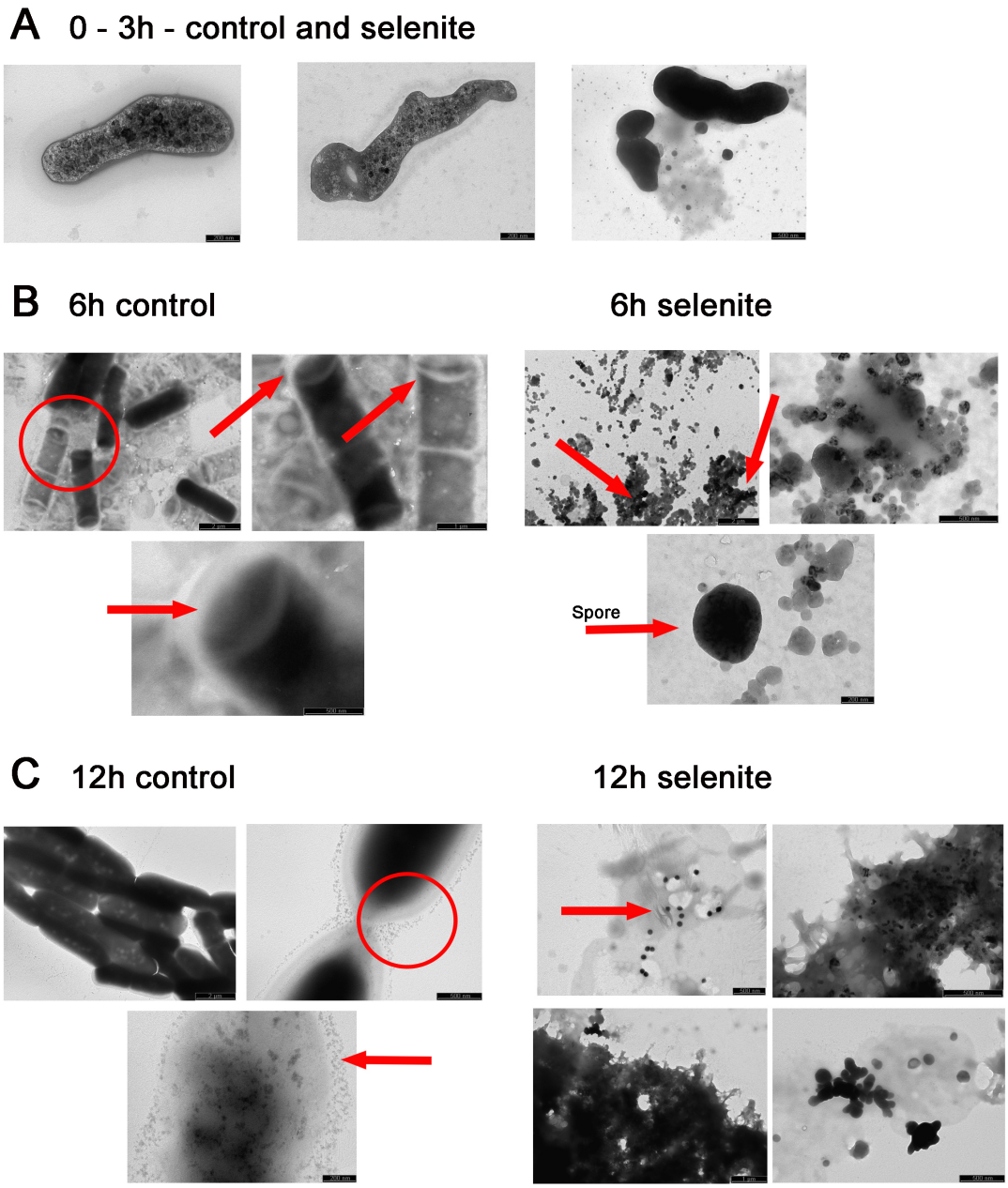

Figure 6.6: TEM images after 3 (A), 6 (B), 12h (C) of growth with or without 2mM selenite. Formation of vesicles is visible even in the control sample after 6h of growth (B, left side), while electron-dense material starts to associate to vesicle-like structures for cells grown with selenite (B, right side). Moderately electron-dense material, probably secreted, is visible surrounding cells in control samples (C, left side). SeNPs and aggregates start to appear in selenite-grown cells, associated with organic material (C, right side). Images were obtained through direct observation of untreated cells, air-dried on TEM grids

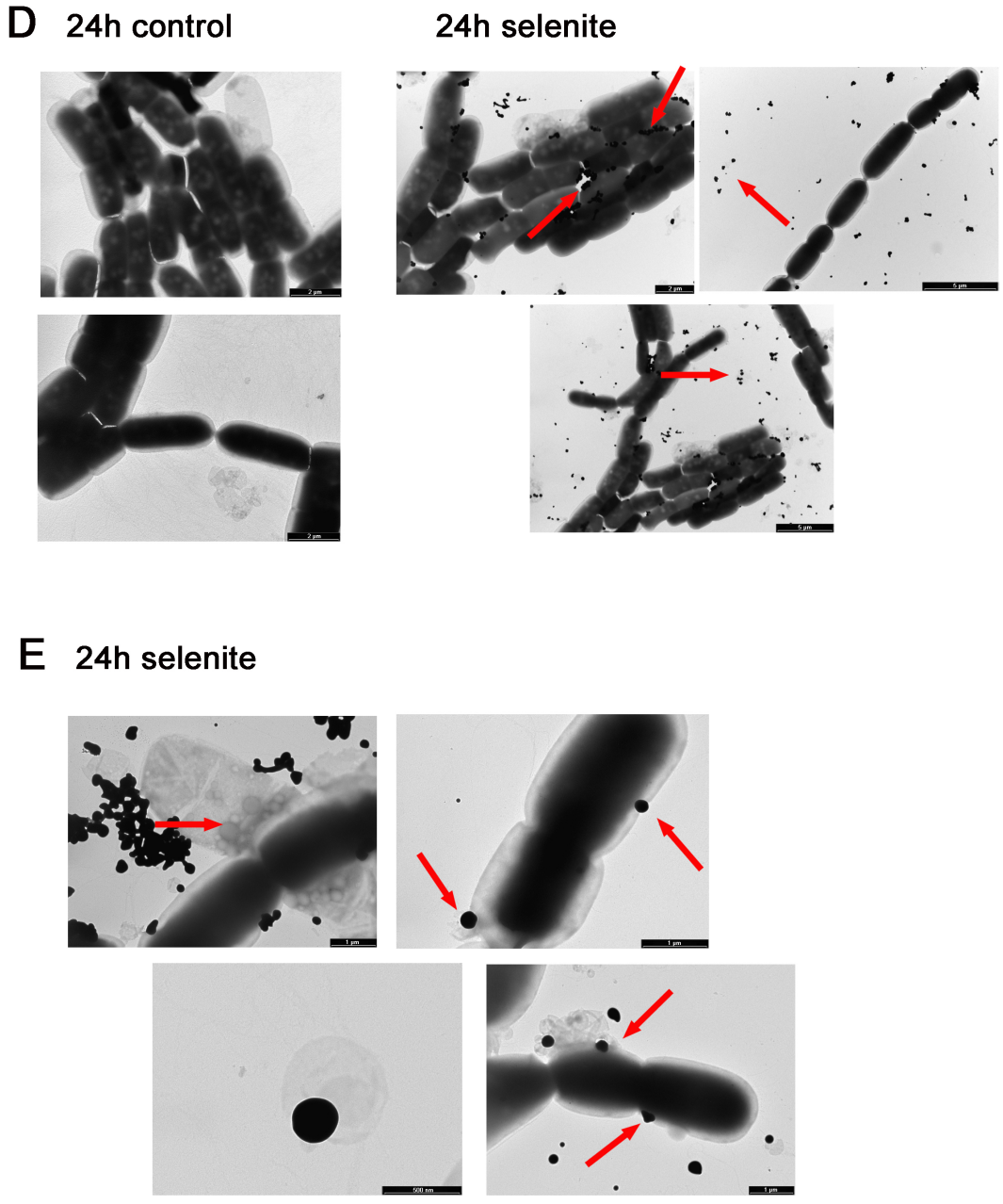

Figure 6.7: TEM images after 24h of growth with or without 2mM selenite (D) and SeNPs-cell interactions (E). SeNPs are clearly visible in selenite-treated cells (D, right side), while absent for control cells (D, left side). SeNPs seem to interact with the cell wall similarly to Figure 6.5 (E). Images were obtained through direct observation of untreated cells, air-dried on TEM grids

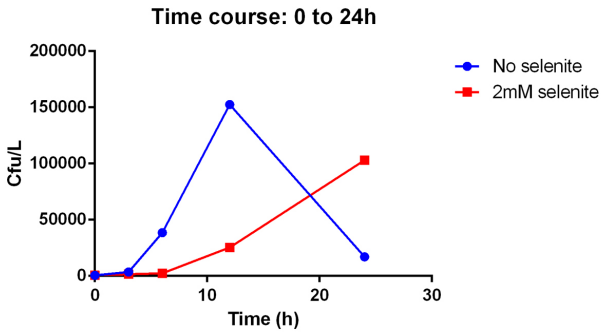

Figure 6.8: Number of CFU of SeITE01 after 3, 6, 12 and 24h growth with 2mM selenite (red line) or without selenite (blue line); representative curve from one trial

similarly shaped material was also observed by Piacenza *et al.* associating to SeITE01 SeNPs under different culture conditions, aimed to increase the presence of organic material after SeNPs extraction (*68*). On the other hand, selenite-treated samples show the presence of both SeNPs (50-70nm) and thick electron-dense aggregates, probably including amorphous Se and bacterial cells (Figure 6.6, panel C). It is not clear, if such aggregates are formed by the previously observed vesicles, or if Se starts to aggregate on the surface of cells. On the other hand, SeNPs (about 70nm) are clearly visible surrounded by organic material.

In Figure 6.7, panel D, cells from control and selenite-treated samples are compared after 24h of growth, when SeNPs are extracted. Both TEM images show the presence of cells with whitish (non electron-dense) spheres, probably polyhydroxibutyrate produced by bacteria (*97*). The only difference seems to be the presence of extracellular SeNPs in the selenite-grown culture. In Figure 6.7 - panel E, presence of cells together with SeNPs is shown. Notably, dimension of SeNPs close to cell walls range from 50 (usually distinguishable inside Se-aggregates) to 200-300nm, while bigger particles (up to 500nm) can be seen not aggregating. Interestingly, images from Figure 6.7 - panel E, strongly resemble pictures previously obtained with thin sections (Figure 6.5).

Such images, together with the presence of cell wall metabolism proteins associating to BioSeNPs and proteomic data about proteins localization and roles, support this new model of a mechanism of SeNPs transport linked to vesiculation processes.

However, TEM images and activity assay also confirm the hypothesis of a periplasmic reduction of selenite, followed by SeNPs formation. The new hypothesis is schematized in Figure 6.9 as a new model. In panel A, the periplasmic formation of SeNPs is shown. The precise mechanism is still unknown, but it could involve membrane proteins or even be not enzymatic (since activity assay showed formation of Se^0 even without NADH).

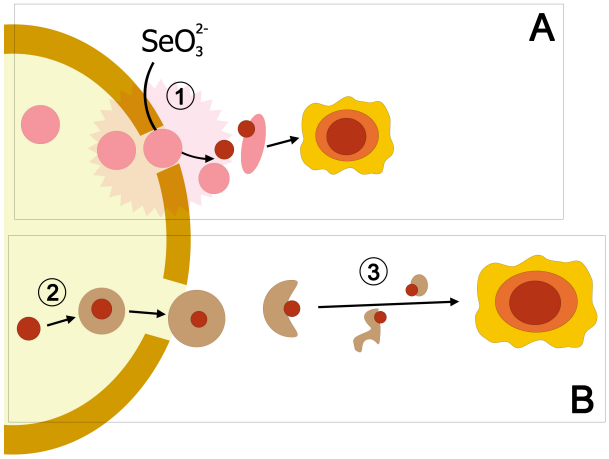

Figure 6.9: Scheme of proposed model. panel A: selenite is reduced in the periplasmic compartment (1), forming SeNPs seeds. Vesicle-like structures secreted from the cell attach to the nascent SeNPs, forming the capping layer. panel B: SeNPs seeds form in the cytoplasm (2) and are secreted by vesiculation. Once outside the cell, they grow through an Ostwald ripening mechanism (3), maintaining part of the transport vesicles as a capping layer

Vesicles containing cytoplasmic material could possibly contribute to form the capping layer. TEM images show in fact the presence of vesicles close to SeNPs. In panel B, the original hypothesis is shown in schematic form, involving intracellular reduction of selenite and formation of nascent SeNPs. Such nascent SeNPs are secreted outside the cell through discontinuities in the cell wall. Once outside the cell, organic material also secreted by the cell could contribute to SeNPs growth and stabilization.

6.4.6 Comparison of different biogenic SeNP formation models

In Figure 6.10, current and new models for SeNPs synthesis in SeITE01 are shown. Current model from Lampis *et al.* (*16*) in panel I shows a number of possible pathways including both extracellular and intracellular formation of SeNPs. Particularly, when SeNPs are proposed to be synthesized intracellularly (I, (1)), they are released in the extracellular matrix after cell lysis (I, (3)).

In the present study, SeNPs are proposed to be secreted by the cell or form in the periplasmic compartment (panel II, A). Two possible pathways are proposed to complete the current model (I). Periplasmic reduction of selenite is hypothesized to occur (II, (1)) based on data from native assay (see Section 6.4.5). Such model was already present in model I (I, (4)), where membrane reductases are responsible of selenite reduction to Se^0.

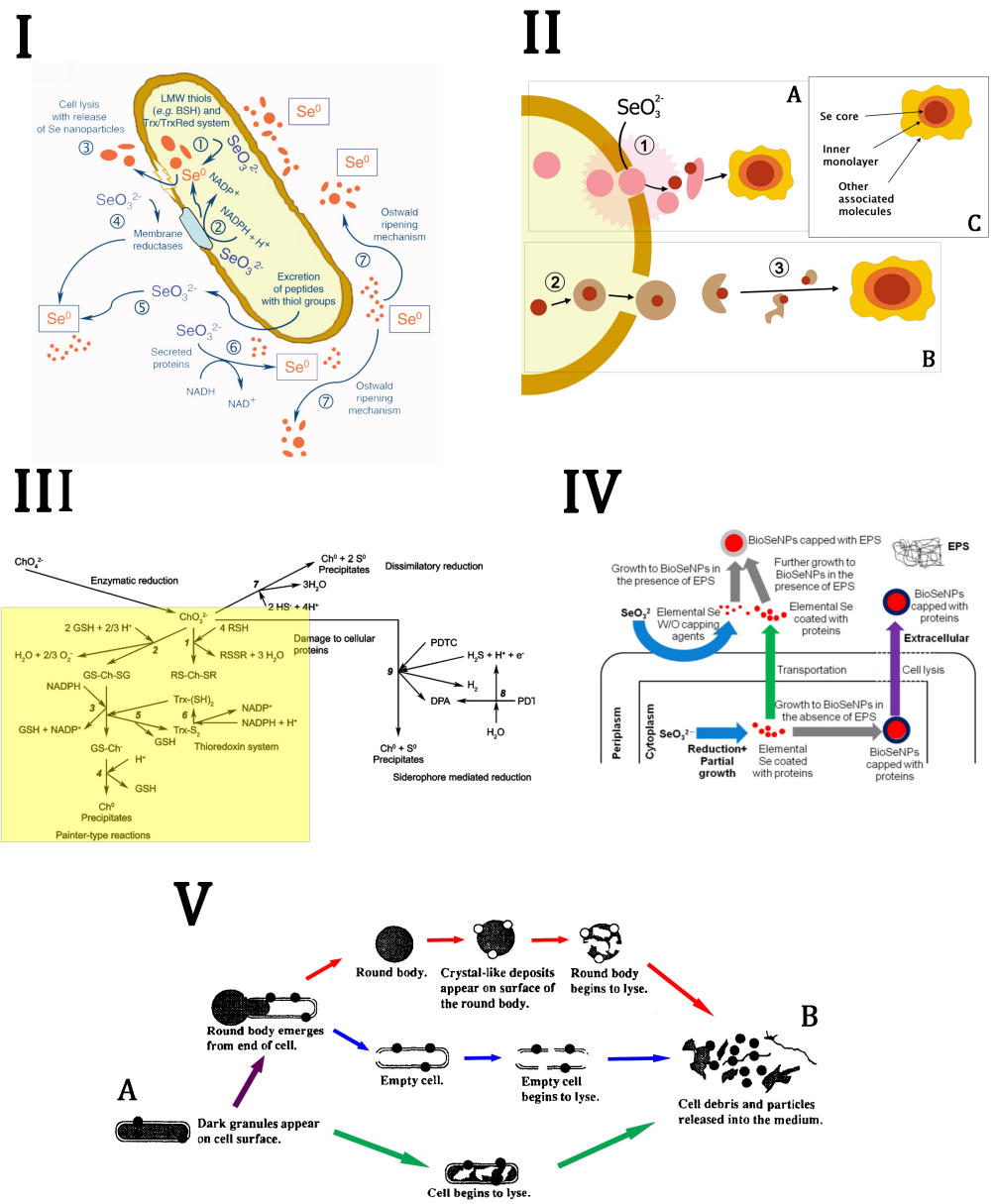

Figure 6.10: Overview of SeNPs biosynthesis pathways and capping layer formation: current model for SeITE01 by Lampis *et al.*, 2014 (*16*) (I); proposed new model (II); Se-oxyanions reduction pathways in bacteria from Zannoni *et al.*, 2008 (*2*) (III); capping layer formation in granular sludge bacteria by Jain *et al.*, 2015 (*52*) (IV); and morphological changes during SeNPs synthesis in*Bacillus subtilis* from Garbisu *et al.*, 1999 (*39*) (modified image) (V)

Moreover, Jain *et al.* already described a similar mechanism in synthesis by granular sludge bacteria (panel IV), where nascent SeNPs are formed in the periplasm without capping agents and start to grow in the presence of EPS (*52*). In this study, since proteomic analysis provided evidence for the presence of both cytoplasmic, membrane and cell wall proteins in SeNPs capping layer, SeITE01 SeNPs are proposed to form extracellularly after formation of Se^0 in the periplasmic compartment and grow in the presence of secreted material and possibly vesicles (panel II, A). This cellular material could constitute the capping layer.

The other pathway proposed in this study (panel I, B), based on the TEM observation and identified proteins, is an intracellular formation of SeNPs nucleation seeds (II, (2)) followed by secretion by vesiculation and Ostwald ripening growth outside the cell (II, (3)). Intracellular reduction was already described by Lampis *et al.* (*16*) to occur for SeITE01 (panel I, (1)) by the interaction with bacillithiol (BSH) and possibly involving Trx/Trx reductase system. Such pathway was reviewed by Zannoni *et al.* to likely occur for all chalcogens ("Ch" in the figure) and is shown in panel III (highlighted part) (*2*). However, differently from model I, where SeNPs occurs directly in the cytoplasm and is followed by cell lysis, in model II intracellular formation of Se^0 is followed by formation of SeNPs nucleation seeds, which are secreted before growth and consequently do not damage the cell. Part of the capping layer could originate from cytoplasmic reduction, potentially acting as a stabilizing agent. Part of it could instead originate from vesicles during translocation through the cell wall or during Ostwald ripening growth.

It is important to note that, as hypothesized in Chapter 4, Figure 4.22 and observed by other authors (*37*), some proteins and other molecules constituting the capping layer are more tightly bound to SeNPs than others. In this thesis, the most tightly bound part of the capping layer is referred as "inner monolayer" (panel II, C). Currently it is unknown which molecules are more tightly bound than others and what is the origin of such molecules (if they associate during cytoplasmic reduction, transport, intra- or extracellular growth, etc.). Moreover, since the extraction procedure includes a sonication step, in this study intra- and extacellular SeNPs were analyzed together. Jain *et al.* propose a different composition for SeNPs secreted after cell lysis, transported and grown outside the cell in the presence of EPS, or formed directly outside the cell in the presence of EPS (panel IV). Capping layer composition would be composed of proteins, proteins and EPS material, or just EPS material, respectively (*52*). Further studies are necessary to understand the exact composition and association strength of SeITE01 SeNPs capping layer molecules.

Finally, the proposed model II does not substitute pathways showed in model I, but it is proposed to complete it. Extracellular production (I, (5, 6)), as well as release due to cell lysis (I, (3)) cannot be excluded, especially considering that more selenite reduction pathways are likely to coexist.

Moreover, it cannot be excluded that different parts of the bacterial population could detoxify selenite through different pathways. In 1999, Garbisu *et al.* observed this phenomenon in *B. subtilis* culture (panel V), where SeNPs, described as "dark granules" (V, A) started to form on the surface of a subpopulation (about 10% of bacteria), finally resulting in SeNPs and cell debris released into the medium (V, B). SeNPs production by this subpopulation could follow three pathways: formation on the surface followed by cell lysis (V, green pathway) or formation of protoplast-like structures called round bodies (V, red pathway) and empty cells (V, blue pathaway), both resulting in lysis and formation of Se^0 deposits (*39*).

6.5 Conclusions

B. mycoides SeITE01 is able to produce SeNPs when exposed to sodium selenite. Such SeNPs display a capping layer also constituted by proteins. In this study, a proteomic analysis was performed on SeITE01 SeNPs. Affinity to Se, role, subcellular localization and secretion pathway of identified proteins were analyzed in order to understand the possible production pathway of SeNPs from selenite reduction to NPs growth outside the cell. Identified proteins displayed different roles and affinity to selenium or metal NPs in general. Some of these proteins are possibly involved in the initial oxidoreductase reactions, while others (membrane and cell wall proteins) probably associate during SeNPs transport and maturation.

A new model is proposed for SeNPs nucleation seeds transport outside the cells: since little activity was previously observed in the cytosol and many cytoplasmic proteins are present in the capping layer, but SeNPs are mainly observable outside the cell (*16*), there should be a way for nascent SeNPs to be transported outside the cell through the cell wall. For this, we observed a number of proteins belonging to cell wall metabolism and/or linked to vesiculation and sporulation processes associated to SeITE01 SeNPs.

A mechanism for SeNPs formation inside the cell had already been proposed by Lampis *et al.* in 2014 (*16*). The research of this thesis modifies this model to propose a transport step to this mechanism, instead of a cell lysis event as the cause of the SeNPs release outside the cell. The model formulated in this study is supported by TEM images showing vesicles and holes in the cell wall in the presence of nascent SeNPs. Selenite reduction activity was also observed in the membrane fraction both dependent and independent on addition of an electron donor. Given the high presence of lipids in the capping layer of SeNPs (see Section 4.4.1), there is the possibility of a reaction with membrane portions with selenite or nascent SeNPs. Membrane and cell wall proteins, proteins linked with vesiculation and sporulation were identified belonging to SeNPs capping layer.

Additional analyses will be necessary to further support the new model.

Experiments for lipid identification and the formation and role of the capping layer are already under investigation. The work of this thesis now provides a new and novel mechanism of SeNP production to add to the models in the literature.

Chapter 7

Conclusion

A comparative analysis involved two Gram-positive and three Gram-negative strains through quantification of capping layer components and parameters associated to SeNPs stability. It showed that:

1. **Quantitative microplate assays can be a useful tool for a routine screening** of many strains/culture conditions/treatments in order to compare BioSeNPs capping layer different compositions.

2. **Not all the capping layer components strongly associate to SeNPs**, as some can disassociate and be found in the supernatant after SeNPs precipitation. On the other hand, some molecules are so strongly bound with SeNPs, not even harsh detergent treatments can remove them.

3. **Gram-negative strains show similar composition and response to detergent treatments in a similar fashion**. Lipids appear to be the most abundant component of the capping layer in terms of µg/mg SeNPs, followed by proteins and then carbohydrates. When treated with detergents, SDS is the most effective, removing most of the proteins and carbohydrates, while Triton treatment is not as much effective. Lipids content is not significantly affected by those treatments.

4. **Gram-positive strains show more variability in composition and response to treatments**. Lipids are still the most abundant component in terms of µg/mg SeNPs, while the other two components differ depending on the strain. SDS treatment is still the most effective treatment in removing carbohydrates and proteins compared to Triton treatment.

5. **Stability of SeNPs is influenced by the presence of the capping layer**. Parameters such as hydrodynamic diameter, polydispersion and surface charge are associated to SeNPs stability and tendency

to aggregate in bigger particles. As evident by the different effects of detergent treatments in removing the capping layer molecules, a model has been hypothesized.

6. **The new model distinguishes strongly bound molecules, called *inner monolayer*, from molecules weakly bound to SeNPs, called *outer monolayer***. The inner monolayer would provide stability to SeNPs and is most probably formed by molecules with a strong affinity to Se. The outer monolayer is easier to remove and has probably the function to keep SeNPs suspended in water solutions. It can detach from SeNPs and reach thermodynamic equilibrium between the molecules bound to SeNPs and free in the solvent.

7. **Different detergents interact differently with the capping layer**. Despite being the most effective in the removal of the capping layer, SDS has minor effects of SeNPs stability. Such detergent could probably bind to the inner layer and keep SeNPs suspended in water. On the other hand, Triton treatment has significant effects on stability, despite quantitatively removing less material than SDS.

Finally, an analysis focused on SeNPs synthesis was carried out through proteomic and microscopy techniques on a Gram-positive strain (SeITE01 (*16*)). As a model for SeNPs synthesis by this strain was already been suggested and previous studies on another *Bacillus* strain (*39*) was used as comparison, this background allowed for a new mechanistic model to be proposed. This research showed that:

1. **Some proteins specifically associate with BioSeNPs** during biosynthesis. In fact, there is no difference in proteomic profile of BioSeNPs extracted by different methods. On the other hand, proteins that bind ChSeNPs exposed to a cell extract show more variability in proteomic profiles. This is not related to the strength of such bound.

2. **Some proteins associate with SeNPs by chance**, probably due to the affinity for the metalloid. By exposing ChSeNPs to a cell extract, we obtained a sort of artificial capping layer containing also proteins. It is not possible to distinguish the strength or the specificity of such bound, but it is likely that proteins only found on BioSeNPs and not on exposed ChSeNPs do bind BioSeNPs during synthesis, probably in a specific manner.

3. **Amongst proteins only found in BioSeNPs there are membrane proteins and proteins linked to vesiculation and sporulation processes**. This led to the hypothesis, that SeNPs synthesis could involve vesicles or occur on the plasma membrane. Since it was

already hypothesized, that SeNPs synthesis could involve different independent pathways, the model already formulated for SeITE01 was updated.

4. **BioSeNPs synthesis by SeITE01 probably involves an extracellular pathway**: Se oxyanions are reduced by membrane enzymes (as confirmed by activity assay) and nascent SeNPs grow outside the cell stabilized by material secreted by vesicles, or interacting with the surface of vesicles themselves (as suggested by TEM images).

5. **BioSeNPs synthesis by SeITE01 probably also involves an intracellular pathway**: the presence of intracellular proteins in the capping layer also suggests a first step of the synthesis inside the cell, followed by cell lysis (in the previous model) and/or transport of the SeNPs nucleation seeds outside the cell inside vesicles or discontinuities in the cell wall (as suggested by TEM images).

6. **Several pathways can likely coexist in the single cells, and some cells in the culture could follow unique pathways**. Due to physiological diversity of cells in a culture community, with more than one process possible, not all cells may be producing the SeNPs in the same fashion.

Acknowledgements

I would like to acknowledge the Environmental Microbiology research group of University of Verona: my supervisor, Prof. Giovanni Vallini, for his advice and support, for giving me the opportunity to work in this research group on this exciting topic.

Dr. Silvia Lampis for her advice, encouragement and guidance, especially in the experimental part.

Prof. Raymond Joseph Turner from University of Calgary (AB, Canada) for giving me the opportunity to work in his research group, for his ideas and support, and for his important help with writing my thesis.

Dr. Daniela Cecconi of the Proteomic research group of University of Verona, for her collaboration in the proteomic part and bioinformatic analysis and her helpful suggestions.

Elena Piacenza and Dr. Alessandro Presentato for their help in the nanoparticles microscopy analysis and my colleagues of the Environmental Microbiology group of University of Verona: Greta, Marco, Chiara, Nazanin and Emanuele for their support during my PhD study period.

I would also like to thank my PhD colleagues of the Computer Science department and Oscar for his help in LaTeX formatting of this thesis and the graphic part.

Finally, I would like to thank my family for their constant support during this exciting yet difficult period of my studies.

Appendix A

Capping layer components quantification: Protocol commentaries

A.1 Total soluble sugars quantification assay

Protocol modified and optimized from Chow and Landhäusser, 2004 (*76*) and Masuko *et al.*, 2005 (*75*).

Reagents:

- 96-well plate + reader
- Sulfuric acid
- Phenol 2%
- "GFG" standard solution (glucose:fructose:galactose, 1:1:1)

Procedure:

- Set a standard curve: 0 (blank) and 0.195 to 12.5µM (lineariy range)
- For each well: add 50µl standard solution, blank or sample (ChSeNPs can be used as a control)
- Read absorbance (Abs) at 490nm (background Abs)
- Add ChSeNPs to standard curve solutions to match background Abs values. Add the new calibration curves to the 96-well plate
- Add 150 µl sulfuric acid
- Quickly add 30 µl of 2% phenol

- Heat the microplate 15min at 90°C in a static water bath
- Cool the microplate 15-20min to room T (do not read if hot)
- Read Abs at 490nm after 18-24h
- When determining the carbohydrates concentration for each sample, refer to the corresponding calibration curve

Commentary:

- In order for the colorimetric reaction to correctly work, timing must be respected. Using a multichannel 200µl pipette would be better to make adding reagents quicker
- Standard curve stock:
  - Standards can be prepared and stored at 4°C. Each can be prepared separately as a concentrated stock for each of the three sugars; a useful concentration is 100mg/ml. A heating stir plate can help dissolve the sugars; however avoid temperatures higher than 100°C to prevent sugars from caramelizing
  - Sterilize the stock solutions and water through a 0.2 µm polyethersulfone filter
  - Prepare all subsequent solutions under a biological hood using sterile tubes and water. First, prepare a GFG stock mixing the three solutions in equal amounts. To obtain 1ml of 1mM (18mg/ml) GFG solution, mix 90µl of each individual sugar stock with 730µl sterile water
  - Dilute the GFG stock to obtain all concentrations of the calibration curves
  - Perform an assay to verify linearity of the standard curve, then store all solutions at 4°C
- Sterile microplates filled with calibration curve solutions can also be prepared one day before performing the assay, sealed and stored at 4°C
- Reaction:
  - Phenol solution should be prepared fresh each time prior filling the microplate with sulfuric acid
  - If using a multichannel pipette, pour in a glass container enough sulfuric acid to be easily pipetted. Do not clean with pure cellulose paper

  - When heating the microplate in the static water bath, make sure it is sealed and cannot flip or spill
  - To maximize linearity of the results, let the reaction occur completely overnight and read Abs after 18-24h (18h is the best timing)

- After the assay, discard the solutions under the chemical hood and leave the microplate under the hood overnight before discarding it

A.2 Solid phase protein quantification assay

Protocol modified and optimized from Minamide and Bamburg, 1990 (*77*).

Reagents:

- Whatman n.1 paper
- 96-well plate + reader
- Absolute methanol
- Staining solution: 0.5% Coomassie Brilliant Blue G in 7% acetic acid (filtered)
- Destaining solution: 7% acetic acid
- Extraction buffer: 66% methanol, 33% water, 1% ammonium hydroxide
- BSA standard solution (2mg/ml)

Procedure:

- Draw a rectangle on a Whatman paper sheet with a pencil and divide it into 1x1cm squares (to avoid contamination, don't touch the squares without gloves). Fold the sheet and make it stand on its edges during application of samples
- Prepare BSA standard solutions: 0 (blank), 0.016 to 2 mg/ml (linearity range)
- Apply 8µl of samples, blanks and standard BSA solutions. Air-dry the sheet (for bigger sample volumes, air-dry and apply multiple times) *
- Rinse in absolute methanol for 10-20sec and air-dry *
- Place in 200ml of Staining solution for 30min at room T with gentle agitation

- Place in 200ml of Destaining solution with gentle agitation for 30min/3h to reduce background (for a better destaining, change the solution after 1h). Air-dry *
- Cut the squares and place them in 2ml eppendorf tubes *
- Add 1ml of Extraction buffer and mix on a vortex
- Leave samples at room T for 5min, then mix again on a vortex
- Transfer 200µl from each tube to a 96-well-plate
- Read Abs at 595nm

* stars indicate possible stopping points

Commentary:

- The assay makes it possible to quantify proteins in the presence of ammonium sulfate, urea, DTT, amino acids, DNA, ionic and nonionic detergents, acids or bases
- Staining solution is reusable several times
- Before starting, clean all surfaces and objects (including pencil, scissors, etc.) to avoid external contamination. Never touch the Whatman paper without gloves. When preparing more Whatman sheets, store them in a sealed container to avoid external contaminations
- Leave the paper sheet under the hood to air-dry more quickly. If stopping the protocol, remove the sheet from the hood and place it in a sealed container to avoid external contaminations
- Make sure to completely cover the Whatman sheet with the staining solution
- For destaining, make sure the paper sheet is not stuck to bottom of container, but can float. To make destaining quicker, change the destaining solution after 1h. It is possible to add a little sponge to absorb the Coomassie excess, but it could leave little spots on the paper if it sits on it, so attention is needed
- Do not pour the destaining solution directly on the paper, as it could destain too much the point where it is poured, causing errors in measurements
- For a more efficient extraction of the Coomassie blue from the squares, cut each square in two pieces along the diagonal, then place both halfs in a 2ml eppendorf tube

- When all samples are extracted, put immediately the solutions into the microplate, as Whatman paper tends to slowly dissolve inside the extraction buffer

A.3 Total lipids quantification assay

Protocol modified and optimized from Cheng *et al.*, 2011 (*78*).

Reagents:

- 96-well plate + reader
- Sulfuric acid
- VP reagent: 0.2mg/ml vanillin in 17% phosphoric acid
- lipid standard solution: oleic acid
- solvent: chloroform:methanol 2:1

Procedure:

- Solubilize the standard lipid in chloroform:methanol 2:1 solvent
- Extract lipids from the samples with the chloroform:methanol 2:1 solvent
- Add samples and standard solution to the 96-well plate, in order to reach the amount of standard lipid the calibration curve (considering less than 100µl/well): 0 (blank), 0.78 to 100µg/well lipid (linearity range)
- Evaporate solvent
- Add 100 µl sulfuric acid/well
- Heat the microplate 20min at 90°C in a static water bath
- Cool the microplate 2min in ice water
- Add 50µl VP reagent/well
- Incubate at room T for 10min
- Read Abs at 540nm after 18h

Commentary:

- VP reagent and solvent should be prepared fresh each time or stored at room temperature for no more than 3 days
- Do not use this protocol for oxidizing samples
- Always work under chemical hood, close the microplate prior moving it to reader or water bath
- When evaporating solvent, pay attention not to let it dry too much, as it could form a spot on the bottom of the wells, causing errors in Abs measurements. It is better to start pipetting the bigger volumes first, then the smaller to allow a more uniform evaporation
- Linearity works better when reading after 18h. Do not wait more than 24h

Appendix B

Identified proteins, supplemental tables

Name	Origin	NCBI num.	Loc	Metabolism	Secretion pathway	Transmembrane domains
translation elongation factor Tu	*B. mycoides*	WP_042981370.1	Cytoplasmic	Protein	no	no
ATP synthase subunit beta	*B. mycoides*	WP_042981037.1	Membrane	Primary	no	no
alanine dehydrogenase	*B. mycoides*	WP_042980294.1	Cytoplasmic	Aminoacid	no	no
elongation factor G	*B. mycoides*	WP_033797762.1	Cytoplasmic	Protein	no	no
formate acetyltransferase	*B. mycoides*	WP_033733733.1	Cytoplasmic	Primary	no	no
methionine adenosyltransferase	*B. mycoides*	WP_003208790.1	Cytoplasmic	Aminoacid	no	no
aminopeptidase	*B. mycoides*	WP_003202305.1	Extracellular	Protein	signal peptide	2
branched-chain alpha-keto acid dehydrogenase subunit E2	*B. mycoides*	WP_003199953.1	Cytoplasmic	Redox	no	no
MULTISPECIES: type I glyceraldehyde-3-phosphate dehydrogenase	*B. cereus* group	WP_002112805.1	Cytoplasmic	Primary	no	no
MULTISPECIES: molecular chaperone GroEL	*B. cereus* group	WP_002029451.1	Cytoplasmic	Protein	no	no
MULTISPECIES: 30S ribosomal protein S3	*B. cereus* group	WP_002009771.1	Cytoplasmic	Protein	no	no
dihydrolipoyl dehydrogenase	*B. cereus* group	WP_000260101.1	Cytoplasmic	Redox	no	no
MULTISPECIES: molecular chaperone DnaK	*B. cereus* group	WP_000034694.1	Cytoplasmic	Protein	no	no
5-methyltetrahydropteroyltriglutamate-homocysteine methyltransferase	*B. mycoides*	KZE07161.1	Cytoplasmic	Aminoacid	no	no
enolase	*B. cereus*	KWW52376.1	Cytoplasmic	Primary	no	no
Pyruvate dehydrogenase E1 component subunit beta	*B. cereus*	CUB10128.1	Cytoplasmic	Primary	no	no

Table B.1: Localization of exposed ChSeNPs proteins: name of the protein (Name) and microorganism (Origin), NCBI database classification number (NCBI num), subcellular localization based on PSORTdb database (Loc), role in cell metabolism (Metabolism), type of secretion pathway based on SecretomeP database (Secretion pathway), presence of transmembrane domain based on TMHMM database (Transmembrane domains)

Name	Origin	NCBI num.	*B. cereus* spores (*96*)	*B. anthracis* spores (*95*)
translation elongation factor Tu	*B. mycoides*	WP_042981370.1	x	x
ATP synthase subunit beta	*B. mycoides*	WP_042981037.1	x	x
alanine dehydrogenase	*B. mycoides*	WP_042980294.1	—	—
elongation factor G	*B. mycoides*	WP_033797762.1	x	x
formate acetyltransferase	*B. mycoides*	WP_033733733.1	—	—
methionine adenosyltransferase	*B. mycoides*	WP_003208790.1	x	—
aminopeptidase	*B. mycoides*	WP_003202305.1	—	—
branched-chain alpha-keto acid dehydrogenase subunit E2	*B. mycoides*	WP_003199953.1	—	—
MULTISPECIES: type I glyceraldehyde-3-phosphate dehydrogenase	*B. cereus* group	WP_002112805.1	x	x
MULTISPECIES: molecular chaperone GroEL	*B. cereus* group	WP_002029451.1	x	x
MULTISPECIES: 30S ribosomal protein S3	*B. cereus* group	WP_002009771.1	—	—
dihydrolipoyl dehydrogenase	*B. cereus* group	WP_000260101.1	x	x*
MULTISPECIES: molecular chaperone DnaK	*B. cereus* group	WP_000034694.1	x	x
5-methyltetrahydropteroyltriglutamate-homocysteine methyltransferase	*B. mycoides*	KZE07161.1	x	—
enolase	*B. cereus*	KWW52376.1	x	x
Pyruvate dehydrogenase E1 component subunit beta	*B. cereus*	CUB10128.1	x	x

Table B.2: Proteins identified also in spore proteome of other members of *B. cereus sensu lato* group: name of the protein (Name) and microorganism (Origin), NCBI database classification number (NCBI num), presence of the same protein in spore proteome of other members of *B. cereus sensu lato* group: *B. cereus* spores (*96*), *B. anthracis* spores (*95*)

* present as dihydrolipoamide dehydrogenase

Name	Origin	NCBI num.	Loc	PSORT score	PSORT e-value	Secr. pathway	SecP score	SignalP pred.
lysozyme, partial	*B. mycoides*	WP_088004971.1	Membrane	813	1E-107	non-classic	0.889192	no
stress protein	*B. mycoides*	WP_078213816.1	Cytoplasmic	972	1E-133	no	0.195888	no
peptide ABC transporter substrate-binding protein	*B. mycoides*	WP_078206463.1	Cellwall	2511	0	signal peptide	0.848139	yes
30S ribosomal protein S7	*B. cereus*	WP_063222353.1	Cytoplasmic	816	1E-111	no	0.063674	no
lysozyme family protein	*B. mycoides*	WP_060751007.1	Membrane	1346	0	non-classic	0.888749	no
peptidoglycan endopeptidase	*B. mycoides*	WP_059038255.1	Cellwall	1641	0	signal peptide	0.891461	yes
peptidase P60	*Bacillus* sp. LK2	WP_048372757.1	Cellwall	1476	0	signal peptide	0.885737	yes
thiol:disulfide interchange protein	*B. mycoides*	WP_044441543.1	Cellwall	749	1E-100	non-classic	0.854366	no
NADH dehydrogenase family protein	*B. mycoides*	WP_044439292.1	Membrane	1842	0	no	0.088997	no
glutamate dehydrogenase	*B. mycoides*	WP_042982821.1	Cytoplasmic	2270	0	no	0.066848	no
translation elongation factor Tu	*B. mycoides*	WP_042981370.1	Cytoplasmic	1851	0	no	0.070478	no
ATP synthase subunit alpha	*B. mycoides*	WP_042981039.1	Cytoplasmic	2531	0	no	0.058480	no
elongation factor G	*B. mycoides*	WP_033797762.1	Cytoplasmic	3662	0	no	0.079899	no
MULTISPECIES: 50S ribosomal protein L5	*B. cereus* group	WP_016116955.1	Cytoplasmic	920	1E-126	no	0.075181	no
penicillin-binding protein	*B. cereus*	WP_002119238.1	Membrane	3378	0	non-classic	0.937360	no
MULTISPECIES: 30S ribosomal protein S5	*B. cereus* group	WP_002063426.1	Cytoplasmic	833	1E-113	no	0.033661	no
MULTISPECIES: protein translocase subunit SecDF	*B. cereus* group	WP_001119051.1	Membrane	3631	0	non-classic	0.902367	no
ATP synthase subunit beta	*Bacillus*	WP_001032596.1	Membrane	2368	0	no	0.077759	no
glyceraldehyde-3-phosphate dehydrogenase, partial	*B. cereus*	KWW52438.1	Cytoplasmic	1392	0	no	0.076361	no

Table B.3: Prediction databases scores for SeITE01 BioSeNPs proteins: sample type (Sample), name of the protein (Name) and microorganism (Origin), NCBI database classification number (NCBI num). Predicted localization (Loc), PSORTdb prediction score (PSORT score) and e-value (PSORT e-value) (*93*): e-value indicates the probability of the resulting match being casual. Predicted secretion pathway (Secr. pathway), SecretomeP score (SecP) (*89*) and presence of a signal peptide (SinalIP pred.) (*98*): a protein is secreted in a non-classical way when the score is >0.5 and SignalP software predicts the absence of a signal peptide

Name	Origin	NCBI num.	Loc	PSORT score	PSORT e-value	Secr. pathway	SecP score	SignalP pred.
translation elongation factor Tu	*B. mycoides*	WP_042981370.1	Cytoplasmic	1851	0		0.070478	no
ATP synthase subunit beta	*B. mycoides*	WP_042981037.1	Membrane	2353	0		0.078539	no
alanine dehydrogenase	*B. mycoides*	WP_042980294.1	Cytoplasmic	1932	0		0.060656	no
elongation factor G	*B. mycoides*	WP_033797762.1	Cytoplasmic	3662	0		0.079899	no
formate acetyltransferase	*B. mycoides*	WP_033733733.1	Cytoplasmic	3971	0		0.130647	no
methionine adenosyltransferase (s-adenosylmethionine synthetase)	*B. mycoides*	WP_003208790.1	Cytoplasmic	2042	0		0.076570	no
aminopeptidase	*B. mycoides*	WP_003202305.1	Extracellular	2429	0	signal peptide	0.751870	yes
branched-chain alpha-keto acid dehydrogenase subunit E2	*B. mycoides*	WP_003199953.1	Cytoplasmic	1827	0		0.072987	no
MULTISPECIES: type I glyceraldehyde-3-phosphate dehydrogenase	*B. cereus* group	WP_002112805.1	Cytoplasmic	1552	0		0.114718	no
MULTISPECIES: molecular chaperone GroEL	*B. cereus* group	WP_002029451.1	Cytoplasmic	2470	0		0.034861	no
MULTISPECIES: 30S ribosomal protein S3	*B. cereus* group	WP_002009771.1	Cytoplasmic	1127	1E-156		0.051619	no
dihydrolipoyl dehydrogenase	*B. cereus* group	WP_000260101.1	Cytoplasmic	2287	0		0.049486	no
MULTISPECIES: molecular chaperone DnaK	*B. cereus* group	WP_000034694.1	Cytoplasmic	2756	0		0.095556	no
5-methyltetrahydropteroyltriglutamate-homocysteine methyltransferase	*B. mycoides*	KZE07161.1	Cytoplasmic	3996	0		0.119376	no
enolase	*B. cereus*	KWW52376.1	Cytoplasmic	2245	0		0.080961	no
Pyruvate dehydrogenase E1 component subunit beta	*B. cereus*	CUB10128.1	Cytoplasmic	1621	0		0.047843	no

Table B.4: Prediction databases scores for SeITE01 exposed ChSeNPs proteins: sample type (Sample), name of the protein (Name) and microorganism (Origin), NCBI database classification number (NCBI num). Predicted localization (Loc), PSORTdb prediction score (PSORT score) and e-value (PSORT e-value) (*93*): e-value indicates the probability of the resulting match being casual. Predicted secretion pathway (Secr. pathway), SecretomeP score (SecP) (*89*) and presence of a signal peptide (SinalIP pred.) (*98*): a protein is secreted in a non-classical way when the score is >0.5 and SignalP software predicts the absence of a signal peptide

Bibliography

(*1*) Wiberg, E., and Wiberg, N., *Inorganic Chemistry*; Academic Press: 2001.

(*2*) Zannoni, D., Borsetti, F., Harrison, J. J., and Turner, R. J., (2008). The bacterial response to the chalcogen metalloids Se and Te. *Advances in Microbial Physiology 53*, 1–72.

(*3*) Antonioli, P., Lampis, S., Chesini, I., Vallini, G., Rinalducci, S., Zolla, L., and Righetti, P. G., (2007). *Stenotrophomonas maltophilia* SeITE02, a new bacterial strain suitable for bioremediation of selenite-contaminated environmental matrices. *Applied and Environmental Microbiology 73*, 6854–63.

(*4*) Chhabria, S., and Desai, K., (2016). Selenium Nanoparticles and Their Applications. *Encyclopedia of Nanoscience and Nanotechnology 20*, 1–32.

(*5*) Fordyce, F. M., (2013). Selenium deficiency and toxicity in the environment. *Essentials of Medical Geology 16*, 375–416.

(*6*) Tapiero, H, Townsend, D. M., and Tew, K. D., (2003). The antioxidant role of selenium and seleno-compounds. *Biomedicine & Pharmacotherapy 57*, 134–44.

(*7*) Fleming, J, Ghose, A, and Harrison, P. R., (2001). Molecular mechanisms of cancer prevention by selenium compounds. *Nutrition and Cancer 40*, 42–9.

(*8*) Lenz, M., and Lens, P. N. L., (2009). The essential toxin: the changing perception of selenium in environmental sciences. *Science of the Total Environment 407*, 3620–33.

(*9*) Keller, E. A., *Environmental Geology (9th Edition)*; Pearson: 2000.

(*10*) Vallini, G., Gregorio, S. D., and Lampis, S., (2005). Rhizosphere-induced selenium precipitation for possible applications in phytoremediation of se polluted effluents. *Zeitschrift fur Naturforschung. C, Journal of Biosciences 60*, 349–56.

(*11*) Jain, R., Dominic, D., Jordan, N., Rene, E. R., Weiss, S., van Hullebusch, E. D., Hübner, R., and Lens, P. N. L., (2016). Preferential adsorption of Cu in a multi-metal mixture onto biogenic elemental selenium nanoparticles. *Chemical Engineering Journal 284*, 917–925.

(*12*) Jain, R., Jordan, N., Schild, D., van Hullebusch, E. D., Weiss, S., Franzen, C., Farges, F., Hübner, R., and Lens, P. N., (2015). Adsorption of zinc by biogenic elemental selenium nanoparticles. *Chemical Engineering Journal 260*, 855–863.

(*13*) Fellowes, J. W., Pattrick, R. A. D., Green, D. I., Dent, A, Lloyd, J. R., and Pearce, C. I., (2011). Use of biogenic and abiotic elemental selenium nanospheres to sequester elemental mercury released from mercury contaminated museum specimens. *Journal of Hazardous Materials 189*, 660–9.

(*14*) Jiang, S., Ho, C. T., Lee, J.-H., Duong, H. V., Han, S., and Hur, H.-G., (2012). Mercury capture into biogenic amorphous selenium nanospheres produced by mercury resistant *Shewanella putrefaciens* 200. *Chemosphere 87*, 621–4.

(*15*) Lampis, S., Zonaro, E., Bertolini, C., Cecconi, D., Monti, F., Micaroni, M., Turner, R. J., Butler, C. S., and Vallini, G., (2017). Selenite biotransformation and detoxification by *Stenotrophomonas maltophilia* SeITE02: Novel clues on the route to bacterial biogenesis of selenium nanoparticles. *Journal of Hazardous Materials 324*, 3–14.

(*16*) Lampis, S., Zonaro, E., Bertolini, C., Bernardi, P., Butler, C. S., and Vallini, G., (2014). Delayed formation of zero-valent selenium nanoparticles by *Bacillus mycoides* SeITE01 as a consequence of selenite reduction under aerobic conditions. *Microbial Cell Factories 13*, 35.

(*17*) Ramos, J. F., and Webster, T. J., (2012). Cytotoxicity of selenium nanoparticles in rat dermal fibroblasts. *International Journal of Nanomedicine 7*, 3907–3914.

(*18*) Lin, Z.-H., and Wang, C. C., (2005). Evidence on the size-dependent absorption spectral evolution of selenium nanoparticles. *Materials Chemistry and Physics 92*, 591–594.

(*19*) Kessi, J., (2006). Enzymic systems proposed to be involved in the dissimilatory reduction of selenite in the purple non-sulfur bacteria *Rhodospirillum rubrum* and *Rhodobacter capsulatus*. *Microbiology (Reading, Engl.) 152*, 731–43.

(*20*) Butler, C. S., Debieux, C. M., Dridge, E. J., Splatt, P., and Wright, M., (2012). Biomineralization of selenium by the selenate-respiring bacterium *Thauera selenatis*. *Biochemical Society Transactions 40*, 1239–43.

(*21*) Prasada, K. S., Patel, H., Patel, T., Patel, K., and Selvaraj, K., (2013). Biosynthesis of Se nanoparticles and its effect on UV-induced DNA damage. *Colloids and Surfaces B: Biointerfaces 103*, 261–266.

(*22*) Zhang, J.-S., Gao, X.-Y., Zhang, L.-D., and Bao, Y.-P., (2001). Biological effects of a nano red elemental selenium. *Biofactors 15*, 27–38.

(*23*) Xiao, Y., Huang, Q., Zheng, Z., Guan, H., and Liu, S., (2017). Construction of a *Cordyceps sinensis* exopolysaccharide-conjugated selenium nanoparticles and enhancement of their antioxidant activities. *International Journal of Biological Macromolecules 99*, 483–491.

(*24*) Jain, R., Seder-Colomina, M., Jordan, N., Dessi, P., Cosmidis, J., van Hullebusch, E. D., Weiss, S., Farges, F., and Lens, P. N., (2015). Entrapped elemental selenium nanoparticles affect physicochemical properties of selenium fed activated sludge. *Journal of Hazardous Materials 295*, 193–200.

(*25*) Jain, R., Matassa, S., Singh, S., van Hullebusch, E. D., Esposito, G., and Lens, P. N. L., (2015). Reduction of selenite to elemental selenium nanoparticles by activated sludge. *Environmental Science and Pollution Research*.

(*26*) Prokisch, J., and Zommara, M. A., Process for producing elemental selenium nanospheres., Patent US 20100189634 A1, 2010.

(*27*) Shakibaie, M., Forootanfar, H., Golkari, Y., Mohammadi-Khorsanda, T., and Shakibaie, M. R., (2015). Anti-biofilm activity of biogenic selenium nanoparticles and selenium dioxide against clinical isolates of *Staphylococcus aureus*, *Pseudomonas aeruginosa*, and *Proteus mirabilis*. *Journal of Trace Elements in Medicine and Biology 29*, 235–241.

(*28*) Srivastava, N., and Mukhopadhyay, M., (2015). Green synthesis and structural characterization of selenium nanoparticles and assessment of their antimicrobial property. *Bioprocess and Biosystems Engineering 38*, 1723–1730.

(*29*) Chudobova, D., Cihalova, K., Dostalova, S., Ruttkay-Nedecky, B., Rodrigo, M. A. M., Tmejova, K., Kopel, P., Nejdl, L., Kudr, J., Gumulec, J., Krizkova, S., Kynicky, J., Kizek, R., and Adam, V., (2014). Comparison of the effects of silver phosphate and selenium nanoparticles on *Staphylococcus aureus* growth reveals potential for selenium particles to prevent infection. *FEMS Microbiology Letters 351*, 195–201.

(*30*) Zonaro, E., Lampis, S., Turner, R. J., Qazi, S. J. S., and Vallini, G., (2015). Biogenic selenium and tellurium nanoparticles synthesized by environmental microbial isolates efficaciously inhibit bacterial planktonic cultures and biofilms. *Frontiers in Microbiology 6*, 584.

(*31*) Cremonini, E., Zonaro, E., Donini, M., Lampis, S., Boaretti, M., Dusi, S., Melotti, P., Lleo, M. M., and Vallini, G., (2016). Biogenic selenium nanoparticles: characterization, antimicrobial activity and effects on human dendritic cells and fibroblasts. *Microbial Biotechnology 9*, 758–771.

(*32*) Painter, E. P., (1941). The Chemistry and Toxicity of Selenium Compounds, with Special Reference to the Selenium Problem. *Chemical Reviews 28*, 179–213.

(*33*) Hockin, S. L., and Gadd, G. M., (2003). Linked redox precipitation of sulfur and selenium under anaerobic conditions by sulfate-reducing bacterial biofilms. *Applied and Environmental Microbiology 69*, 7063–72.

(*34*) Zawadzka, A. M., Crawford, R. L., and Paszczynski, A. J., (2006). Pyridine-2,6-bis(thiocarboxylic acid) produced by *Pseudomonas stutzeri* KC reduces and precipitates selenium and tellurium oxyanions. *Applied and Environmental Microbiology 72*, 3119–29.

(*35*) Ridley, H., Watts, C. A., Richardson, D. J., and Butler, C. S., (2006). Resolution of distinct membrane-bound enzymes from *Enterobacter cloacae* SLD1a-1 that are responsible for selective reduction of nitrate and selenate oxyanions. *Applied and Environmental Microbiology 72*, 5173–80.

(*36*) Kessi, J., and Hanselmann, K. W., (2004). Similarities between the abiotic reduction of selenite with glutathione and the dissimilatory reaction mediated by *Rhodospirillum rubrum* and *Escherichia coli*. *Journal of Biological Chemistry 279*, 50662–9.

(*37*) Dobias, J, Suvorova, E. I., and Bernier-Latmani, R, (2011). Role of proteins in controlling selenium nanoparticle size. *Nanotechnology 22*, 195605.

(*38*) Choudhury, H. G., Cameron, A. D., Iwata, S., and Beis, K., (2011). Structure and mechanism of the chalcogen-detoxifying protein TehB from *Escherichia coli*. *Biochemical Journal 435*, 85–91.

(*39*) Garbisu, C, Carlson, D, Adamkiewicz, M, Yee, B. C., Wong, J. H., Resto, E, Leighton, T, and Buchanan, B. B., (1999). Morphological and biochemical responses of *Bacillus subtilis* to selenite stress. *Biofactors 10*, 311–9.

(*40*) Oremland, R. S., Herbel, M. J., Blum, J. S., Langley, S., Beveridge, T. J., Ajayan, P. M., Sutto, T., Ellis, A. V., and Curran, S., (2004). Structural and spectral features of selenium nanospheres produced by Se-respiring bacteria. *Applied and Environmental Microbiology 70*, 52–60.

(*41*) Blum, J. S., Bindi, A. B., Buzzelli, J, Stolz, J. F., and Oremland, R. S., (1998). *Bacillus arsenicoselenatis*, sp. nov., and *Bacillus selenitireducens*, sp. nov.: two haloalkaliphiles from Mono Lake, California that respire oxyanions of selenium and arsenic. *Archives of Microbiology 171*, 19–30.

(*42*) Lenz, M., Kolvenbach, B., Gygax, B., Moes, S., and Corvini, P. F. X., (2011). Shedding light on selenium biomineralization: proteins associated with bionanominerals. *Applied and Environmental Microbiology 77*, 4676–80.

(*43*) Leaver, J. T., Richardson, D. J., and Butler, C. S., (2008). *Enterobacter cloacae* SLD1a-1 gains a selective advantage from selenate reduction when growing in nitrate-depleted anaerobic environments. *Journal of Industrial Microbiology & Biotechnology 35*, 867–73.

(*44*) Debieux, C. M., Dridge, E. J., Mueller, C. M., Splatt, P., Paszkiewicz, K., Knight, I., Florance, H., Love, J., Titball, R. W., Lewis, R. J., Richardson, D. J., and Butler, C. S., (2011). A bacterial process for selenium nanosphere assembly. *PNAS U.S.A. 108*, 13480–5.

(*45*) Dridge, E. J., and Butler, C. S., (2010). Thermostable properties of the periplasmic selenate reductase from *Thauera selenatis*. *Biochimie 92*, 1268–73.

(*46*) Lowe, E. C., Bydder, S., Hartshorne, R. S., Tape, H. L. U., Dridge, E. J., Debieux, C. M., Paszkiewicz, K., Singleton, I., Lewis, R. J., Santini, J. M., Richardson, D. J., and Butler, C. S., (2010). Quinol-cytochrome c oxidoreductase and cytochrome c4 mediate electron transfer during selenate respiration in *Thauera selenatis*. *Journal of Biological Chemistry 285*, 18433–42.

(*47*) Hunter, W. J., (2014). A *Rhizobium selenitireducens* Protein Showing Selenite Reductase Activity. *Current Microbiology 68*, 311–316.

(*48*) Tugarova, A. V., Vetchinkina, E. P., Loshchinina, E. A., Burov, A. M., Nikitina, V. E., and Kamnev, A. A., (2014). Reduction of selenite by *Azospirillum brasilense* with the formation of selenium nanoparticles. *Microbial Ecology 68*, 495–503.

(*49*) Pearce, C. I., Coker, V. S., Charnock, J. M., Pattrick, R. A. D., Mosselmans, J. F. W., Law, N., Beveridge, T. J., and Lloyd, J. R., (2008). Microbial manufacture of chalcogenide-based nanoparticles via the reduction of selenite using *Veillonella atypica*: an in situ EXAFS study. *Nanotechnology 19*, 155603.

(*50*) Zhang, W., Chen, Z., Liu, H., Zhang, L., Gao, P., and Li, D., (2011). Biosynthesis and structural characteristics of selenium nanoparticles by *Pseudomonas alcaliphila*. *Colloids and Surfaces B: Biointerfaces 88*, 196–201.

(*51*) Ostwald, W., *Lehrbuch Der Allgemeinen Chemie*; W. Engelmann: 1896; Vol. 2.

(*52*) Jain, R., Jordan, N., Weiss, S., Foerstendorf, H., Heim, K., Kacker, R., Hübner, R., Kramer, H., van Hullebusch, E. D., Farges, F., and Lens, P. N. L., (2015). Extracellular polymeric substances govern the surface charge of biogenic elemental selenium nanoparticles. *Environmental Science & Technology 49*, 1713–20.

(*53*) Dwivedi, S., Alkhedhairy, A. A., Ahamed, M., and Musarrat, J., (2013). Biomimetic synthesis of selenium nanospheres by bacterial strain JS-11 and its role as a biosensor for nanotoxicity assessment: a novel se-bioassay. *PLoS ONE 8*, e57404.

(*54*) Lortie, L, Gould, W. D., Rajan, S, McCready, R. G., and Cheng, K. J., (1992). Reduction of Selenate and Selenite to Elemental Selenium by a *Pseudomonas stutzeri* Isolate. *Applied and Environmental Microbiology 58*, 4042–4.

(*55*) Dhanjal, S., and Cameotra, S. S., (2010). Aerobic biogenesis of selenium nanospheres by *Bacillus cereus* isolated from coalmine soil. *Microbial Cell Factories 9*, 52.

(*56*) Fleet-Stalder, V. V., Gürleyük, H, Bachofen, R, and Chasteen, T. G., (1997). Effects of growth conditions on production of methyl selenides in cultures of *Rhodobacter sphaeroides*. *Journal of Industrial Microbiology & Biotechnology 19*, 98–103.

(*57*) Bebien, M, Chauvin, J. P., Adriano, J. M., Grosse, S, and Verméglio, A, (2001). Effect of selenite on growth and protein synthesis in the phototrophic bacterium *Rhodobacter sphaeroides*. *Applied and Environmental Microbiology 67*, 4440–7.

(*58*) Sarret, G., Avoscan, L., Carrière, M., Collins, R., Geoffroy, N., Carrot, F., Covès, J., and Gouget, B., (2005). Chemical forms of selenium in the metal-resistant bacterium *Ralstonia metallidurans* CH34 exposed to selenite and selenate. *Applied and Environmental Microbiology 71*, 2331–7.

(*59*) Zhang, S.-Y., Zhang, J., Wang, H.-Y., and Chen, H.-Y., (2004). Synthesis of selenium nanoparticles in the presence of polysaccharides. *Materials Letters 58*, 2590–2594.

(*60*) Palomo-Siguero, M., and Madrid, Y., (2017). Exploring the Behavior and Metabolic Transformations of SeNPs in Exposed Lactic Acid Bacteria. Effect of Nanoparticles Coating Agent. *International Journal of Molecular Sciences 18*.

(*61*) Stark, W. J., (2011). Nanoparticles in Biological Systems. *Angewandte Chemie International Edition 50*, 1242–1258.

(*62*) Cheng, Y., Xiao, X., Li, X., Song, D., Lu, Z., Wang, F., and Wang, Y., (2017). Characterization, antioxidant property and cytoprotection of exopolysaccharide-capped elemental selenium particles synthesized by *Bacillus paralicheniformis* SR14. *Carbohydrate Polymers*, 18–26.

(*63*) Piacenza, E., Presentato, A., Zonaro, E., Lemire, J. A., Demeter, M., Vallini, G., Turner, R. J., and Lampis, S., (2017). Antimicrobial activity of biogenically produced spherical Se-nanomaterials embedded in organic material against *Pseudomonas aeruginosa* and *Staphylococcus aureus* strains on hydroxyapatite-coated surfaces. *Microbial Biotechnology 10*, 804–818.

(*64*) Cheng, G., Fan, J., Sun, W., Cao, J., Hu, C., and Peng, X., (2014). A near-infrared fluorescent probe for selective detection of HClO based on Se-sensitized aggregation of heptamethine cyanine dye. *Chemical Communications 50*, 1018–1020.

(*65*) Gonzalez-Gil, G., Lens, P. N. L., and Saikaly, P. E., (2016). Selenite Reduction by Anaerobic Microbial Aggregates: Microbial Community Structure, and Proteins Associated to the Produced Selenium Spheres. *Frontiers in Microbiology 7*, 571.

(*66*) Yang, S. I., George, G. N., Lawrence, J. R., Kaminskyj, S. G. W., Dynes, J. J., Lai, B., and Pickering, I. J., (2016). Multispecies Biofilms Transform Selenium Oxyanions into Elemental Selenium Particles: Studies Using Combined Synchrotron X-ray Fluorescence Imaging and Scanning Transmission X-ray Microscopy. *Environmental Science & Technology 50*, 10343–10350.

(*67*) Jain, R., Jordan, N., Tsushima, S., Hübner, R., Weiss, S., and Lens, P., (2017). Shape Change of Biogenic Elemental Selenium Nanomaterials From Nanospheres to Nanorods Decreases Their Colloidal Stability. *Environmental Science: Nano.*

(*68*) Piacenza, E., Bulgarini, A., Lampis, S., Vallini, G., and Turner, R. J., (2017). Biogenic SeNPs from *Bacillus mycoides* SelTE01 and *Stenotrophomonas maltophilia* SelTE02: Characterization with reference to their associated organic coating. *AIP Conference Proceedings.*

(*69*) Prateeksha, Singh, B. R., Shoeb, M, Sharma, S, Naqvi, A. H., Gupta, V. K., and Singh, B. N., (2017). Scaffold of Selenium Nanovectors and Honey Phytochemicals for Inhibition of *Pseudomonas aeruginosa* Quorum Sensing and Biofilm Formation. *Frontiers in Cellular and Infection Microbiology 7*, 93.

(*70*) Di Gregorio, S., Lampis, S., and Vallini, G., (2005). Selenite precipitation by a rhizospheric strain of *Stenotrophomonas* sp. isolated from the root system of *Astragalus bisulcatus*: a biotechnological perspective. *Environmental International 31*, 233–241.

(*71*) Okinaka, R. T., and Keim, P., (2016). The Phylogeny of *Bacillus cereus sensu lato*. *Microbiology Spectrum 4*.

(*72*) Bradford, M. M., (1976). A rapid and sensitive method for the quantitation of microgram quantities of protein utilizing the principle of protein-dye binding. *Analytical Biochemistry 72*, 248–54.

(*73*) Smith, P. K., Krohn, R. I., Hermanson, G. T., Mallia, A. K., Gartner, F. H., Provenzano, M. D., Fujimoto, E. K., Goeke, N. M., Olson, B. J., and Klenk, D. C., (1985). Measurement of protein using bicinchoninic acid. *Analytical Biochemistry 150*.

(*74*) Zhang, S.-Y., Zhang, J., Wang, H.-Y., and Chen, H.-Y., (2004). Synthesis of selenium nanoparticles in the presence of polysaccharides. *Materials Letters 58*.

(*75*) Masuko, T., Minami, A., Iwasaki, N., Majima, T., Nishimura, S.-I., and Lee, Y. C., (2005). Carbohydrate analysis by a phenol-sulfuric acid method in microplate format. *Analytical Biochemistry 339*, 69–72.

(*76*) Chow, P. S., and Landhäusser, S. M., (2004). A method for routine measurements of total sugar and starch content in woody plant tissues. *Tree Physiology 24*, 1129 –1136.

(*77*) Minamide, L. S., and Bamburg, J. R., (1990). A filter paper dye-binding assay for quantitative determination of protein without interference from reducing agents or detergents. *Analytical Biochemistry 190*, 66–70.

(*78*) Cheng, Y.-S., Zheng, Y., and VanderGheynst, J. S., (2011). Rapid quantitative analysis of lipids using a colorimetric method in a microplate format. *Lipids 46*, 95–103.

(*79*) DuBois, M., Gilles, K. A., Hamilton, J. K., Rebers, P. A., and Smith, F., (1956). Colorimetric Method for Determination of Sugars and Related Substances. *Analytical Chemistry 28*, 350–356.

(*80*) Panfoli, I., Calzia, D., Santucci, L., Ravera, S., and Candiano, M. B. G., (2012). A blue dive: from 'blue fingers' to 'blue silver'. A comparative overview of staining methods for in-gel proteomics. *Expert Review of Proteomics 6*, 627–634.

(*81*) Knight, J. A., Anderson, S., and Rawle, J. M., (1972). Chemical Basis of the Sulfo-phospho-vanillin Reaction for Estimating Total Serum Lipids. *Clinical Chemistry 18*, 199–202.

(*82*) Cronan, J. E., (2003). Bacterial Memebrane Lipids: Where Do We Stand? *Annual Review of Microbiology 57*, 203–224.

(*83*) Baldin, A., *Isolamento e caratterizzazione preliminare di ceppi batterici selenito-resistenti da suoli contaminati*; Bachelor Thesis, University of Verona: 2014.

(*84*) Ferron, E., *Studio della biogenesi di nanoparticelle di Selenio e Tellurio elementale in ceppi batterici isolati presso un sito contaminato ungherese*; Bachelor Thesis, University of Verona: 2014.

(*85*) Sehgal, P., and Otzen, D. E., (2006). Thermodynamics of unfolding of an integral membrane protein in mixed micelles. *Protein Science 15*, 890–899.

(*86*) Romero-Pérez, A., García-García, E., Zavaleta-Mancera, A., Ramírez-Bribiesca, J. E., Revilla-Vázquez, A., Hernández-Calva, L. M., López-Arellano, R., and Cruz-Monterrosa, R. G., (2010). Designing and evaluation of sodium selenite nanoparticles in vitro to improve selenium absorption in ruminants. *Veterinary Research Communications 34*, 71–79.

(*87*) Laemmli, U. K., (1970). Cleavage of structural proteins during the assembly of the head of bacteriophage T4. *Nature 227*, 680–5.

(*88*) Mascot, http://www.matrixscience.com/search_form_select.html.

(*89*) SecretomeP, http://www.cbs.dtu.dk/services/SecretomeP/.

(*90*) Bendtsen, J. D., Jensen, L. J., Blom, N., Heijne, G. V., and Brunak, S., (2004). Feature-based prediction of non-classical and leaderless protein secretion. *Protein Engineering, Design and Selection 17*, 349–56.

(*91*) TMHMM, http://www.cbs.dtu.dk/services/TMHMM/.

(*92*) Sonnhammer, E. L., von Heijne, G, and Krogh, A, (1998). A hidden Markov model for predicting transmembrane helices in protein sequences. *Proceedings of the 6th International Conference on Intelligent Systems for Molecular Biology 6*, 175–82.

(*93*) PSORTdb, http://www.psort.org/psortb/.

(*94*) Zhang, L., Li, D., and Gao, P., (2012). Expulsion of selenium/protein nanoparticles through vesicle-like structures by *Saccharomyces cerevisiae* under microaerophilic environment. *World Journal of Microbiology and Biotechnology 28*, 3381–6.

(*95*) Mukhopadhyay, S., Akmal, A., Stewart, A. C., Hsia, R.-C., and Read, T. D., (2009). Identification of *Bacillus anthracis* spore component antigens conserved across diverse *Bacillus cereus sensu lato* strains. *Molecular & Cellular Proteomics 8*, 1174–91.

(*96*) Delvecchio, V. G., Connolly, J. P., Alefantis, T. G., Walz, A., Quan, M. A., Patra, G., Ashton, J. M., Whittington, J. T., Chafin, R. D., Liang, X., Grewal, P., Khan, A. S., and Mujer, C. V., (2006). Proteomic profiling and identification of immunodominant spore antigens of *Bacillus anthracis*, *Bacillus cereus*, and *Bacillus thuringiensis*. *Applied and Environmental Microbiology 72*, 6355–63.

(*97*) Narayanan, A., and Ramana, K. V., (2012). Polyhydroxybutyrate production in *Bacillus mycoides* DFC1 using response surface optimization for physico-chemical process parameters. *3 Biotech*, 287–296.

(*98*) SignalP, http://www.cbs.dtu.dk/services/SignalP/.